AD_____

Award Number: DAMD17-95-C-5063

TITLE: Molecular Targets for Organophosphates in the Central Nervous System

PRINCIPAL INVESTIGATOR: Dr. Edson X. Albuquerque

CONTRACTING ORGANIZATION: University of Maryland
Baltimore, MD 21201

REPORT DATE: April 2006

TYPE OF REPORT: Final

PREPARED FOR: U.S. Army Medical Research and Materiel Command
Fort Detrick, Maryland 21702-5012

REPORT DOCUMENTATION PAGE

Form Approved
OMB No. 0704-0188

1. REPORT DATE	2. REPORT TYPE	3. DATES COVERED
01-04-2006	Annual	18 May 1995 – 14 Mar 2006

4. TITLE AND SUBTITLE

Molecular Targets for Organophosphates in the Central Nervous System

5a. CONTRACT NUMBER

5b. GRANT NUMBER
DAMD17-95-C-5063

5c. PROGRAM ELEMENT NUMBER

6. AUTHOR(S)

Dr. Edson X. Albuquerque

Email: ealbuque@umaryland.edu

5d. PROJECT NUMBER

5e. TASK NUMBER

5f. WORK UNIT NUMBER

7. PERFORMING ORGANIZATION NAME(S) AND ADDRESS(ES)

University of Maryland
Baltimore, MD 21201

8. PERFORMING ORGANIZATION REPORT NUMBER

9. SPONSORING / MONITORING AGENCY NAME(S) AND ADDRESS(ES)
U.S. Army Medical Research and Materiel Command
Fort Detrick, Maryland 21702-5012

10. SPONSOR/MONITOR'S ACRONYM(S)

11. SPONSOR/MONITOR'S REPORT NUMBER(S)

12. DISTRIBUTION / AVAILABILITY STATEMENT
Approved for Public Release; Distribution Unlimited

13. SUPPLEMENTARY NOTES
Original contains colored plates: ALL DTIC reproductions will be in black and white.

14. ABSTRACT

This project was a major effort to determine the effects of low-level exposure to the nerve agents sarin, soman, and VX in the mammalian CNS. Actions on synaptic transmission and neuronal cell death were assessed. Studies gave us clues to the mechanism of action of the agents, particularly in regard to cognitive function in humans that could be exposed to nerve agents in a chemical warfare attack. Reversible cholinesterase (ChE) inhibitors were tested for their ability to counteract nerve agent effects. Galantamine, a reversible ChE inhibitor with nicotinic allosteric potentiating actions currently used to treat mild to moderate Alzheimer's disease, was found to be effective in counteracting nerve agent toxicity. In vitro studies were therefore employed to determine the mechanism of action of galantamine. In vivo studies in guinea pigs were ultimately begun to assess the effectiveness of a pre- and/or post-treatment regimen of galantamine in protecting against multiple LD50 challenges with nerve agents. We compared the effectiveness of pre- and post-treatment with galantamine with other reversible ChE inhibitors in preventing lethality of the nerve agents and examined potential mechanisms underlying the effectiveness of the best treatment.

15. SUBJECT TERMS
Organophosphates

16. SECURITY CLASSIFICATION OF:			17. LIMITATION OF ABSTRACT	18. NUMBER OF PAGES	19a. NAME OF RESPONSIBLE PERSON
a. REPORT	b. ABSTRACT	c. THIS PAGE			USAMRMC
U	U	U	UU	102	19b. TELEPHONE NUMBER *(include area code)*

Standard Form 298 (Rev. 8-98)
Prescribed by ANSI Std. Z39.18

FORWORD

Opinions, interpretations, conclusions and recommendations are those of the author and are not necessarily endorsed by the U.S. Army.

( ) Where copyrighted material is quoted, permission has been obtained to use such material.

( ) Where material from documents designated for limited distribution is quoted, permission has been obtained to use the material.

(x) Citations of commercial organizations and trade names in this report do not constitute an official Department of the Army endorsements or approval of the products or services of these organizations.

(x) In conducting research using animals, the Investigator(s) adhered to the "Guide for the Care and Use of Laboratory Animals," prepared by the Committee on Care and Use of Laboratory Animals of the Institute of Laboratory Animals Resources, National Research Council (NIH Publication No. 86-23, Revised 1985).

( ) For the protection of human subjects, the Investigator(s) have adhered to policies of applicable Federal Law 32 CFR 219 and 45 CFR 46.

( ) In conducting research utilizing recombinant DNA technology, the Investigator(s) adhered to current guidelines promulgated by the National Institutes of Health.

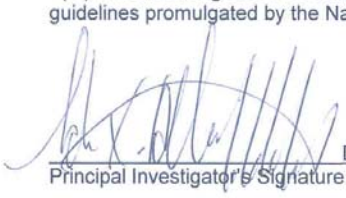

December 14, 2006

Principal Investigator's Signature Date

DAMD17-95-C-5063

Table of Contents

Page Number

Index to Figures in this Report:

INTRODUCTION

The organophosphorus compounds (OPs) soman, sarin, VX and tabun, referred to as nerve agents, are among the most lethal chemical weapons ever developed (Coupland and Leins, 2005). Some of them were used with catastrophic results in wars and in the terrorist attacks in Japan in the 1990's (Romano and King, 2001). The majority of insecticides are also OPs, and intoxication with these compounds represents a major public health concern worldwide (Karalliedde and Senanayake, 1989; Buckley *et al.*, 2004). The possibility of further terrorist attacks with nerve agents and the escalating use of OP insecticides underscore the urgent need to develop effective and safe antidotes against OP poisoning.

The acute toxicity of OPs results primarily from their action as irreversible inhibitors of AChE (Bajgar, 2004). In the periphery, ACh accumulation leads to persistent muscarinic receptor stimulation that triggers a syndrome whose symptoms include miosis, profuse secretions, bradycardia, bronchoconstriction, hypotension, and diarrhea. It also leads to overstimulation followed by desensitization of nicotinic receptors causing severe skeletal muscle fasciculations and subsequent weakness. Central nervous system (CNS)-related effects include anxiety, restlessness, confusion, ataxia, tremors, seizures, cardiorespiratory paralysis, and coma.

Current therapeutic strategies to decrease OP toxicity include atropine to reduce the muscarinic syndrome, oximes to reactivate OP-inhibited AChE, and benzodiazepines to control OP-triggered seizures (Bajgar, 2004). The limitations of these treatments are well recognized (4), and alternative therapies have been sought. Among these are phosphotriesterases and butyrylcholinesterase (BuChE), enzymes that act as OP scavengers (Doctor *et al.*, 1991; Ghanem and Raushel, 2005). However, potential adverse immunological reactions and the difficulty in delivering these large molecules systemically have slowed progress in this field.

Pyridostigmine bromide, a quaternary carbamate that does not cross the blood brain barrier (BBB) appreciably and inhibits reversibly AChE and BuChE with similar potencies has been approved for use by military personnel under threat of exposure to nerve agents. Pre-treatment with pyridostigmine prevents OP-induced irreversible AChE inhibition in the periphery and increases survival of animals acutely exposed to lethal doses of nerve agents, provided that atropine and oximes are administered promptly after an OP exposure (Bajgar, 2004; Wetherell *et al.*, 2002; Leadbeater *et al.*, 1985). When used acutely prior to an OP exposure, reversible inhibitors of AChE that are capable of crossing the BBB, including physostigmine, tacrine and huperzine A (herein referred to as huperzine), afford better protection than pyridostigmine against OP toxicity, but generally at doses that produce significant incapacitation and CNS impairment (Deshpande *et al.*, 1986; Grunwald *et al.*, 1994; Fricke *et al.*, 1994; Fricke *et al.*, 1994; Lallement *et al.*, 2002).

Galantamine, a drug approved for treatment of mild-to-moderate AD (Corey-Bloom, 2003), has properties appropriate for an antidotal therapy against OP poisoning. Briefly, galantamine: (i) is a reversible AChE inhibitor that crosses the BBB (Corey-Bloom, 2003), (ii) has anticonvulsant properties (Dreyer, 1968; Losev and Tkachenko, 1986), and (iii) prevents neurodegeneration (Pereira *et al.*, 2002; Arias *et al.*, 2004; Kihara *et al.*, 2004), a hallmark of OP poisoning (Shih *et al.*, 2003). Thus, this study was designed to test the hypothesis that galantamine can be a safe countermeasure against OP intoxication in guinea pigs, the best non-primate model for predicting the effectiveness of antidotal therapies for OP poisoning in humans (Maxwell *et al.*, 1988). Due to their low levels of circulating carboxylesterases, guinea pigs, like non-human primates, are considerably more sensitive to OPs and respond better to antidotal therapies consisting of pretreatment with reversible AChE inhibitors and post-

treatment with atropine, than rats or mice (Maxwell *et al.*, 1988).

This report summarizes all of our studies attempting to identify specific cellular and molecular mechanisms by which different OPs affect neuronal viability and synaptic plasticity and to characterize the mechanisms that can contribute to the effectiveness of a given medical countermeasure against OP poisoning.

BODY

Section 1. Effects of nerve agents on spontaneous and evoked release of neurotransmitters

1.1. Low concentrations of the organophosphate VX affect spontaneous and evoked transmitter release from hippocampal neurons: toxicological relevance ofcholinesterase-independent actions

Introduction

Organophosphate compounds (OPs) include, in addition to insecticides and other compounds used to treat schistosomiasis and Alzheimer's disease (Tariot *et al.*, 1997), the highly toxic and lethal nerve gases VX, soman, sarin, and tabun. These "nerve agents" represent a major threat to soldiers in battle fields and occasionally have been used by terrorists against civilians (Gunderson *et al.*, 1992; Solberg and Belking, 1997). Although it has long been accepted that inhibition of cholinesterase is the mechanism underlying the toxic effects of OPs, these compounds have been shown to interact with molecular targets other than cholinesterases in the peripheral and central nervous systems (Idriss *et al.*, 1986; Rao *et al.*, 1987; Albuquerque *et al.*, 1985, 1987, 1988, 1994; Rocha *et al.*, 1992, 1996c). Of particular interest is the report that at the neuromuscular junction VX increases acetylcholine (ACh) release by a mechanism unrelated to cholinesterase inhibition (Rao *et al.*, 1987). Similarly, it has been observed that VX and tabun as well as the carbamate pyridostigmine increase spontaneous glutamate release at the locust nerve-muscle synapse, causing firing of spontaneous action potentials (Idriss *et al.*, 1986).

Of major importance for the understanding of the actions underlying the neurotoxic effects of OPs is the fact that the mechanisms regulating the release of neurotransmitters from neurons of the central nervous system (CNS) are different from those modulating the release of ACh at the neuromuscular junction. Not only do the voltage-gated channels have a key role in controlling release of transmitters from CNS neurons, but also, when present on presynaptic CNS neurons, ligand-gated channels, including neuronal nicotinic receptors (nAChRs) and the *N*-methyl-D-aspartate (NMDA)-type of glutamate receptors, as well as metabotropic receptors, including the muscarinic receptors and some subtypes of glutamate receptors, are capable of modulating differently the release of a variety of neurotransmitters. For instance, activation of neuronal nAChRs has been implicated in the release of GABA and glutamate (Alkondon *et al.,* 1997; Gray *et al.,* 1996). Thus, considering that OPs can interact directly with nAChRs (reviewed in Albuquerque *et al.*, 1987), muscarinic (Jett *et al.*, 1991; Silveira *et al.*, 1990), and glutamatergic receptors (Gray *et al.*, 1996), the question is raised of whether OPs can alter transmitter release from CNS neurons, and, if so, by what mechanism.

By means of the patch-clamp technique, we demonstrated for the first time that at toxicologically relevant, low concentrations VX blocks the tetrodotoxin (TTX)-sensitive release of GABA and glutamate from hippocampal neurons, with estimated IC_{50} values of 1 nM and >30 nM, respectively. Whereas the effect of VX on GABA release is partially reversible upon washing and is mediated by its direct interactions with presynaptic muscarinic receptors, that on glutamate release is not reversible and could be accounted for by VX-induced decrease in the firing rate and amplitude of action potentials. Also, we provided evidence that VX (10 nM) increases the action potential-independent, TTX-insensitive release of GABA and glutamate via a Ca^{2+}-dependent mechanism.

Materials and Methods

Animals. Pregnant Sprague-Dawley rats were kept for two days in the animal facility of the University of Maryland, Baltimore. The animals were given rodent chow and tap water *ad libitum* and, on the day of culture preparation, were sacrificed by cervical dislocation after being anesthetized in a CO_2 atmosphere.

Neuronal Culture. Cultures of hippocampal neurons were prepared as described previously (Alkondon and Albuquerque, 1993). Briefly, the hippocampi of 18-day-old fetal rats were dissected out and incubated at 36 °C for 30 min with trypsin (0.25%). After the enzymatic treatment, the neurons were dissociated in Minimal Essential Medium (MEM) supplemented with glutamine (2 mM), 10% heat-inactivated horse serum (GIBCO BRL, Grand Island, NY), 10% fetal-bovine serum (JRH Bioscience, Lenex, KS) and deoxyribonuclease II (20 µg/ml, type V). The neurons were plated at a density of 175,000 to 350,000/ml on a collagen-coated culture dish, and were incubated at 36 °C in a 10% CO_2 - 90% air atmosphere saturated with water. At 24 h after plating the neurons, MEM supplemented with 10% heat-inactivated horse serum and glutamine (2 mM) was substituted for the original culture medium. Non-neuronal cell proliferation was inhibited at the seventh day of culture by adding to the medium 5-fluor-2'2-deoxyuridine (final concentration = 13.3 µg/ml) and uridine (final concentration = 6.7 µg/ml) for 24 h. Neurons cultured for 15 to 30 days were used.

Electrophysiological Recordings. A culture dish was perfused continuously at 1.52 ml/min with external solution that contained (in mM): NaCl, 165; KCl, 5; $CaCl_2$, 2; glucose, 10; 4-(2-hydroxy ethyl)-1-piperazineethanesulfonic acid (HEPES), 10 (the pH was adjusted to 7.3 with NaOH). Whenever stated, TTX (150 nM) was added to the external solution, and when miniature postsynaptic currents (MPSCs) were recorded, the muscarinic blocker atropine (1 µM) was also added to the external solution. Experiments were performed at room temperature (20-24^{o}C).

Drug-containing external solution was applied to the neurons by a procedure similar to that described previously (Rocha *et al.*, 1996c). Briefly, sets of six to eleven coplanar-parallel tubes (400-µm inner diameter) were used to provide the continuous gravity-driven flow of several different solutions to the neurons. A microcomputer-controlled, motor-driven system (Newport Corporation, Irvine, CA) was used to position a selected tube at approximately 350 µm from the neurons. The time to switch between two neighboring tubes was 30 msec.

The whole-cell mode of the patch-clamp technique (Hamill *et al.*, 1981) was used to record postsynaptic currents from hippocampal neurons using an Axopatch 200A (Axon Instruments, Inc. CA) or an LM-EPC-7 (List Electronic, Darmstadt, FRG). The internal solution used to fill the pipettes consisted of (in mM): CsCl, 80; CsF, 80; Cs-ethylene glycol bis (β-amino-ethyl ether)-N,N-tetraacetic acid, 10; and HEPES, 10 (the pH was adjusted to 7.3 with CsOH). For studies of action potentials, CsCl and CsF were substituted with KCl.

The series resistance was not compensated, and any patch that had more than 10% fluctuation in its series resistance was discarded. The signals were filtered at 2.3 kHz, stored on VCR tapes and digitized to a microcomputer at 10-20 kHz. The frequency, peak amplitude and decay-time constant of the MPSCs were analyzed by the programs CDR and SCAN (Dempster, 1989).

Field stimulation-evoked postsynaptic currents were elicited by the application of an electrical stimulus of 20–60-µsec duration and supra-maximal intensities (6-10 V) via a bipolar

electrode constructed with platinum wires (50-100 μm, diameter; Karma Co. N.J). The neurons to be stimulated were carefully positioned between the poles of the bipolar electrode. The electrode was connected to a digital-to-analog interface (TL-1 DMA, Axon Instrument, Inc., Foster City, CA) of the microcomputer via an isolated stimulator (Digitimer Ltd., Medical System Corp, New York, NY). Possible changes in series resistance were detected by applying, on line, a 3-mV-peak-amplitude hyperpolarizing pulse before the stimulus pulse.

Statistical Analysis. Data are expressed as mean ± standard error (S.E.). Differences in the populations were analyzed with the Student's t test.

Drugs and biological hazards. VX (O-Ethyl S-[2-(diisopropyl-amino)ethyl] methylphosphono-thiolate) and soman (1,2,2-Trimethylpropyl methylphosphonofluoridate) were obtained from the U.S. Army Medical Research and Development Command (USAMRDC). Methyllycaconitine citrate (MLA) was a gift from Prof. M.H. Benn (Department of Chemistry, University of Calgary, Calgary, Alberta, Canada). Dihydro-β-erythroidine hydrobromide (DHβE) was a gift from Merck, Sharp & Dohme (Rahway, NJ). Other chemicals were purchased from Sigma Chemical Co., St. Louis, MO.

Safety handling OPs was assured according to USAMRDC's recommendation. These compounds were stored at 80□C and diluted daily by using an OP vapor-proof hood. All OP- or TTX-containing solutions were inactivated with 5% sodium hypochlorite. Latex gloves and proper goggles were used throughout the day of the experiment.

Results

Two transmitter release processes were analyzed in the presence and in the absence of the nerve agent VX, *i.e.* the action potential-dependent and the action potential-independent release of GABA and glutamate from hippocampal neurons. The action potential-dependent release of each neurotransmitter was the result of field stimulation of neurons synapsing onto the neurons from which recordings were obtained. Application of a supra-maximal electrical stimulus via a bipolar electrode to neurons synaptically connected to the neuron under study always led to the activation of a postsynaptic current that was mediated by the evoked release of either glutamate or GABA. In this study, glutamatergic and GABAergic currents, which are herein referred to as excitatory postsynaptic currents (EPSCs) and inhibitory postsynaptic currents (IPSCs), respectively, were pharmacologically isolated; evoked EPSCs were recorded from neurons that were perfused with the $GABA_A$-receptor antagonist picrotoxin (100 μM) and evoked IPSCs were recorded from neurons that were perfused with the α-amino-3-hydroxy-5-methyl-4-isoxazolepropionic acid (AMPA)-receptor antagonist 6-cyano-7-nitroquinoxaline-2,3-dione (CNQX; 10 μM). It should be noted that under our recording conditions the contribution of the NMDA receptor activity to glutamate-mediated EPSCs is negligible (see Rocha *et al.*, 1996b; Braga *et al.*, 1999). If VX would not interfere with the activity of the postsynaptic receptors mediating the EPSCs and IPSCs, measurements of the amplitude of these currents in the presence and in the absence of this OP would provide direct evidence of its effect on the action potential-dependent release of the neurotransmitters. The action potential-independent release of both GABA and glutamate was studied in neurons that were continuously perfused with TTX-containing external solution. Under this experimental condition, miniature postsynaptic currents (MPSCs) could be recorded from the hippocampal neurons. GABAergic MPSCs were selectively recorded in the presence of CNQX (10 μM), and glutamatergic MPSCs were selectively recorded in the presence of picrotoxin (100 μM). If VX did not affect the activity of the postsynaptic receptors mediating the MPSCs, changes in frequency of MPSCs would be indicative of alterations in transmitter release.

VX reduces the amplitude of GABA-mediated IPSCs and glutamate-mediated EPSCs evoked by field stimulation of cultured hippocampal neurons.

In the presence of picrotoxin, superfusion of hippocampal neurons with external solution containing VX (0.1 nM) resulted in a concentration-dependent reduction of the peak amplitude of evoked EPSCs (Fig. 1.1.1A). This effect was not reversible during 5 min of washing the neurons with VX-free external solution. Much lower concentrations of VX were necessary to block IPSCs. In the presence of CNQX, superfusion of hippocampal neurons with external solution containing 0.01 1 nM VX resulted in a significant reduction of the amplitude of the IPSCs (Fig. 1B). Whereas at 50 nM VX decreased by only 30% the amplitude and the area under the curve of evoked EPSCs (n=9) (Fig. 1.1.1A), at 1 nM it decreased by 50% the amplitude of evoked IPSCs (Fig. 1.1.1B). The effect of VX on the IPSCs was partially reversible upon washing of the neurons with VX-free external solution.

Atropine prevents VX-induced reduction of the action potential-dependent release of GABA.

In an attempt to elucidate the mechanism underlying the effect of VX on the evoked IPSCs, we considered the fact that OPs can directly or indirectly affect the activity of nAChRs and muscarinic receptors, which are known to modulate the action potential-dependent release of GABA from hippocampal neurons.

In the presence of CNQX, perfusion of the hippocampal neurons with atropine (1 μM)-containing external solution resulted in a 30% reduction of the amplitude of evoked IPSCs (Fig. 1.1.2A), indicating that there should be a basal muscarinic receptor activity controlling the release of GABA from the hippocampal neurons in culture. Such activity could be maintained by ACh released from cholinergic neurons in our culture. In the continuous presence of atropine, exposure of the neurons to VX (1 nM) resulted in no significant further reduction of the IPSC amplitude (Fig. 1.1.2A). Contrariwise, in neurons that were continuously perfused with external solution containing MLA (2 nM) and DHβE (200 nM) -- antagonists of the two major subtypes of nAChRs present in hippocampal neurons, *i.e.* the α7 and α4β2 nAChRs, respectively (Alkondon and Albuquerque, 1993) -- VX was still capable of reducing the amplitude of the IPSCs (Fig. 1.1.2B).

As stated above, following the blockade of the muscarinic receptors with atropine (1 μM), VX (1 nM) could no longer affect the amplitude of the IPSCs (see Fig. 1.1.2A). However, upon washing of the neurons with atropine-free, VX (1 nM)-containing external solution, the amplitude of the evoked IPSCs was decreased to approximately 50% of control values. Subsequently, perfusion of the neurons with external solution containing both atropine and VX did not reverse the effect of the OP on the amplitude of evoked IPSCs (Fig. 1.1.2A).

VX decreases the rate of firing and the amplitude of evoked action potentials in hippocampal neurons.

Perfusion of current-clamped hippocampal neurons with VX (0.150 nM)-containing external solution changed the pattern and amplitude of evoked action potentials recorded from hippocampal neurons in culture. VX (0.1 nM) decreased the amplitude of the action potentials and reduced the occurrence of repetitive firing (Fig 1.1.3). These effects of VX, which were concentration dependent and were only partially reversible upon washing of the cells with VX-free external solution, were observed starting 10 30 sec after its application to the neurons. Also, these effects of VX were neither related to membrane depolarization (data not shown) nor accompanied by changes in the input resistance of the neurons. The input resistance of the neurons was continuously monitored throughout the experiments by the application of 100-

300-msec hyperpolarizing pulses of 10-30-pA amplitude just before the application of the depolarizing pulses (50-100 pA) that triggered the action potentials. In the presence of VX, the input resistance of the cultured neurons was not significantly different from that obtained under control conditions and had a mean value of 400±36 MΩ (n = 14).

Under voltage-clamp conditions, the current transients elicited by depolarizing steps applied to neurons held at 80 mV had a Na^+ component and a K^+ component, which could be isolated from one another by the use of Cs^+ (which blocks the K^+ channels) in the internal solution or TTX (which blocks the Na^+ channels) in the external solution. In the presence of VX (1 μM), K^+-current transients were not significantly different from those observed in the absence of VX (Fig. 1.1.4). Therefore, VX-induced reduction of repetitive firing observed in neurons under current-clamp conditions was not due to modulation by VX of voltage-activated K^+ channels, and was probably accounted for by an effect of VX on the voltage-activated Na^+ channels subserving the Na^+-current transients. Additional studies are underway to elucidate the mechanisms by which VX inhibits the activity of voltage-gated Na^+ channels.

VX facilitates TTX-insensitive release of glutamate and GABA from hippocampal neurons.

Glutamatergic and GABAergic MPSCs could be recorded from hippocampal neurons perfused continuously with TTX-containing external solution. In recordings where a low frequency of MPSCs was detected (< 15 events/sec), the occurrence of events followed a random pattern so that the plot of the time interval between two consecutive events versus the number of events could be fitted by a single exponential function. Because the frequency of MPSCs varied from patch to patch, VX was applied to patches in which a low frequency of MPSCs was detected under control conditions. In about 70-80% of the experiments, the MPSC frequency under control condition remained constant over time.

The plot of the cumulative number of detected MPSCs versus recording time revealed that VX increased the frequency of MPSCs and that this effect was persistent throughout the recording time (5-30 min). VX-induced increased MPSC frequency could be detected starting 1-2 min after the initiation of the superfusion of the neurons with VX-containing solution and continuing for 30 min (n = 8). Considering that the onset of the application of VX-containing solution to the neurons occurred 30 msec after the moment that the motor-driven, drug-delivery system was activated, the 1-2-min latency for the effect of VX could be attributed to an interaction of this OP with extracellular presynaptic targets associated with second messenger-dependent pathways or with intracellular targets within the presynaptic terminals.

The enhancement by VX (1 nM-10 μM) of the frequency of glutamate- and GABA-mediated MPSCs was concentration dependent (Fig. 1.1.5). At 10 nM, VX increased the MPSC frequency to 195 ± 15% of the control, whereas at 1 μM, it increased the MPSC frequency to 556 ± 95 % of the control (Fig. 1.1.5). Such an effect was not reversible upon washing of the neurons for 10 min with VX-free external solution.

Analysis of results obtained from patches in which the time interval between two consecutive events was long enough to allow a reasonable fit of the decay-time constant as well as the measurement of the peak amplitude of isolated MPSCs indicated that VX (50 nM) had no significant effect on the mean peak amplitude or decay-time constant of MPSCs mediated by glutamate (Fig. 1.1.6) or GABA (Data not shown). These findings demonstrate that VX does not interact with postsynaptic $GABA_A$ or AMPA receptors and indicate that VX-induced increase of the frequency of GABAergic and glutamatergic MPSCs is exclusively due to an enhancement by VX of the TTX-insensitive release of neurotransmitters.

Mechanisms underlying the ability of VX to increase the TTX-insensitive release of glutamate and GABA from cultured hippocampal neurons.

If cholinesterase inhibition was responsible for the effect of VX on GABA- and glutamate-mediated MPSCs, any cholinesterase inhibitor should have the same effect as VX on the MPSCs. However, a 5-min perfusion of the neurons with soman at a concentration (2 μM) sufficient to inhibit completely the cholinesterase activity had no effect on the frequency, kinetics or amplitude of the MPSCs. In addition, following complete blockade of cholinesterase by soman, VX (10 nM) was still capable of increasing the frequency of GABA- and glutamate-mediated MPSCs (Fig. 1.1.7).

Many studies have indicated that presynaptic metabotropic receptors such as the muscarinic receptors, and ligand-gated channels, including glutamate ionotropic receptors, can modulate the TTX-insensitive transmitter release from hippocampal neurons (Jarolimek and Misgeld, 1997; Cunha *et al.*, 1997). However, the effect of VX on the frequency of glutamate- and GABA-mediated spontaneous MPSCs could be observed in the presence of the NMDA-type glutamate receptor antagonists APV (50 μM) and Mg^{2+} (1 mM) and of the muscarinic receptor antagonist atropine (1 μM). In addition, VX (50 nM) had no effect on whole-cell currents induced by the admixture of NMDA (50 μM) plus glycine (10 μM) (Fig. 1.1.8 top). Similarly VX (1 μM) did not interact with the inhibitory strychnine-sensitive glycine receptors (Fig. 1.1.8 bottom, left traces). Moreover, the lack of changes in the amplitude and kinetics of the GABA- and glutamate-mediated MPSCs indicates that VX does not interact with $GABA_A$ or AMPA receptors, respectively. Therefore, it can be concluded that VX-induced facilitation of TTX-insensitive transmitter release is not due to modulation by VX of presynaptic $GABA_A$, glycine, AMPA, NMDA, and muscarinic receptors.

To investigate whether the effects of VX on the TTX-insensitive release of GABA and glutamate was Ca^{2+} dependent, a Ca^{2+}-free external solution was used. The occurrence of MPSCs was substantially reduced during perfusion of the neurons with nominally Ca^{2+}-free external solution, and the addition of VX (50 nM-1 μM) (n = 6) to this solution did not change the frequency of MPSCs.

Discussion

The present investigation demonstrates for the first time that synaptic transmission in the mammalian CNS is affected by toxicologically relevant concentrations of the nerve agent VX via mechanisms that are unrelated to cholinesterase inhibition. At picomolar concentrations, VX blocks the action potential-dependent release of GABA as evidenced by its ability to reduce the amplitude of IPSCs evoked by field stimulation of presynaptic neurons. Only at nanomolar concentrations did VX inhibit significantly the action potential-dependent release of glutamate. Also at nanomolar concentrations, VX increased the action potential-dependent release of GABA and glutamate as evidenced by an increase in the frequency and no changes in the kinetics of GABA- and glutamate-mediated MPSCs recorded from hippocampal neurons in the presence of TTX. The mechanisms underlying the effects of VX on synaptic transmission and the relevance of the present findings are discussed herein.

A direct interaction of VX with presynaptic muscarinic receptors accounts for its ability to block the action potential-dependent release of GABA from hippocampal neurons.

The finding that the muscarinic receptor antagonist atropine prevents VX (0.1-1 nM) from blocking the evoked release of GABA from hippocampal neurons indicates that such an effect is probably mediated by muscarinic receptors. Numerous studies have reported that muscarinic receptors modulate GABA-mediated inhibitory neurotransmission in the mammalian CNS (Morton and Davies, 1997; Sanz *et al.*, 1997) and that the major subtypes of muscarinic receptors present in hippocampal neurons are M2 and M4 (McKinney *et al.*, 1993).

Inhibition by VX of evoked GABA release could have been explained by the activation of presynaptic muscarinic receptors by excess of ACh generated as a consequence of VX-induced inhibition of acetylcholinesterase (Pitler and Alger, 1992). However, at 10 pM, VX inhibited the evoked release of GABA to a much greater extent than it would have blocked cholinesterase activity (Sawyer *et al.*, 1991). It is most likely that VX-induced blockade of evoked release of GABA is mediated by a direct interaction of this OP with presynaptic muscarinic receptors. This notion is supported by previous reports that several OPs can bind with high affinity to muscarinic receptors (Silveira *et al.*, 1990; Jett *et al.*, 1991).

VX-induced reduction of the amplitude of action potentials could underlie the ability of this OP to block the action potential-dependent release of glutamate from hippocampal neurons.

Our results indicate that VX reduces both the firing rate and the amplitude of action potentials recorded from hippocampal neurons. These effects, which appear to be a consequence of changes in the activation/inactivation properties of voltage-gated Na^+ channels (see *Results*), were only observed at VX concentrations $\geq$ 100 pM. Since 0.1 nM VX decreased by about 10% the amplitude of both evoked action potentials and evoked EPSCs, the reduction by VX of the amplitude of action potentials could account for the ability of this OP to decrease the evoked release of glutamate.

The interaction of VX with presynaptic muscarinic receptors is undoubtedly a more specific mechanism by which synaptic transmission can be altered. However, it has been reported that the muscarinic receptor subtypes mostly associated with modulation of glutamate release in the CNS are the M1 and M3 (Cox *et al.*, 1994). Thus, even if VX was capable of interacting with M1/M3 receptors, no signigicant changes in glutamate release would have been detected in our preparation, because these receptor subtypes do not appear to be the predominant muscarinic receptor subtypes present in hippocampal neurons (McKinney *et al.*, 1993). Alterations of the firing rate and amplitude of action potentials may represent a less selective mechanism of action of VX, since it will result in the reduction of the action potential-dependent release of all neurotransmitters. Thus, whereas at picomolar concentrations, VX should alter the function of synapses that are modulated by the activity of presynaptic muscarinic receptors, at nanomolar concentrations, VX should cause a generalized reduction of the action potential-dependent synaptic transmission.

VX-induced enhancement of action potential-independent release of neurotransmitters is unrelated to cholinesterase inhibition and is Ca^{2+} dependent.

At nanomolar concentrations, VX increased the action potential-independent release of GABA and glutamate from hippocampal neurons. Such an effect, which was observed in the presence of atropine, had the same magnitude regardless of the neurotransmitter being released by the neurons, indicating that VX acted via a mechanism common to the spontaneous, action potential-independent release of all neurotransmitters. Also, this effect of

VX could still be detected when cholinesterase was fully inhibited by soman. Given that soman by itself did not have a significant effect on the spontaneous release of GABA and glutamate, cholinesterase inhibition would not account for the ability of VX to increase the action potential-independent release of neurotransmitters.

The finding that in the absence of extracellular Ca^{2+} VX did not alter transmitter release suggested a Ca^{2+}-dependent mechanism of action for this OP. The influx of Ca^{2+} into the neurons appears to be necessary for the effect of VX to take place. Thus, it could be hypothesized that VX interacts directly with Ca^{2+} channels, prolonging their open time or reducing their kinetics of inactivation. Alternatively, it could be hypothesized that VX interacts with an extracellular target that is associated with second messenger pathways or affects a Ca^{2+}-dependent mechanism within the presynaptic terminals. The slow onset of action of VX on spontaneous transmitter release favors the second hypothesis.

Toxicological relevance of cholinesterase-unrelated, VX-induced changes in synaptic transmission in the hippocampus.

It has been classically thought that OP-induced seizures are the ultimate consequence of cholinesterase inhibition. However, the present study demonstrates that at concentrations that produce little, if any, effect on cholinesterase, VX, by directly interacting with presynaptic muscarinic receptors, causes a selective inhibition of the evoked release of GABA. The net effect of such interaction would be the prevalence of the excitatory transmission in the CNS of VX-intoxicated subjects. This imbalance between excitatory and inhibitory transmission in the CNS resulting from the direct blockade by VX of the inhibitory synaptic transmission could account for the ability of this OP to induce convulsions, which are apparently responsive for the neuronal damage observed in various areas of the brain, including the hippocampus, of rats that receive intra-amygdaloid injections of VX (McDonough *et al.*, 1987).

It should be taken into account that although atropine is able to prevent VX-induced block of the evoked release of GABA, atropine itself reduces (to a lesser extent than VX does) the muscarinic cholinergic modulation of GABA release. Thus, muscarinic antagonists, although useful to some extent, may not be the best therapeutic countermeasure to prevent VX-induced neurotoxicity in the mammalian CNS. It appears more likely that a drug capable of enhancing the GABAergic activity would be better able to prevent (or even reverse) the neurotoxic effects of VX.

In conclusion, the present study indicates that the excitotoxic effects of VX in the CNS can be attributed to a direct interaction of this OP with presynaptic muscarinic receptors and subsequent blockade of the action potential-dependent release of GABA. Also, it provides evidence that, via cholinesterase-independent actions, nanomolar concentrations of VX can severely affect synaptic transmission in the hippocampus, blocking the action potential-dependent release of glutamate and facilitating the action potential-independent release of both GABA and glutamate. These findings may set the stage for the development of more efficacious measures to treat and/or prevent VX-induced neurotoxicity.

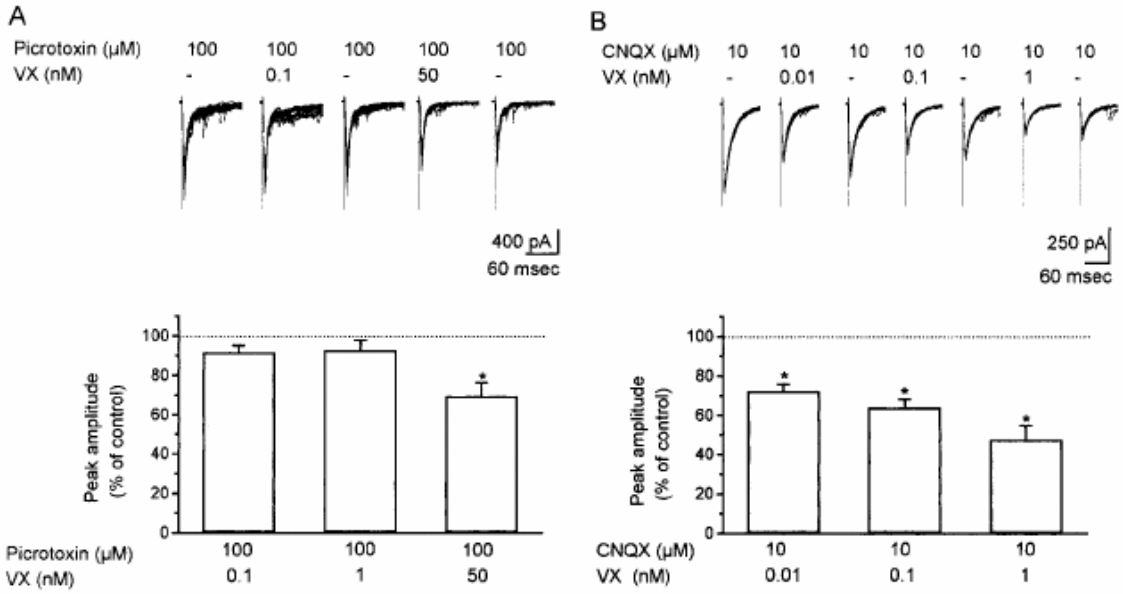

Figure 1.1.1. *VX reduces the amplitude of evoked EPSCs and IPSCs recorded from cultured hippocampal neurons.* **A.** Top traces: Samples of evoked EPSCs recorded from hippocampal neurons continuously perfused with picrotoxin (100 μM)-containing external solution prior to, during, and after their exposure to VX (0.1 or 50 nM). Bottom graph: Concentration-response relationship for VX-induced reduction of the EPSC peak amplitude. The peak amplitude of the EPSCs recorded prior to exposure of the neurons to VX was taken as 100% and was used to normalize the peak amplitude of the EPSCs recorded under each of the experimental conditions. Results are mean ± S.E. of 5 experiments. **B.** Top traces: Samples of evoked IPSCs recorded from hippocampal neurons continuously perfused with CNQX (10 μM)-containing external solution prior to, during, and after their exposure to VX (0.01, 0.1, or 1 nM). Bottom graph: Concentration-response relationship for VX-induced reduction of the IPSC peak amplitude. The peak amplitude of the IPSCs recorded prior to exposure of the neurons to VX was taken as 100% and was used to normalize the peak amplitude of the IPSCs recorded under each of the experimental conditions. Results are mean ± S.E. of 6 experiments. Each concentration was tested on a neuron that had not been previously exposed to VX. VX was applied to the neurons for 5 min. Membrane potential, –30 to –40 mV.
* Significantly different from control groups at P<0.01 in the Student's *t* test.

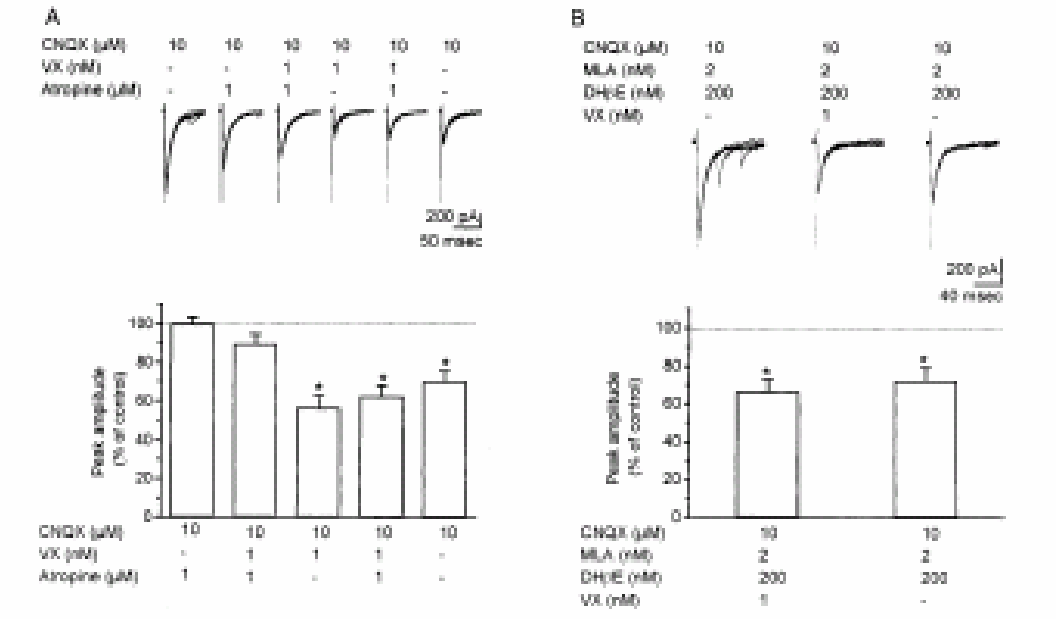

Figure 1.1.2. *VX-induced reduction of the amplitude of IPSCs is prevented by the muscarinic receptor antagonist atropine.* **A.** Top traces: Samples of evoked IPSCs recorded from hippocampal neurons that were continuously perfused with CNQX (10 μM)-containing external solution and subjected to the following sequential treatment: (i) 5-min exposure to atropine (1 μM); (ii) 5 min exposure to the admixture of atropine plus VX (1 nM); (iii) 5-min exposure to VX (1 nM); (iv) 5-min exposure to the admixture of VX plus atropine; and (v) 5-min washing with atropine- and VX-free external solution. Membrane potential, –30 to –40 mV. Bottom graph: Plot of the peak amplitude of evoked IPSCs recorded under the different experimental conditions. The peak amplitude of evoked IPSCs recorded prior to the exposure of the neurons to atropine or VX was taken as 100% and was used to normalize the peak amplitude of the currents recorded under each experimental condition. Results are mean ± S.E. of 5 experiments. **B.** Top traces: Samples of IPSCs recorded in the presence of the nicotinic receptor blockers MLA and DHβE prior to and after exposure of the neurons for 5 min to VX (1 nM). Membrane potential, –30 to –40 mV. Bottom graph: Plot of the peak amplitude of evoked IPSCs recorded from hippocampal neurons that were continuously perfused with external solution containing the nicotinic receptor blockers in the presence and in the absence of VX. The amplitude of the IPSCs recorded prior to the exposure of the neurons to VX was taken as 100% and was used to normalize the peak amplitude of the IPSCs recorded during and after perfusion of the neurons with VX-containing external solution. Results are mean ± S.E. of 3 experiments.
* Significantly different from control groups at P<0.01 in the Student's *t* test.

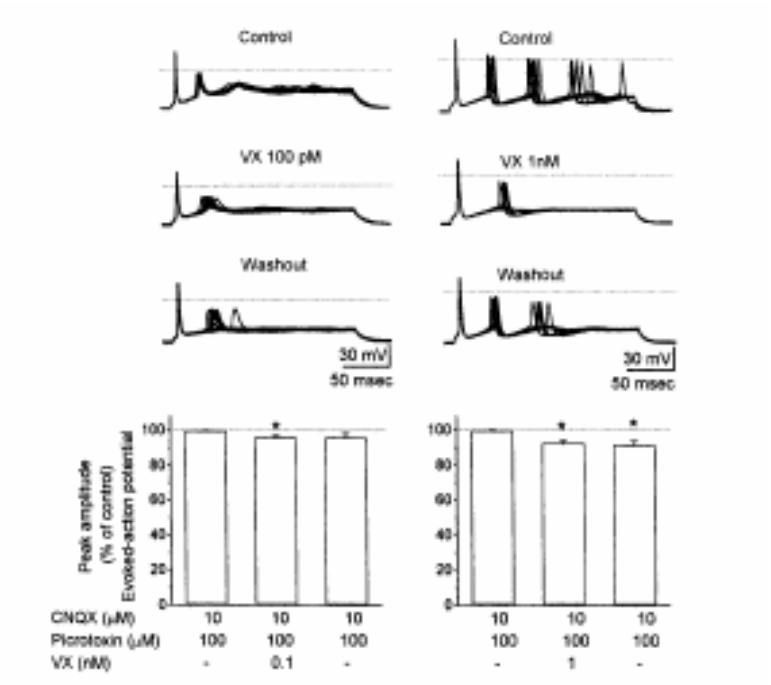

Figure 1.1.3. *VX reduces the rate of firing and the amplitude of action potentials recorded from hippocampal neurons in culture.* Top traces: Samples of action potentials recorded from each of two current-clamped hippocampal neurons before, during, and after their exposure to VX (0.1 or 1 nM). Action potentials were elicited every 3 sec by 50-100-pA depolarizing currents following 20-30-pA hyperpolarizing currents applied to the hippocampal neurons via the recording pipette. Membrane potentials were approximately –70 mV. Horizontal doted lines indicate 0 mV level. Recordings on the left were obtained from a neuron that fired action potentials phasically, whereas those in the right were obtained from a neuron that fired action potentials tonically. Notice that exposure of the neurons to VX reduced the rate of firing and the amplitude of the action potentials, and that the effects of this OP were only partially reversible upon washing of the neurons with VX-free external solution. All recordings were obtained in the presence of CNQX (10 μM) and picrotoxin (100 μM). Bottom graph: Quantification of the effects of VX (0.1-1 nM) on the peak amplitude of the evoked action potentials.
* Significantly different from control groups, P<0.05 in the Student's *t* test.

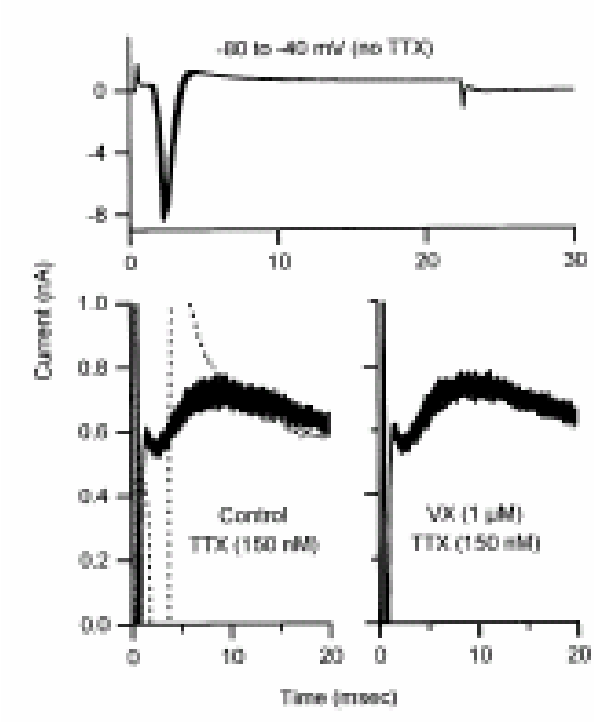

Figure 1.1.4. *VX does not affect voltage-gated K^+ currents recorded from hippocampal neurons.* Top traces: Samples of voltage-gated currents induced by the application of depolarizing voltage steps via the patch pipette to the hippocampal neurons in the absence of TTX. Bottom, left graph: Samples of voltage-gated K^+ currents recorded from the same neuron subjected to the same experimental protocol but in the presence of TTX. Dotted line represents the time course of averaged recordings obtained from the neuron in the absence of TTX. Notice that the fast current transient, corresponding to the activation of voltage-gated Na^+ channels was not detected in the presence of TTX. Bottom, right graph: 5-min perfusion of the neurons with external solution containing TTX and VX changed neither the kinetics nor the amplitude of the voltage-gated K^+ currents.

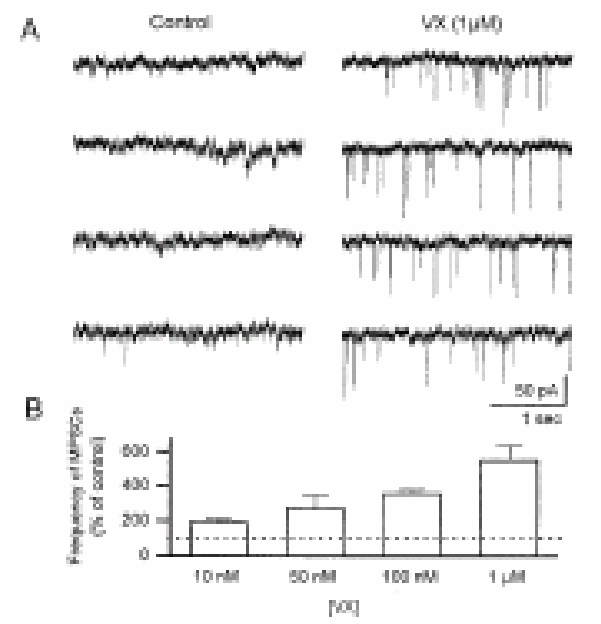

Figure 1.1.5. *VX increases the frequency of MPSCs recorded from hippocampal neurons.* Top traces: Samples of MPSCs recorded from a TTX-perfused hippocampal neuron before and during its exposure to VX (1 nM). The neuron was exposed to VX for 30 min. Membrane potential: –70 mV. Bottom graph: Quantification of the effect of various concentrations of VX (10 nM-1 μM) on the frequency of MPSCs. The frequency of MPSCs recorded prior to the exposure of the neurons to VX and calculated as the number of events recorded for 5 min divided by the recording time was taken as 100% and was used to normalize the frequency of MPSCs recorded after 30-min exposure of the neurons to the OP. Each VX concentration was tested in a neuron that had not been previously exposed to VX. Results are mean ± S.E. from 4 experiments.

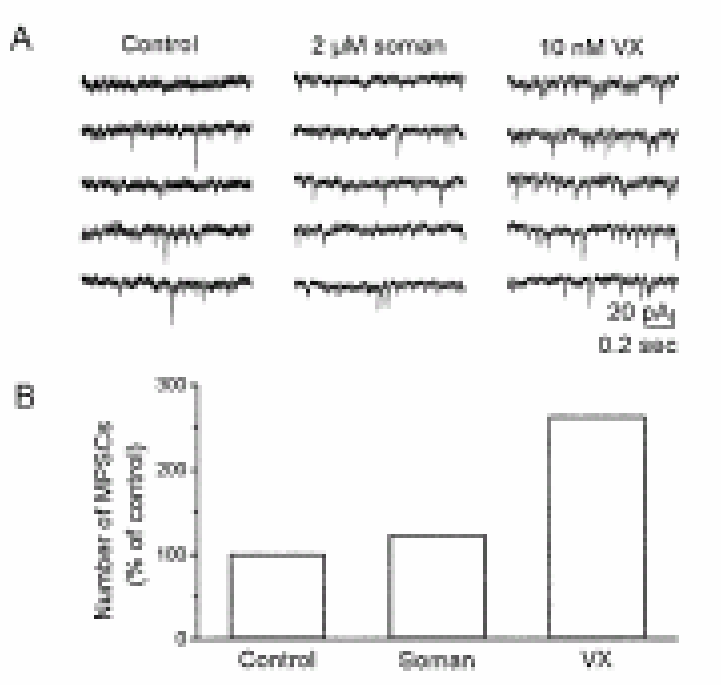

Figure 1.1.6. *VX does not affect the peak amplitude and decay-time constant of glutamatergic MPSCs.* Top graphs: Histograms of the distribution of the peak amplitude of MPSCs recorded from four different neurons continuously perfused with external solution containing TTX and picrotoxin (100 μM) before (solid lines) and after (dotted lines) their exposure to VX (1 nM). VX was applied to the neurons for 30 min. Bottom graphs: Histograms of the distribution of the decay-time constant of MPSCs recorded from four different neurons continuously perfused with external solution containing TTX and picrotoxin (100 μM) before (solid lines) and after (dotted lines) their exposure to VX (1 nM). All results were obtained from neurons that were held at –70 mV. Notice that the modes of the distributions of the peak amplitude and decay-time constant of the glutamatergic MPSCs were not altered by VX.

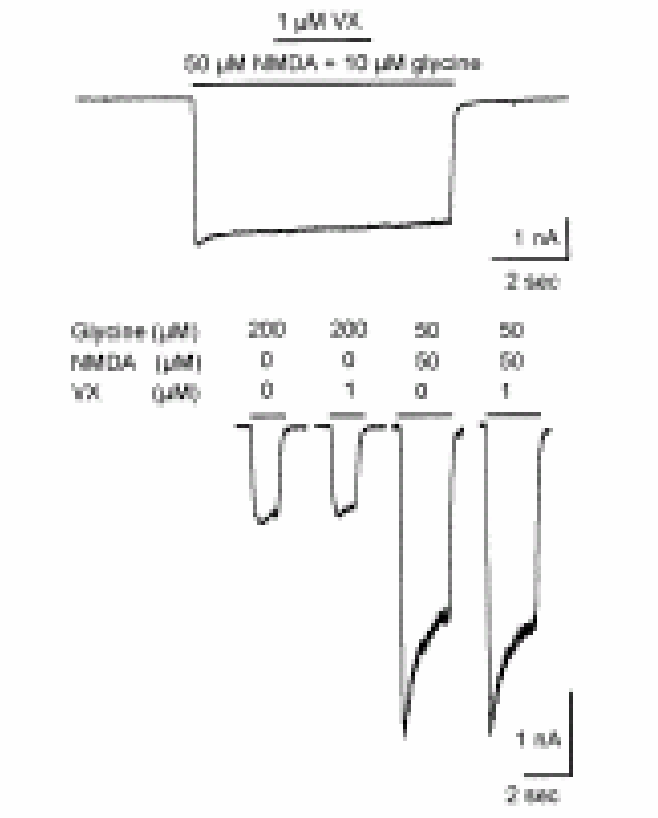

Figure 1.1.7. *VX causes significant increase in the frequency of MPSCs recorded from hippocampal neurons.* Top traces: Samples of MPSCs recorded from a TTX-perfused hippocampal neuron before and during its exposure to soman (2 μM) and VX (10 nM). Membrane potential, -70 mV. The neuron was exposed to soman for 10 min and to VX for 5 min. Bottom graph: Plot of the cumulative number of MPSCs under different experimental conditions. Note that exposure of the neuron to soman does not increase the number of MPSCs, whereas exposure to VX increases the number of MPSCs by approximately 4 times.

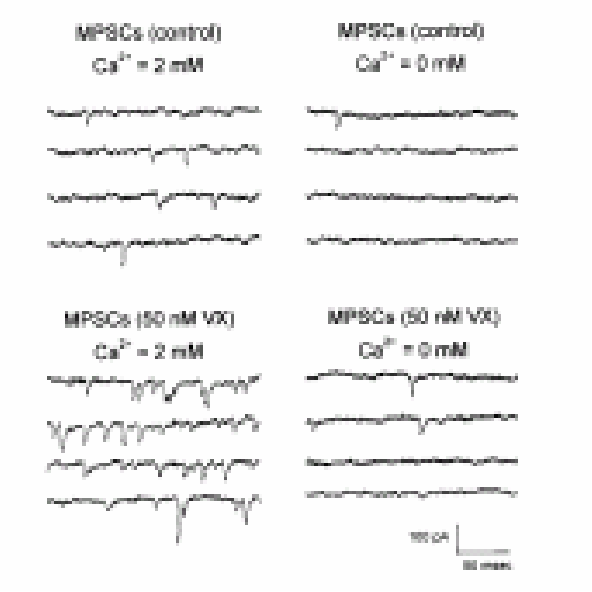

Figure 1.1.8. *VX does not alter the kinetics or amplitude of glycine- or NMDA-plus-glycine-evoked whole-cell currents in cultured hippocampal neurons.* Top trace: Recording sample of a whole-cell current evoked by the application of an admixture of NMDA (50 μM) and glycine (10 μM) to a hippocampal neuron. VX was applied to the neuron for 2 sec during the time when the NMDA receptors were activated. Bottom traces: Samples of whole-cell currents evoked by either glycine alone or the admixture of glycine-plus-NMDA before and following a 5-min exposure of a hippocampal neuron to VX (1 μM). Membrane potential, 70 mV. Similar results were obtained from 5 neurons.

1.2. The organophosphate sarin, at low concentrations, inhibits the evoked release of GABA in rat hippocampal slices

Introduction

Organophosphates (OPs) represent a class of compounds that includes insecticides, therapeutic agents, and a group of highly toxic compounds, the nerve gases (tabun, sarin, soman and VX; Taylor, 1996). These nerve agents, known as weapons of mass destruction, have been used in recent years in the Middle East (Sapolsky, 1998; Haley and Kurt 1997). The high toxicity of these compounds is primarily attributed to their ability to inhibit the enzyme acetylcholinesterase (AChE). However, several lines of evidence indicate that their life threatening effects are related to their direct interactions with targets other than AChE in the central nervous system (CNS) (Albuquerque *et al.*, 1994; Eldefrawi *et al.*, 1992; Idriss *et al.*, 1986; McDonough and Shih 1997; Raveh *et al.*, 1993; Rocha *et al.*, 1999). As a consequence, subjects who have been exposed to these nerve gases present a wide range of neurological dysfunctions (Albuquerque *et al.*, 1994).

One of the toxic signs following acute intoxication by OPs is the occurrence of convulsions (Lallement *et al.*, 1998). These convulsions may be precipitated by an imbalance between the excitatory and the inhibitory systems caused indirectly through the inhibition of AChE or by a direct action of the OPs on synaptic activity.

Recent data have shown that inhibitory GABAergic and excitatory glutamatergic transmission can be modulated by presynaptically located ligand-gated ion channels and metabotropic receptors (Alkondon *et al.*, 1999; Gray *et al.*, 1996). For example, nicotinic acetylcholine receptors (nAChRs) bearing the α7-subunit and muscarinic receptors, once stimulated, increase the spontaneous and decrease the evoked release of GABA from hippocampal neurons (Albuquerque *et al.*, 1998; Pitler and Alger, 1992). Furthermore, glutamatergic spontaneous transmission in the CNS is enhanced by the activation of nicotinic receptors sensitive to methyllycaconitine and α-bungarotoxin (Alkondon *et al.*, 1996; Gray *et al*, 1996; Marin *et al.*, 1997; Aramakis and Metherate, 1998). Data in the literature suggest that various OPs interact with the above mentioned receptors (Albuquerque *et al.*, 1985, 1987, 1988, 1994, Rocha *et al.*, 1996; Rao *et al.*, 1987).

The objective of this study was to investigate whether sarin affects excitatory and/or inhibitory transmission in the hippocampus, and, if so, by what mechanism. To this end, the whole-cell mode of the patch-clamp technique was applied to CA1 neurons in rat hippocampal slices to record GABAergic and glutamatergic postsynaptic currents (PSCs) that were either evoked by field stimulation of neurons synaptically connected to the neurons under study or tetrodotoxin (TTX)-insensitive GABAergic and glutamatergic PSCs. The results presented herein demonstrate that sarin, at concentrations lower than the IC_{50} for AChE inhibition (5 nM), selectively decreases the evoked release of GABA and that this effect, which is partially reversible upon washing of the neurons, is mediated by the interaction of the OP with presynaptic muscarinic receptors. These findings lay the groundwork for better understanding the neurotoxic effects of sarin, and may be relevant for the development of more efficacious treatments against sarin-induced acute intoxication.

Materials and Methods

Hippocampal slices. Slices of 250 μm thickness were obtained from the hippocampi of 22̣26 day-old Sprague-Dawley rats according to the procedure described earlier (Alkondon *et al.*,

1997). The slices were stored in a holding chamber containing artificial cerebrospinal fluid (ACSF) bubbled with 95% O_2 and 5% CO_2, and maintained at room temperature. Each slice, as needed, was transferred to a recording chamber (capacity of 2.0 ml) and held submerged by a nylon net. The recording chamber was continuously perfused with bubbled (95% O_2 and 5% CO_2) ACSF, which had the following composition (in mM): NaCl, 125; $NaHCO_3$, 25; KCl, 2.5; NaH_2PO_4, 1.25; $CaCl_2$, 2; $MgCl_2$, 1 and glucose, 25 (osmolarity, 340 mOsm).

Electrophysiological recordings. PSCs were recorded from neurons of the CA1 pyramidal layer of rat hippocampal slices. The signal was recorded by means of an LM-EPC-7 (List Electronic, Darmstadt, FRG), filtered at 3 kHz, and either stored on VCR tapes or directly sampled by a microcomputer using the PCLAMP6 software (Axon Instruments, Foster City, CA). Low resistance (2-4 MΩ) electrodes were pulled from borosilicate capillary glass (World Precision Instruments, New Haven, CT) and filled with internal solution containing (mM): CsCl, 80; CsF, 80; EGTA, 10; CsOH, 22.5; HEPES, 10 and QX-314, 5 (pH 7.3, adjusted with CsOH, osmolarity 340 mOsm). In all experiments the membrane potential was held in the range of 55 to 65 mV. The test solutions were applied to the slices through a set of coplanar-parallel glass tubes (400 µm i.d.) glued together and assembled on a Narishige micromanipulator. The tubes were placed at a distance of approximately 100 µm from the slice, and the gravity-driven flow rate was adjusted to 0.8 ml/min. Each tube was connected to a different reservoir filled with test solution. Evoked PSCs were recorded following application of a supra maximal, 20-40-µs electrical stimulus via a bipolar electrode made of thin platinum wires (50-100-µm diameter). The stimulus was delivered by an isolated stimulator unit (Digitimer Ltd., Garden City, England) connected to a digital-to-analog interface (TL-1 DMA, Axon Instrument, Inc., Foster City, CA). The platinum electrode was positioned at the Schaffer collateral fibers at approximately 200 µm away from the neuron under study in the CA1 pyramidal layer of the hippocampal slices. Possible changes in series resistance were detected by applying, online, a 3-mV-peak-amplitude hyperpolarizing pulse before the stimulus pulse. Miniature postsynaptic currents (MPSCs) were recorded from neurons in the CA1 pyramidal layer of hippocampal slices that were continuously perfused with TTX (300 nM)-containing ACSF. Excitatory or inhibitory evoked PSCs and MPSCs were identified pharmacologically by the application of antagonists of the excitatory α-amino-3-hydroxy-5-methyl-4-isoxazolepropionic acid (AMPA) and *N*-methyl-D-aspartate (NMDA) receptors, 6-cyano-7-nitroquinoxaline-2,3-dione (CNQX, 20 µM) and 2-amino-5-phosphono-valeric acid (APV, 50 µM), respectively, or the antagonist of the inhibitory $GABA_A$ receptor, picrotoxin (100 µM). In some experiments, atropine (1 µM) was used to block muscarinic receptors.

Data analysis. Peak amplitude, 10-90% rise time, and decay-time constant for evoked PSCs were determined using the pClamp6 software. MPSCs were analyzed for peak amplitude, decay-time constant and frequency by the programs CDR and SCAN (Dempster, 1989). Results are presented as mean ± S.E. and compared for their statistical significance using the unpaired Student's t test. The level of statistical significance employed in all cases was between $p < 0.05$ and $p < 0.01$.

Drugs and biological hazards. Sarin (Isopropyl methylphosphonofluoridate) and soman (1,2,2-Trimethylpropyl methylphosphonofloridate) were obtained from the U.S. Army Medical Research and Development Command (USAMRDC). MLA citrate was a gift from Prof. M. H. Benn (Department of Chemistry, University of Calgary, Alberta, Canada). DHβE hydrobromide was a gift from Merck, Sharp & Dohme (Rahway, NJ). All other chemicals were purchased from Sigma Chemical Co., St. Louis, MO. A 250 mM stock solution of picrotoxin was made in dimethylsulfoxide, and dilutions were made in the ACSF. NaOH was used to dissolve CNQX (the 10 mM stock of CNQX had 12.2 mM of NaOH).

Safe handling of OPs was assured according to USAMRDC's recommendations. The compounds were stored at 80°C and diluted daily in an OP vapor-proof hood. All OP- or TTX-containing solutions were inactivated with 5% sodium hypochloride. Latex gloves and proper goggles were used throughout the day of the experiment.

Results

Sarin does not affect the TTX-insensitive release of glutamate and GABA in the CA1 field of hippocampal slices.

Perfusion of hippocampal slices with TTX (300 nM)-containing ACSF resulted in blockade of high-amplitude spontaneous PSCs (Fig. 1.2.1). In the presence of TTX, two populations of MPSCs were recorded: one population consisted of currents that had a slow decay-time constant (32.8 ± 8.2 ms) and that were sensitive to blockade by the $GABA_A$ receptor antagonist picrotoxin (100 μM). The other consisted of fast-decaying currents (decay-time constant = 15.75 ± 1.49 ms) that were sensitive to the glutamate receptor antagonists CNQX (20 μM) and APV (50 μM).

Perfusion of hippocampal slices with ACSF containing TTX (300 nM) and sarin (1 nM) did not alter the peak amplitude or the decay-time constant of glutamate- (data not shown) or GABA- (Fig. 1.2.1) mediated MPSCs recorded from neurons in the CA1 pyramidal layer. Because sarin had no effect on the amplitude or the decay-time constant of the MPSCs, it was possible to estimate the MPSC frequency by the area under the curve, which represents the total amount of charge that crosses from one side to the other side of the membrane. To measure the area under the curve, MPSCs were studied in records obtained under control conditions and after 5 min (for stabilization of MPSC frequency) of sarin treatment. The area was calculated over a period of two-mins recording time, and the values expressed as percentage of control. Bath perfusion of the hippocampal slices for 25 min with sarin (1 nM)-containing ACSF did not affect the frequency of either glutamatergic (data not shown) or GABAergic MPSCs (Fig. 1.2.1). These findings indicate that at the concentration tested sarin did not interfere with the TTX-insensitive release of neurotransmitters or with the activity of $GABA_A$ and glutamate receptors.

Sarin selectively reduces the action potential-dependent release of GABA in the CA1 field of hippocampal slices.

Application via a bipolar platinum electrode of supra-maximal stimuli to the Schaffer collateral pathway of the *stratum radiatum* of the CA1 hippocampal field always resulted in activation of PSCs consequent to the evoked release of GABA or glutamate. In each experiment, evoked PSCs had variable amplitudes but did not show any rundown throughout the recording time under control conditions. Inhibitory postsynaptic current (IPSCs) mediated by the evoked release of GABA and excitatory postsynaptic currents (EPSCs) mediated by evoked release of glutamate were pharmacologically and kinetically isolated. Evoked EPSCs were recorded from CA1 neurons perfused with the $GABA_A$-receptor antagonist picrotoxin (100 μM), and evoked IPSCs were recorded from neurons perfused with the AMPA- and NMDA-receptor antagonists CNQX (20 μM) and APV (50 μM), respectively. These currents could also be identified according to their kinetics: (a) the decay-time constant of EPSCs and IPSCs were 7.8±2.3 and 22.3±3.7 ms, respectively, and (b) the zero-current potential for EPSCs and IPSCs were approximately 0 and 20 mV, respectively.

In the presence of CNQX and APV, perfusion of the slices with ACSF containing sarin (100 pM-100 nM) reduced the amplitude of the evoked IPSCs recorded from neurons in the

pyramidal layer of the CA1 field of the hippocampal slices (Fig. 1.2.2). This effect of sarin, which was concentration dependent, was observed 34 min after exposure of the slices to the OP. Saturation of the effect of sarin on the amplitude of IPSCs was observed at 1 nM. In the presence of sarin (1 nM), the amplitude of evoked IPSCs was 57.14 ± 5.12 % of the amplitude of IPSCs recorded under control condition. This effect of sarin was partially reversed upon a 10-min perfusion of the hippocampal slices with sarin-free ACSF (see Fig. 1.2.2), whereas the effect of higher concentrations of the OP on the IPSC peak amplitude could not be reversed even after a 20-min perfusion of the slices with sarin-free ACSF. Although the amplitude of IPSCs was significantly reduced by sarin, the amplitude of EPSCs was not affected by even higher concentrations of the OP. In the presence of picrotoxin, perfusion of the slices with ACSF containing sarin (150 nM) had no effect on the EPSC amplitude recorded from neurons in the pyramidal layer of the CA1 field of the hippocampal slices (Fig. 1.2.3).

At 1nM, sarin had no effect on the rise time or decay-time constant of the IPSCs (Fig. 1.2.4A). These results and the findings that sarin is unable to affect the kinetics or the amplitude of the IPSCs supports the concept that sarin-induced reduction of the evoked IPSC amplitude is due to the reduction by the OP of the evoked release of GABA. Sarin (50 nM) also failed to affect the rise time or decay-time constant of the evoked EPSCs (Fig. 1.2.4B).

Atropine prevents but does not reverse sarin-induced reduction of evoked release of GABA.

In an attempt to elucidate the mechanisms underlying the effect of sarin on IPSCs, we considered that nAChRs and muscarinic receptors are known to modulate the evoked release of GABA in hippocampal neurons and that OPs can directly or indirectly affect both receptors.

In the presence of CNQX, perfusion of the hippocampal slices with atropine (100 nM-3 μM) resulted in a concentration-dependent reduction of the amplitude of the evoked IPSCs (Fig. 1.2.5), indicating that there is a basal control of GABA release by the muscarinic receptors in the pyramidal layer of the CA1 region of the hippocampus. The reduction by atropine of the amplitude of evoked IPSCs saturated at 1 μM. Of interest, in the range of 1 to 10 nM, atropine caused a small, yet significant enhancement of the amplitude of the evoked IPSCs (Fig. 1.2.5).

In the continuous presence of a saturating blocking concentration of atropine (1 μM), exposure of the hippocampal neurons to a saturating concentration of sarin (1 nM) caused no additional reduction of IPSC amplitude (Fig. 1.2.6A). Likewise, after perfusing the neurons with sarin (1 nM)-containing ACSF, exposure of the neurons to ACSF containing an admixture of atropine (1 μM) and sarin (1 nM) did not result in any further reduction of the evoked IPSC amplitude (Fig. 1.2.6B).

Perfusion of the neurons with an external solution containing methyllycaconitine (MLA, 50 nM), mecamylamine (1 μM) and dihydro-β-erythroidine (DHβE, 10 μM), antagonists of the nAChRs in hippocampal neurons, i.e. the α7, α3β4 and α4β2 nAChRs, respectively, (Alkondon and Albuquerque, 1993) did not affect the action of sarin on the amplitude of the evoked IPSCs (Fig. 1.2.7).

Sarin-induced reduction of evoked IPSCs is unrelated to cholinesterase inhibition.

If cholinesterase inhibition were responsible for the effect of sarin on GABA-mediated evoked postsynaptic currents, a pre-exposure of hippocampal neurons to another cholinesterase inhibitor would not result in any additional reduction of the evoked IPSCs.

After a 15-min perfusion of hippocampal slices with ACSF containing soman at a concentration sufficient to block the activity of the enzyme AChE (2 μM), there was a 42% reduction of the amplitude of evoked IPSCs (Fig. 1.2.8). However, following the complete blockade of the enzyme by soman, sarin (1 nM) still caused an additional reduction of the amplitude of evoked IPSCs . As shown in figure 1.2.8, the additional blockade induced by sarin is no larger than 20%. As discussed below, not only do these findings indicate that a significant part of the effect of sarin on the amplitude of evoked IPSCs is independent of the blockade of AChE, but they also suggest that soman and sarin affect the evoked release of GABA via different mechanisms.

Discussion

The data presented in this study demonstrate that sarin, at picomolar concentrations, selectively reduces the action potential-dependent release of GABA in the rat hippocampus, and that this effect is, due, in part to a direct interaction of the OP with muscarinic receptors present on GABAergic neurons. In the same range of concentrations, sarin does not interfere with the glutamatergic neurotransmission in the hippocampus, and even at nanomolar concentrations, sarin is unable to affect the action potential-independent release of GABA or glutamate. The selective blockade by sarin of the action potential-dependent GABAergic transmission sheds new light on understanding the pathophysiology of the intoxication induced by this OP.

A direct interaction of sarin with presynaptic muscarinic receptors contributes to the OP-induced reduction of evoked GABA release from neurons in hippocampal slices.

Modulation by muscarinic receptors of GABA-mediated inhibitory neurotransmission in the mammalian CNS has been reported in numerous studies (Pitler and Alger, 1992; Morton and Davies, 1997; Sanz *et al.*, 1997; Kimura and Baughman, 1997). However, the mechanism by which this modulation occurs is uncertain (Rouse *et al.*, 1997). A study carried out in hippocampal slices demonstrated that the muscarinic antagonist atropine reduces Cl currents carried by $GABA_A$ receptors (Siebler *et al.*, 1988). Other studies have shown that activation of muscarinic receptors has a similar effect on the amplitude of evoked IPSCs (Pitler and Alger, 1992; Behrends and Bruggencate, 1993). It seems that modulation by muscarinic receptors of GABAergic transmission is rather complex, because yet another study (Figenschou *et al.*, 1996) reported that different concentrations of the muscarinic agonist carbachol have opposite actions on evoked action potentials recorded from CA1 pyramidal neurons in rat hippocampal slices. In the present study, experiments carried out with atropine supported this contention, given that atropine had a dual effect on the evoked release of GABA: at low concentrations (1-10 nM) it increased, whereas at high concentrations (100 nM-3 μM) it decreased the release of GABA. Of interest is the observation that the blocking effect of a saturating concentration of atropine on the evoked IPSCs did not add to that of a saturating concentration of sarin, indicating that the effect of sarin on the evoked release of GABA involved an interaction of the OP with presynaptic muscarinic receptors. There is evidence in the literature supporting the idea that OPs can bind with high affinity to a specific subtype of the neuronal muscarinic receptors, the m2 receptors, probably acting as antagonists (Bakry *et al.*, 1988; Eldefrawi *et al.*, 1992).

It is widely known that OPs can act as open channel blockers of the nicotinic receptors in muscle (Albuquerque *et al.*, 1988; Thesleff *et al.*, 1990) and that nicotinic receptors are involved in modulation of the evoked GABA release (Alkondon *et al.*, 1997, 1999; Braga *et al.*, 1999). However, experiments carried out in the presence of the nicotinic blockers showed that the effect of sarin on evoked GABA release does not involve the neuronal nAChRs present in

hippocampal neurons.

Taking into consideration the data in this report, it is reasonable to consider that sarin acts as a muscarinic receptor antagonist inhibiting the evoked release of GABA. A similar effect of OPs on the muscarinic modulation of evoked GABA release was previously reported for the nerve agent VX in cultured hippocampal neurons (Rocha *et al.*, 1999).

Sarin-induced decrease of action potential-dependent release of GABA is not fully accounted for by cholinesterase inhibition.

The finding that even when the cholinesterase enzyme was completely blocked, by pretreatment with 2 μM soman, sarin still caused a reduction in the evoked IPSCs provides strong evidence that sarin has an effect on the action potential-dependent release of GABA that is independent of the blockade of AChE.

The notion that OPs can act at sites other than the cholinesterase enzyme is not recent. Studies have shown that OPs can interact with a variety of different targets inside and outside the CNS (Sivam *et al.*, 1984; Okumura *et al.*, 1996; Karczmar, 1984). At the neuromuscular junction, OPs have been shown to interact directly with cholinergic and glutamatergic terminals (Albuquerque *et al.*, 1985; Rao *et al.*, 1987; Idriss *et al.*, 1986). In the CNS a recent study carried out in cultured hippocampal neurons demonstrated that VX alters spontaneous and evoked transmitter release by interacting with specific presynaptic sites (Rocha *et al.*, 1999). Furthermore, binding studies have shown that OPs can interact directly with muscarinic and nicotinic receptors in the periphery and in the central nervous system (Bakry *et al.*, 1988; Silveira *et al.*, 1990).

Our finding that sarin inhibits the evoked GABA release by a mechanism independent of the cholinesterase inhibition is strengthened by the fact that the concentrations at which sarin blocked the evoked release of GABA were much lower, ranging from 300 pM to 1 nM, than the IC_{50} for sarin (5 nM) in inhibiting AChE activity in the rat hippocampus (Sawyer *et al.*, 1991). Also, if the increase of ACh resulting from blockade of AChE was responsible for the reduction of the IPSCs, the use of antagonists of the neuronal nicotinic receptors should have promoted an additional reduction of the evoked IPSCs (Alkondon *et al.*, 1997; Braga *et al.*, 1999). In conclusion, our data suggest that the effect of sarin-induced reduction of evoked GABA release cannot be accounted for by AChE inhibition and subsequent increase in ACh at the synaptic gap.

Toxicological relevance of sarin-induced reduction of evoked GABA release in the hippocampus.

Seizures and convulsions are the prevalent toxic signs following intoxication with nerve agents. These seizures, if not rapidly reverted, can progress to status epilepticus and contribute to serious brain damage (Kadar *et al.*, 1994; Suzuki *et al.*, 1997). Initially, the seizures were considered to be a consequence of the high concentrations of ACh following blockade of AChE; however, a previous study demonstrated that the OP VX can interfere with neuronal synaptic transmission in different ways, not only causing an imbalance between the action potential-dependent excitatory and inhibitory synaptic transmissions, but also increasing the action potential-independent transmitter release (Rocha *et al.*, 1999) via a mechanism unrelated to the cholinesterase inhibition. In contrast, sarin, at low concentrations, has a more specific effect in the mammalian hippocampus, affecting only the action potential-dependent inhibitory synaptic transmission. A selective blockade by sarin of GABAergic transmission, particularly in the hippocampus, could conceivably contribute to the convulsions caused by the

OP, and, that being the case, compounds that are able to enhance the inhibitory GABAergic transmission in the CNS might be considered as possible countermeasures.

Currently, the management of OP intoxication includes the use of oximes (Brightman *et al.*, 1995), benzodiazepines and the muscarinic antagonist atropine. It is interesting to note that, atropine poorly crosses the blood-brain-barrier, and very low concentrations of this drug are likely to be achieved in the CNS following the regular doses used to prevent and/or treat OP-induced intoxication. Thus, our finding that, at very low concentrations (1-10 nM), atropine increases the GABAergic neurotransmission in the hippocampus, indicates that atropine may be beneficial to prevent and/or reverse the convulsions induced by sarin.

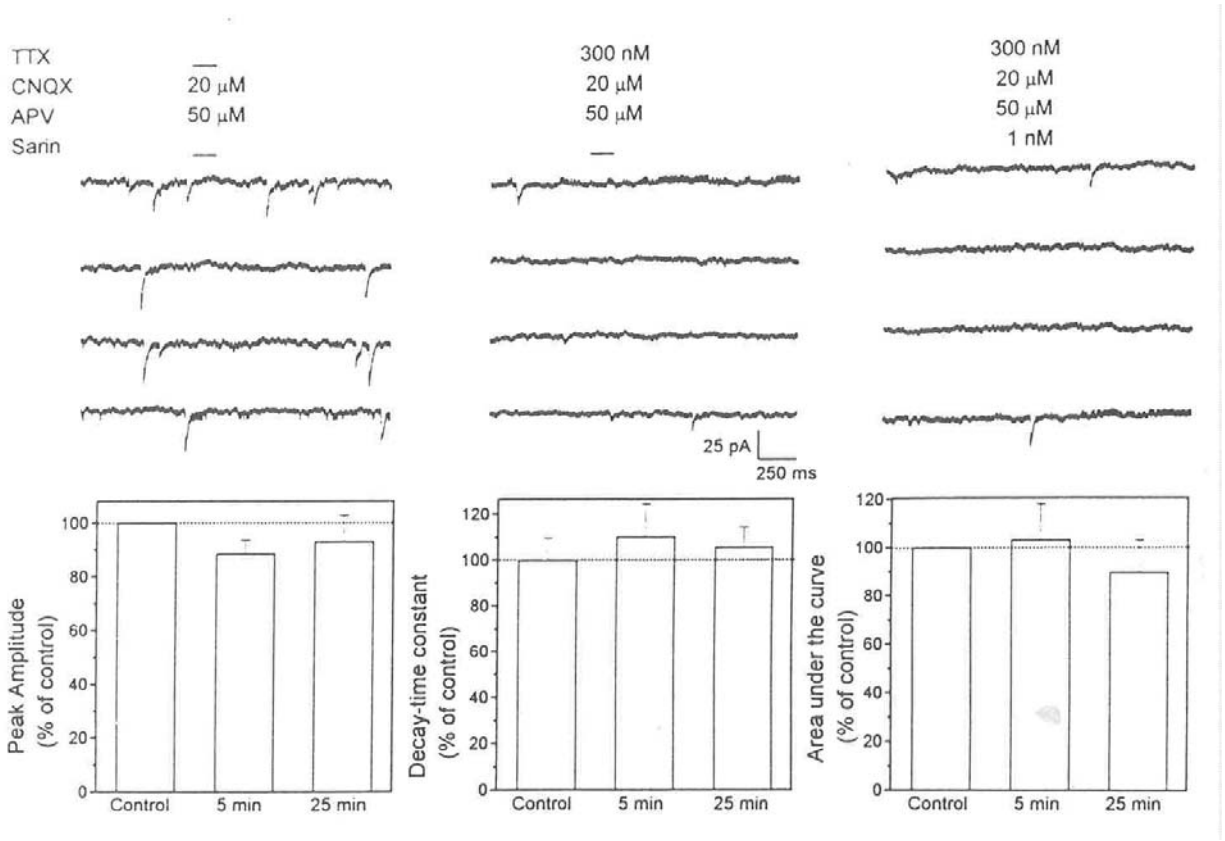

Figure 1.2.1. *Sarin does not induce changes in MPSCs in neurons from hippocampal slices.* Top: Samples of MPSCs recorded from neurons of the pyramidal layer of the CA1 area of hippocampal slices continuously perfused with CNQX (20 μM) and APV (50 μM), in the absence (left panel) and presence (center) of TTX (300 nM), and after adding sarin (1 nM) to the TTX-containing ACSF (right panel). Note that perfusion with TTX abolished the large amplitude postsynaptic currents. Graphs: Quantitative analysis of the effect of sarin on the amplitude, decay-time constant and area under the curve of the MPSCs recorded from neurons of the pyramidal layer of the CA1 area. All data were analyzed at 5 and 25 min of exposure to sarin. Results are mean ± S.E. of 5 experiments. Holding potential: 60 mV.

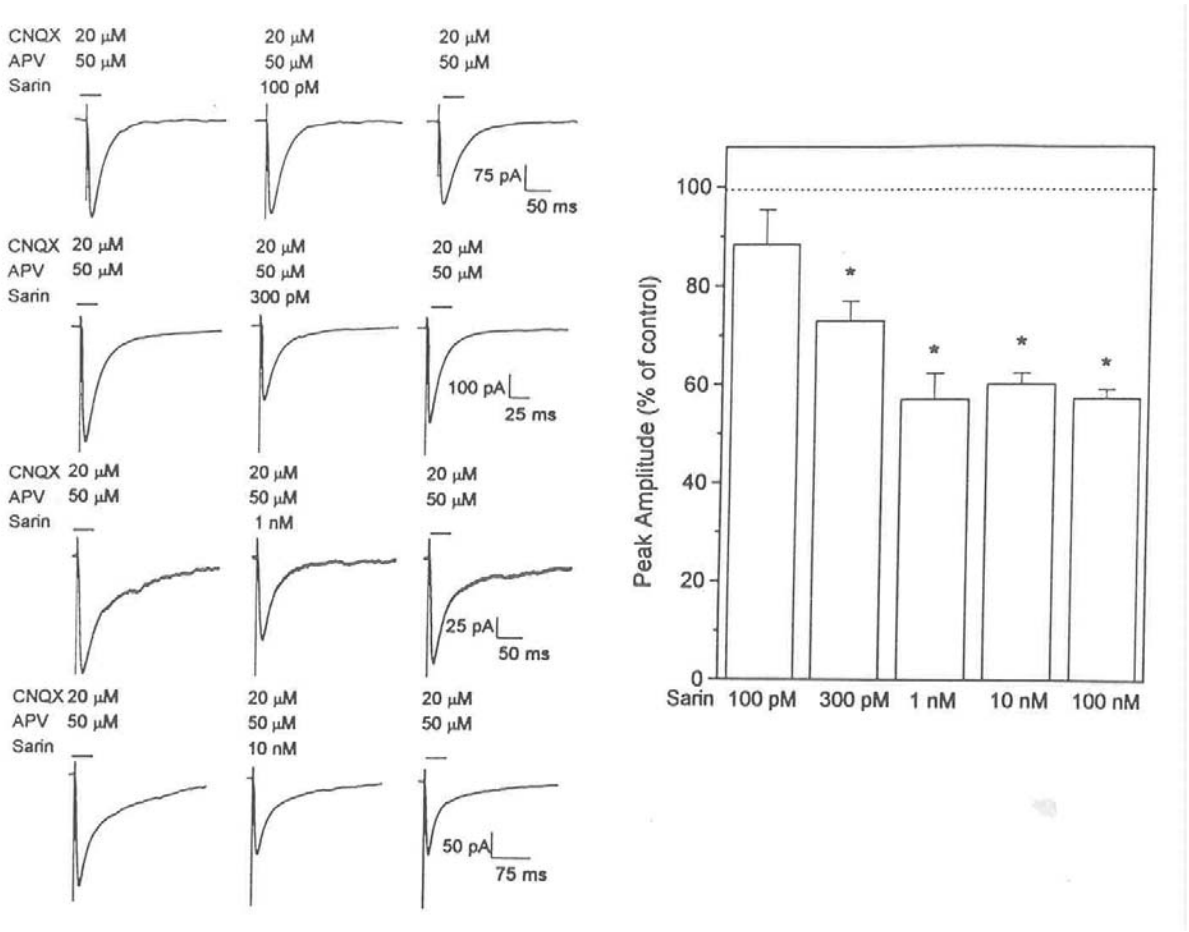

Figure 1.2.2. *Sarin at different concentrations decreases the amplitude of evoked IPSCs recorded from neurons of hippocampal slices.* Traces on the left are samples of evoked IPSCs recorded from neurons of the pyramidal layer of the CA1 area of hippocampal slices continuously perfused with CNQX (20 µM) and APV (50 µM)-containing ACSF prior to and during exposure of the neurons to sarin (100 pM-10 nM), followed by the wash out of sarin. The traces are averages of 50 currents. The graph on the right shows the concentration-response relationship for sarin-induced blockade of IPSCs peak amplitude. The amplitude of the IPSCs recorded under control condition was taken as 100% and used to normalize the amplitude of IPSCs recorded in presence of sarin. Each concentration was tested on a neuron that had not been previously exposed to sarin. Results are mean ± S.E. of 5 experiments. Asterisk indicates difference from control condition with p values < 0.01 according to t-test. Holding potential: -60 mV.

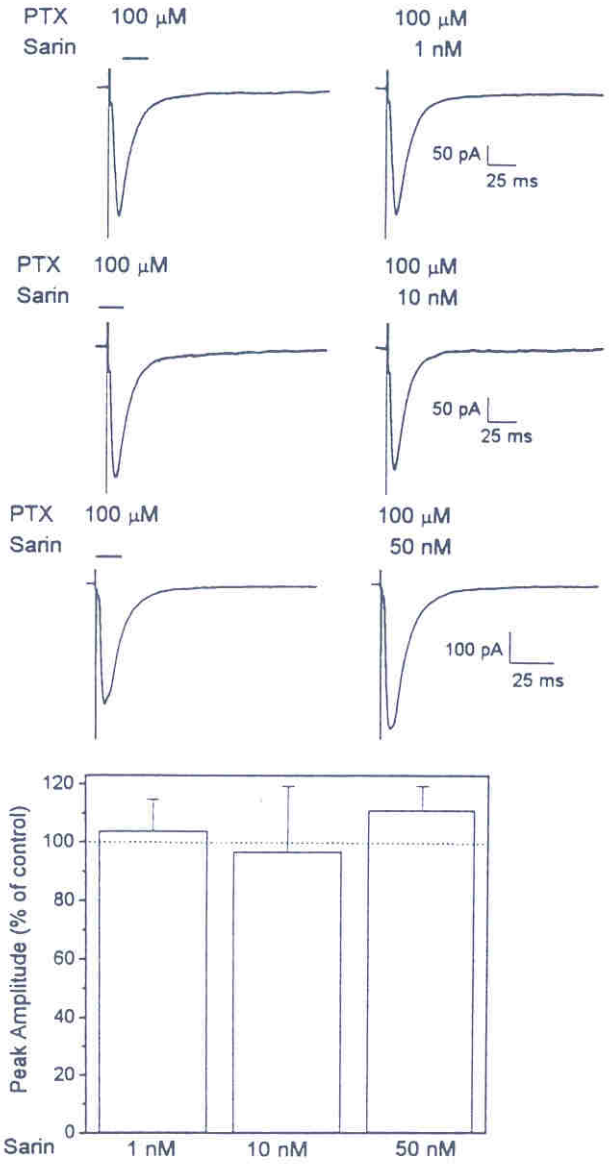

Figure 1.2.3. *Sarin does not affect the amplitude of evoked EPSCs recorded from neurons of hippocampal slices.* Samples of evoked EPSCs recorded from neurons of the pyramidal layer of the CA1 area of the hippocampus in the presence of picrotoxin (100 μM), prior to and during exposure to sarin (1-50 nM). Traces are average of 50 currents. The graph shows the concentration-response relationship for sarin-induced blockade of EPSC peak amplitude. The amplitude of the EPSCs recorded under control condition was taken as 100% and used to normalize the amplitude of EPSCs recorded in the presence of sarin. Each concentration was tested on a neuron that had not been previously exposed to sarin. Results are mean ± S.E. of 5 experiments. Holding potential: -60 mV.

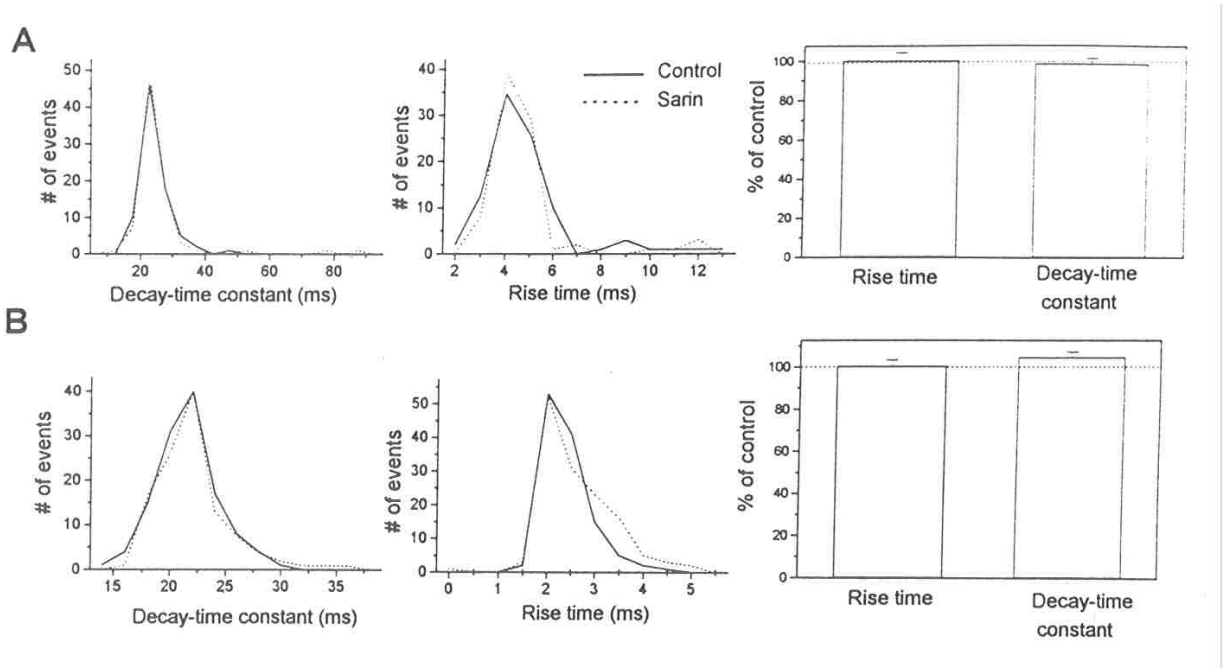

Figure 1.2.4. *Sarin does not affect the rise time or the decay-time constant of the evoked postsynaptic currents from neurons of hippocampus slices.* A: Left: Distributions of the rise times and decay-time constants of the evoked IPSCs of a neuron from the CA1 pyramidal layer of a hippocampal slice perfused with CNQX (20 μM) and APV (50 μM) before (solid lines) and during (dotted lines) exposure to sarin (1 nM). Right: Quantitative analysis of the rise times and decay-time constants of IPSCs recorded prior to and during exposure to sarin. The rise times and the decay-time constants of evoked IPSCs recorded under control condition were taken as 100% and used to normalize the rise time and the decay-time constant of the IPSCs recorded in the presence of sarin. B: Left: Distribution of rise times and decay-time constants of the evoked EPSCs recorded from a neuron of the pyramidal layer of the CA1 area of a hippocampal slice continuously perfused with picrotoxin (100 μM) prior to (solid lines) and during (dotted lines) exposure to sarin (50 nM). Right: Quantitative analysis of the rise times and decay-time constants of the EPSCs recorded prior and during exposure to sarin. The rise times and the decay-time constants of evoked EPSCs recorded under control conditions were taken as 100% and used to normalize the rise times and the decay-time constants of the EPSCs recorded in presence of sarin. The results are mean ± S.E. of 5 experiments. Holding potential: -60 mV.

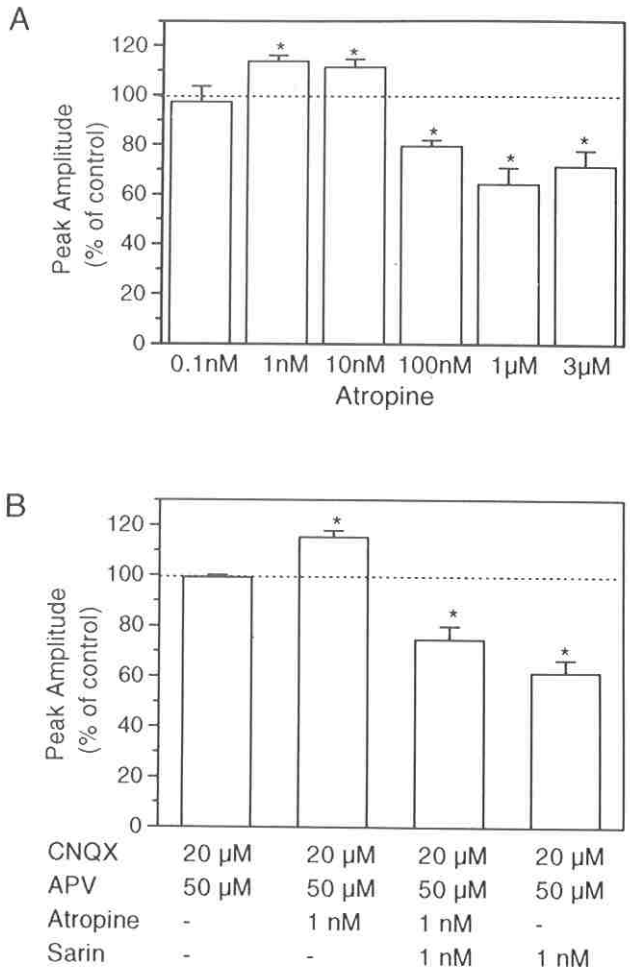

Figure 1.2.5. *Atropine has dual effects on evoked IPSCs.* A: Atropine (100 nM–3 μM) reduced the peak amplitude of IPSCs recorded from hippocampal neurons. However, atropine (1-10 nM) produced an increase in the amplitude of GABA-mediated evoked current. The amplitudes of IPSCs recorded in the absence of atropine were taken as 100% and used to normalize the peak amplitude of IPSCs recorded in presence of atropine. Each concentration was tested on a slice that had not been previously exposed to atropine. B: Plot of the peak amplitude of evoked IPSCs recorded in the presence of atropine (1 nM) and sarin (1 nM). The amplitude of the IPSCs recorded prior to exposure of the slice to atropine and sarin was taken as 100 % and was used to normalize the peak amplitude of the IPSCs recorded during and after perfusion of the slice with atropine and/or sarin-containing external solution Results are mean ± S.E. of 5 experiments for A and 3 experiments for B. Asterisk indicates difference from control condition with p values < 0.01 according to t-test for A and we used one-way ANOVA followed by Dunnett's test for B ($p < 0.05$). Holding potential: 60 mV.

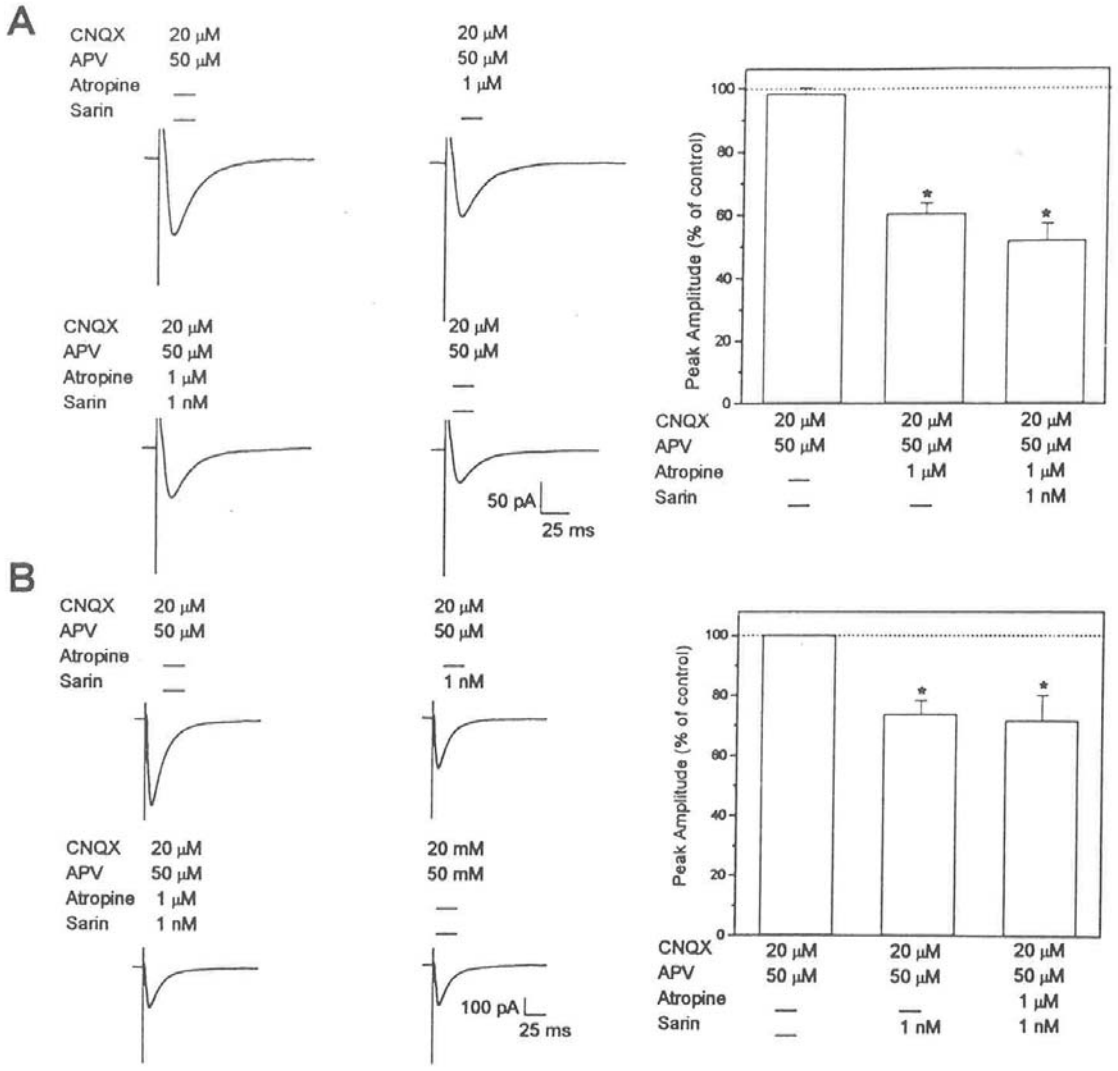

Figure 1.2.6. *Sarin-induced reduction of the amplitude of IPSCs is prevented but not reversed by the muscarinic receptor antagonist atropine recorded from neurons of hippocampus slices.* A: Left: Samples of evoked IPSCs recorded from neurons of the pyramidal layer of the CA1 area of hippocampal slices continuously perfused with CNQX (20 μM) and APV (50 μM) in the presence of atropine (1 μM) and sarin (1 nM). Traces are averages of 50 currents. Right: Quantitative analysis of the effect of sarin on the amplitude of evoked IPSCs in the presence of atropine (1 μM). The amplitude of the evoked IPSCs recorded prior to the exposure of the neurons to atropine or sarin was taken as 100% and used to normalize the peak amplitude of the IPSCs recorded under each experimental condition. B: Left: Samples of IPSCs recorded from neurons of the pyramidal layer of CA1 area of hippocampus slices continuously perfused with CNQX (20 μM) and APV (50 μM) in the presence of sarin (1 nM) prior to and after exposure of the slices to atropine (1 μM). Traces are averages of 50 currents. Right: Quantitative analysis of the effect of atropine (1 μM) on the amplitude of evoked IPSCs recorded in the presence of sarin (1 nM). The amplitude of the evoked IPSCs recorded prior to the exposure of the neurons to atropine or sarin was taken as 100% and used to normalize the peak amplitude of the IPSCs recorded under each experimental condition. Results are mean ± S.E. of 5 experiments. Asterisk indicates the difference from control condition (CNQX-, APV-containing ACSF) with p values < 0.01. Holding potential: -60 mV.

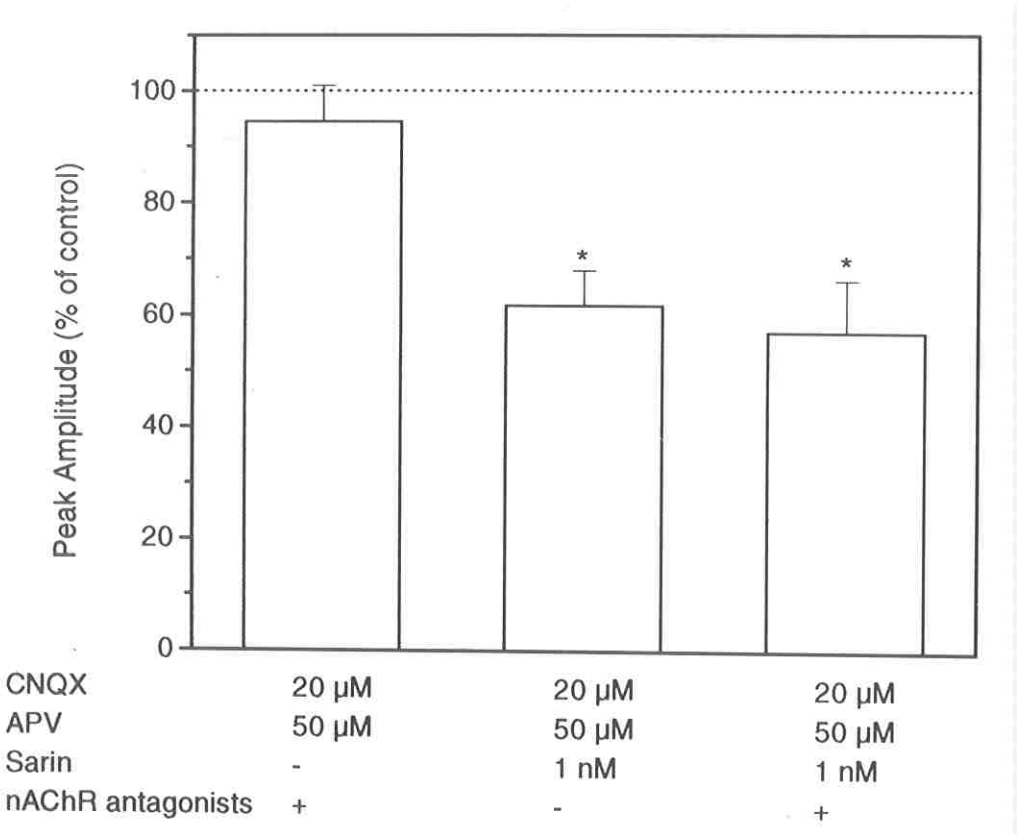

Figure 1.2.7. *Nicotinic receptor antagonists do not interfere with sarin-induced inhibition of IPSCs*. Quantitative analysis of the effect of sarin on IPSCs from neurons of the pyramidal layer of CA1 area of hippocampus slices that were continuously perfused with CNQX (20 μM) and APV (50 μM), in the presence and absence of nicotinic receptor blockers MLA (50 nM), DHβE (10 μM), and mecamylamine (1 μM). The amplitude of the evoked IPSCs recorded prior to the exposure of the neurons to sarin was taken as 100% and used to normalize the peak amplitude of the IPSCs recorded in presence of sarin. Results are mean ± S.E. of 5 experiments. Holding potential: -60 mV.

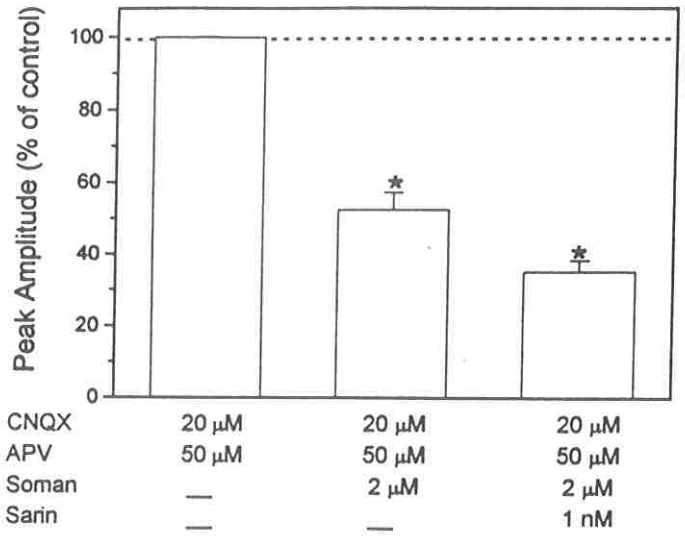

Figure 1.2.8. *Prior inhibition of acetylcholinesterase with soman does not interfere with the inhibitory effect of sarin on evoked IPSCs.* Quantitative analysis of the effect of sarin on IPSCs from neurons of the pyramidal layer of CA1 area of the hippocampus slices that were continuously perfused with CNQX (20 μM) and APV (50 μM), in presence of soman (2 μM). The amplitude of the evoked IPSCs recorded prior to the exposure of the neurons to soman and sarin was taken as 100% and used to normalize the peak amplitude of the IPSCs recorded under each experimental condition. Asterisk indicates the difference from control condition (CNQX-, APV-containing ACSF) with p values < 0.02. Results are mean ± S.E. of 4 experiments. Holding potential: - 60 mV.

Section 2. Antagonism of by pyridostigmine of the effects of nerve agents on neurotransmitter release

2.1. Low concentrations of pyridostigmine prevent soman-induced inhibition of GABAergic transmission in the central nervous system: involvement of muscarinic receptors

Introduction

We have shown (Santos *et al.*, 2003) that soman selectively reduces GABAergic transmission in the hippocampus, and that pyridostigmine, when pre-applied, could prevent the OP's effects. Here we report our detailed analysis of pyridostigmine's ability to block soman-induced reduction in GABAergic transmission, and the analysis of the underlying mechanism.

Materials and methods

Rat hippocampal slices. Hippocampal slices of 250-μm thickness were obtained from 15–25-day-old Sprague-Dawley rats according to the procedure described earlier (Alkondon *et al.*, 1999). The slices were kept in a holding chamber containing artificial cerebrospinal fluid (ACSF) bubbled with 95% O_2 and 5% CO_2, at room temperature. Each slice, as needed, was transferred to a recording chamber (capacity of 2 ml) and held submerged by two nylon fibers. The recording chamber was continuously perfused with bubbled ACSF, which had the following composition (in mM): NaCl, 125; $NaHCO_3$, 25; KCl, 2.5; NaH_2PO_4, 1.25; $CaCl_2$, 2; $MgCl_2$, 1 and glucose, 25 (osmolarity ~340 mOsM).

Electrophysiological recordings. By means of the whole-cell mode of the patch-clamp technique, spontaneous or field stimulation-evoked postsynaptic currents (PSCs) were recorded from neurons of the CA1 pyramidal layer of rat hippocampal slices. Test solutions were applied to the slices through a set of coplanar-parallel glass tubes (400 μm i.d.) glued together and assembled on a motor driven system (Newport Corporation, Irvine, CA) controlled by microcomputer. The tubes were placed at a distance of approximately 100–150 μm from the slice, and the gravity-driven flow rate was adjusted to 1.0 ml/min. Each tube was connected to a different reservoir filled with test solution. Evoked PSCs were recorded following application of a supramaximal 20–60-μs electrical stimulus to afferent fibers via a bipolar electrode made of thin platinum wires (50–100-μm diameter). The stimulus was delivered by an isolated stimulator unit (Digitimer Ltd., Garden City, England) connected to a digital-to-analog interface (TL-1 DMA, Axon Instrument Inc., Foster City, CA). The platinum electrode was positioned at the Schaffer collaterals. Possible changes in series resistance were detected by applying, online, a 5-mV hyperpolarizing pulse before the test pulse.

Electrophysiological signals were recorded by means of an Axopatch 200A (Axon Instruments, Inc. CA) filtered at 2 kHz, and either stored on VCR tapes or directly sampled by a microcomputer using the pClamp6 software (Axon Instruments, Foster City, CA). Low-resistance (2–5 MΩ) electrodes were pulled from borosilicate capillary glass (World Precision Instruments, New Haven, CT) and filled with internal solution. The composition of the internal solution used for voltage-clamp recordings from neurons in the CA1 pyramidal layer was (in mM): CsCl, 80; CsF, 80; EGTA, 10; CsOH, 22.5; HEPES, 10 and QX-314, 5 (pH adjusted to 7.3 with CsOH; 340 mOsM). All experiments were performed at room temperature (20–22^{o}C)

Data analysis. Peak amplitude, 10–90% rise time, and decay-time constant of field stimulation- evoked PSCs were determined using the pClamp6 software. Spontaneously occurring currents were analyzed using the Continuous Data Recording software (Dempster, 1989). All the analyses were made on fixed 3-min recordings. Unless otherwise stated, data

are presented as mean ± S.E.M. The Student's t-test was used for pairwise comparison of results obtained in a test group and its respective control. In addition, one-way analysis of variance (ANOVA) followed by Turkey's post-hoc test was used to compare results of repeated measures and multiple groups.

Cholinesterase assay. Cholinesterase activity was measured by a two-phase radiotopic assay (Johnson and Russel, 1975) using 0.788 mM [3H]ACh chloride, which was sufficient to produce 100,000 cpm when totally hydrolyzed. The reaction (100 µl) was terminated by addition of 100 µl of a termination mixture (1 M monochloroacetic acid, 2 M NaCl, 0.5 M NaOH) to which 4 ml of scintillation mixture (10% isoamyl alcohol, 0.5% diphenyloxazole, 0.02% dimethylphenyloxazolylbenzene in toluene) was added. The hydrolyzed, acidified [3H]acetate partitioned into the organic phase and was subsequently counted. All samples were assayed in the presence of the butyrylcholinesterase inhibitor tetraisopropylpyrophosphoramide (10^{-4} M). Protein assays were performed using a micro BCA Kit (Pierce, Rockford, Il) according to the manufacturer instructions. Two sets of experiments were carried out. In one set, hippocampal slices were first perfused for 15 min with ACSF containing no drug, soman (1 nM) or PB (100 nM) and subsequently washed three times with drug-free ACSF for 1.5 min. Each slice was transferred to a microfuge tube containing 50 µl of extraction buffer (pH = 7.4; NaCl 1 M; $NaH_2PO4.H_2O$ 0.019 M; $NaHPO_4.7H_2O$ 0.081 M; Titron X-100 1%) and snap frozen. Cells within the slices were lysed by five rounds of freeze-thaw, lasting approximately 5 min, and homogenates were centrifuged at 14,000 rpm at 4°C. Cholinesterase activity measured in the supernatant was normalized to the protein contents of the pellets. In the other set of experiments, hippocampal slices were first extracted as above and cholinesterase activity was measured in the supernatants after 0, 15, 30 and 60 min' exposure to PB (100 nM).

Drugs and biological hazards. Soman (1,2,2-trimethylpropyl methylphosphonofloridate) was obtained from the U.S. Army Medical Research and Development Command (USAMRDC). Atropine sulfate, PB, 6-cyano-7-nitroquinoxaline-2,3-dione (CNQX), 2-amino-5-phosphonovaleric acid (APV), picrotoxin and 4-diphenylacetoxy-*N*-methypiperidine (4-DAMP) were purchased from Sigma Chemical Co. (St. Louis, MO). 11-[[[2-diethylamino-*O*-methyl]-1-piperidinyl]acetyl]-5,11-dihydrol-6*H*-pyridol[2,3-*b*][1,4]benzodiazepine-6-one (AFDX-116) was purchased from Tocris Cookson Inc. (Ellisville, MO). Methyllycaconitine (MLA) citrate was a gift from Prof. M. H. Benn (Department of Chemistry, University of Calgary, Alberta, Canada). Dihydro-β-erythroidine (DHβE) hydrobromide was a gift from Merck (Rahway, NJ). A 250 mM stock solution of picrotoxin was made in DMSO, and dilutions were made in the ACSF. NaOH was used to dissolve CNQX and APV (the 10 mM stock solution of CNQX had 12.5 mM NaOH and the 50 mM stock solution of APV had 0.5 M of NaOH). [3H]ACh (specific activity = 55 mCi/mmol) was obtained from Perkins Elmer Life Sciences Inc./New England Nuclear (Boston, MA)

Safe handling of organophosphates was assured according to USAMRDC's recommendations. The compounds were stored at −80°C and diluted daily in an organophosphate vapor-proof hood. All organophosphate- and/or tetrodotoxin-containing solutions were inactivated with 5% sodium hypochloride. Latex gloves and proper goggles were used throughout the experiment.

Results and Discussion

EPSCs evoked by field stimulation of Schaffer collaterals were recorded from CA1 pyramidal neurons in rat hippocampal slices that were continuously perfused with ACSF containing the GABAA receptor antagonist picrotoxin (100 µM). Likewise, IPSCs evoked by field stimulation of Schaffer collaterals were recorded from CA1 pyramidal neurons in rat hippocampal slices that were continuously perfused with ACSF containing the glutamate

receptor antagonists CNQX (20 μM) and APV (50 μM). As shown in Figure 2.1.1, during the recording time, the amplitudes of these synaptic currents were fairly stable.

When the hippocampal slices were perfused with ACSF containing soman (0.1-10 nM), there was a concentration-dependent reduction of the amplitude of the IPSCs evoked by stimulation of the Schaffer collaterals and recorded from CA1 pyramidal neurons (Figure 2.1.2). The effect of soman was selective for GABAergic transmission, because the amplitudes of EPSCs evoked by stimulation of the Schaffer collaterals and recorded from CA1 pyramidal neurons were not affected by soman at concentrations as high as 50 nM (Figure 2.1.3). Exposure of the hippocampal slices to soman also had a selective effect on the spontaneous, action potential-dependent GABAergic transmission between the Schaffer collaterals and CA1 pyramidal neurons. Of interest, however, soman-induced reduction of amplitude and frequency of spontaneously occurring IPSCs was more pronounced when the events were recorded between successive field stimulations of the Schaffer collaterals (see Figure 2.1.4). Soman-induced inhibition of GABAergic transmission in hippocampal slices was mediated exclusively by muscarinic receptors, because it could be prevented by perfusion of the slices with ACSF containing atropine (Figure 2.1.5A) and it was not affected by the nAChR antagonists methyllycaconitine (MLA) and dihydro-β-erythroidine (DHβE) (Figure 2.1.5B).

In contrast to soman, pyridostigmine bromide (PB) at nanomolar concentrations increased the amplitude of IPSCs evoked by field stimulation of the Schaffer collaterals and recorded from CA1 pyramidal neurons in hippocampal slices (Figure 2.1.6A). Like soman, however, PB did not affect glutamatergic transmission in the hippocampal slices (Figure 2.1.6B). The effect of PB on GABAergic transmission was concentration dependent, being maximal at 100 nM (Figure 2.1.6C) and was completely reversible upon washing the preparations with PB-free physiological solution (Figure 2.1.6A). The facilitatory effect of PB on field stimulation-evoked GABAergic transmission in the hippocampus was mediated primarily by muscarinic receptors, as it was selectively blocked by 1 nM atropine (Figure 2.1.7). In addition to increasing the amplitude of field stimulation-evoked IPSCs, PB at nanomolar concentrations also increases the frequency and amplitude of spontaneous IPSCs recorded from CA1 pyramidal neurons and these effects are also blocked by the muscarinic receptor antagonist atropine (Figure 2.1.8).

In an attempt to define pharmacologically the muscarinic receptor subtypes underlying the effects of PB and soman on GABAergic transmission in the rat hippocampus, the m3 receptor-preferring antagonist 4-DAMP and the m2 receptor-preferring antagonist AFDX-116 were used. Evoked IPSCs were recorded from CA1 pyramidal neurons in hippocampal slices that were exposed first to 4-DAMP (100 nM) for 5–8 min and subsequently to the admixture of 4-DAMP (100 nM) plus soman (1 nM) or PB (100 nM) for an additional 10 min. The same protocol was carried out using AFDX-116 instead of 4-DAMP. At the end of the experiments, the preparations were washed for 10 min with drug-free ACSF. The m2 receptor-preferring antagonist AFDX-116 prevented soman from inhibiting GABAergic transmission in the hippocampus, whereas the m3 receptor-preferring antagonist 4-DAMP was unable to affect the inhibitory effect of soman on GABAergic transmission (Figure 2.1.9A). In contrast, PB-induced potentiation of GABAergic transmission in the hippocampus was selectively prevented by 4-DAMP and was not altered by AFDX-116 (Figure 2.1.9B).

To determine how PB could affect soman-induced inhibition of GABAergic transmission in the hippocampus, two sets of experiments were performed. In one set of experiments, IPSCs were recorded from hippocampal slices that were exposed first to PB (100 nM), subsequently to soman (1, 3 or 10 nM) plus PB (100 nM) and finally to PB alone. In the other,

IPSCs were recorded from neurons that were exposed first to PB (300 nM) and subsequently to PB (300 nM) plus soman (3 or 10 nM). Each perfusion lasted 5–8 min. The potentiating effect that 100 nM PB had on GABAergic transmission counteracted the inhibition induced by 1 nM soman. (Figure 2.1.10A and B). Of interest, the inhibitory effect of soman on evoked IPSCs was unaltered when hippocampal slices were first exposed to soman (1 nM) and subsequently to soman (1 nM)-plus-PB (100 nM) (Figure 2.1.10C). Likewise, soman (1 nM)-induced reduction of the frequency and amplitude of spontaneous IPSCs recorded from CA1 pyramidal neurons was prevented by pre-exposure of the hippocampal slices to 100 nM PB (Figure 2.1.11).

Summary and relevance of the studies with pyridostigmine and soman

Potentiation of GABAergic transmission by 100 nM PB functionally antagonized soman-induced inhibition of GABAergic transmission, but only when hippocampal slices were pre-treated with PB. We showed further that, acting via m3 receptors present on GABAergic neurons, PB at 100 nM effectively prevents inhibition of GABAergic transmission induced by the interactions of soman with m2 receptors located on GABAergic neurons. Therefore, PB, acting via m3 receptors, can effectively counteract effects arising from the interactions of soman with m2 receptors in the brain.

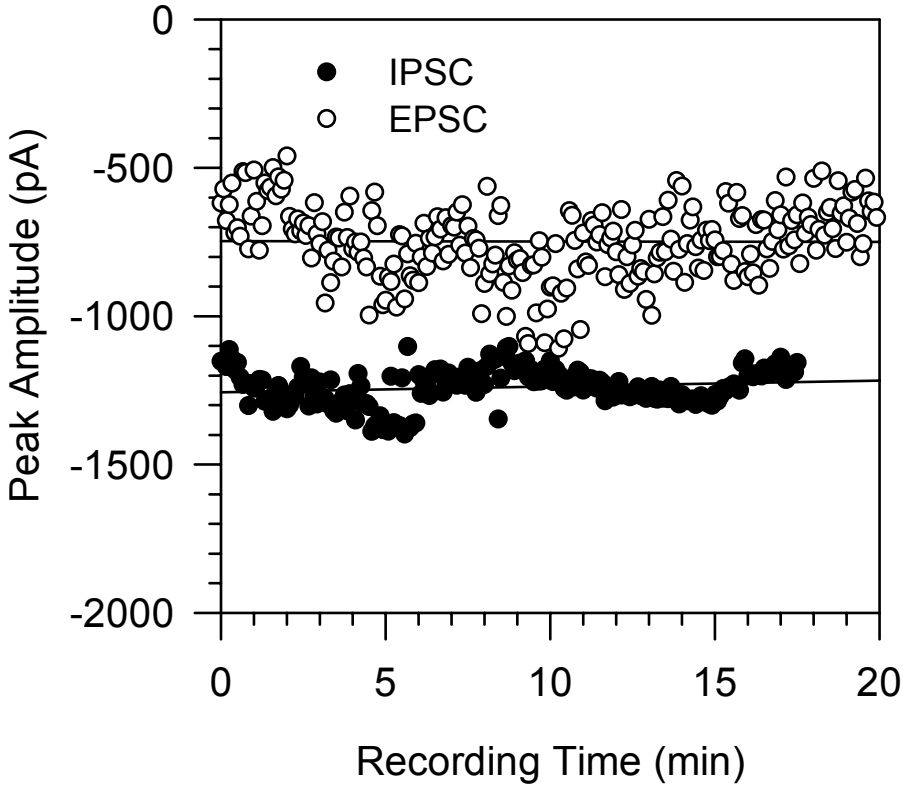

Figure 2.1.1. *Time-dependent changes in the amplitudes of EPSCs and IPSCs evoked by stimulation of the Schaffer collaterals and recorded from CA1 pyramidal neurons in rat hippocampal slices.* Plot of the amplitudes of EPSCs or IPSCs evoked by field stimulation of the Schaffer collaterals at 0.2 Hz and recorded from CA1 pyramidal neurons versus recording time. Holding potential, -60 mV.

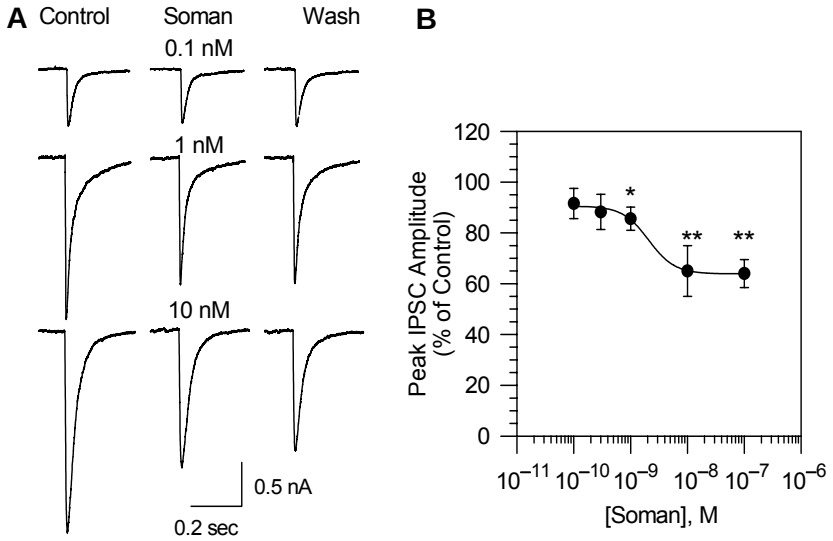

Figure 2.1.2. *Effect of soman on the amplitude of IPSCs evoked by field stimulation of the Schaffer collaterals and recorded from CA1 pyramidal neurons in rat hippocampal slices*. **A.** Representative recording samples of evoked IPSCs obtained (i) under control conditions, (ii) in the presence of 0.1, 1 or 10 nM soman, and (iii) after 10-min washing of the slices with soman-free ACSF. The neurons were exposed for 10 min to soman. All experiments were carried out in the presence of CNQX (20 μM) and APV (50 μM). Membrane potential, -60 mV. **B.** Concentration-dependent effect of soman on evoked IPSCs. Each concentration was tested on a slice that had not been previously exposed to soman. Graph and error bars represent mean and S.E.M., respectively, of results obtained from 4 neurons. According to the unpaired Student's t-test, results are significantly different from control with $p < 0.05$ (*) or $p < 0.01$ (**).

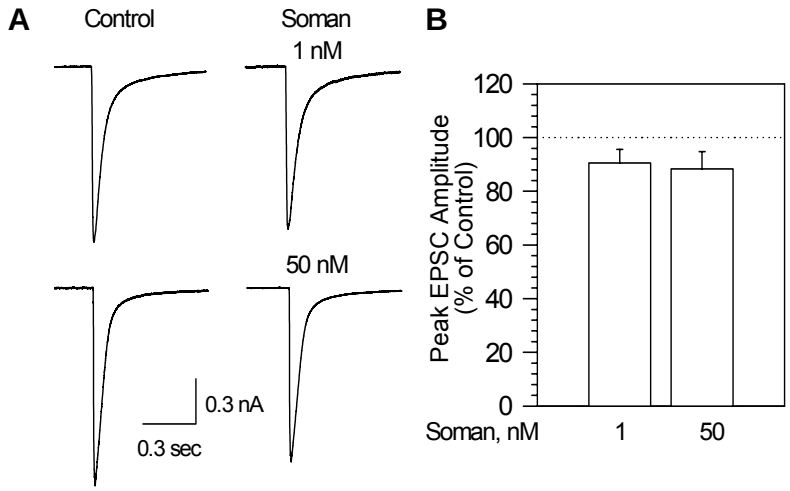

Figure 2.1.3. *Soman does not affect field sitmulation-evoked EPSCs recorded from CA1 pyramidal neurons.* **A.** Samples of evoked EPSCs recorded from neurons at -60 mV before (left traces) and during exposure to 1 or 50 nM soman (right traces). **B.** Quantitative analysis of the effect of soman on evoked EPSCs. Graph and error bars represent mean and S.E.M., respectively, of results obtained from 4 neurons.

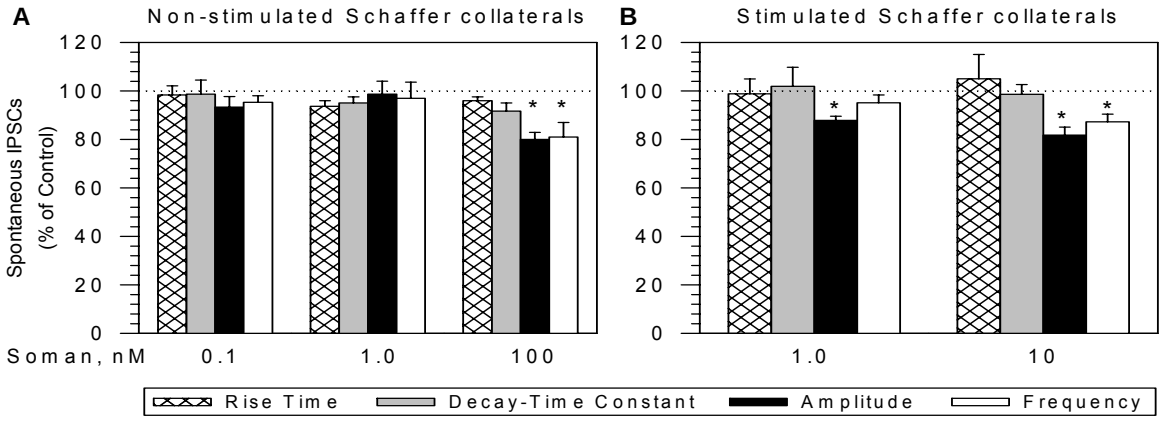

Figure 2.1.4. *Soman decreases the amplitude and frequency of spontaneously occurring IPSCs recorded from CA1 pyramidal neurons in rat hippocampal slices*. **A.** Quantitative analysis of the effects of soman on spontaneous IPSCs recorded from CA1 pyramidal neurons in slices where the Schaffer collaterals had not been field stimulated. The average rise time and decay-time constant of IPSCs recorded from neurons prior to their exposure to soman were 2.5 $\pm$ 0.55 msec and 7.5 $\pm$ 1.44 msec, respectively. **B.** Quantitative analysis of the effects of soman on spontaneous IPSCs recorded from CA1 pyramidal neurons in slices where the Schaffer collaterals were stimulated at 0.2 Hz. The average rise time and decay-time constant of IPSCs recorded under control conditions were 2.03 $\pm$ 0.39 msec and 8.16 $\pm$ 1.73 msec, respectively. Graph and error bars represent mean and S.E.M., respectively, of results obtained from 5 neurons at -60 mV. According to the unpaired Student's t-test, results are significantly different from control with $p < 0.05$ (*).

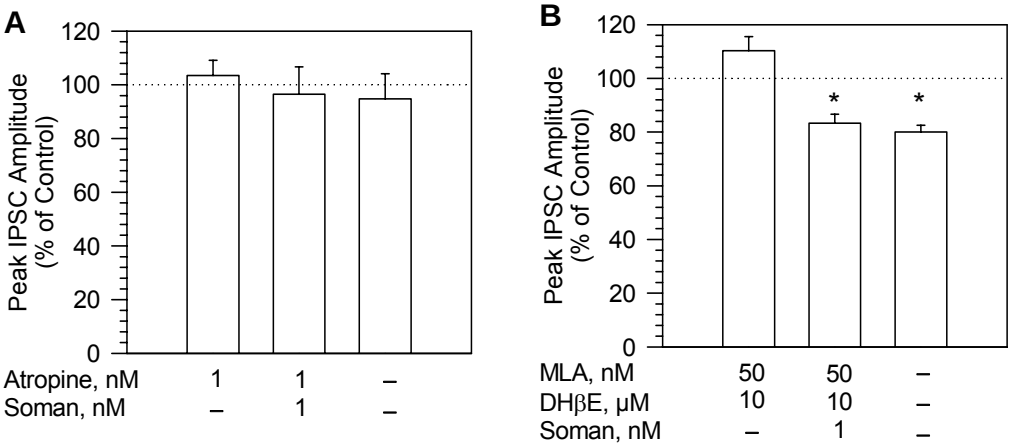

Figure 2.1.5. *Effects of the muscarinic receptor antagonist atropine and the nAChR antagonists MLA and DHβE on soman-induced inhibition of evoked IPSCs in rat hippocampal slices.* **A.** Quantitative analysis of the effect of atropine on evoked IPSCs and on soman-induced inhibition of evoked IPSCs. Evoked IPSCs were recorded from CA1 pyramidal neurons in hippocampal slices that were exposed first to atropine (1nM) for 5-8 min and subsequently to the admixture of atropine (1 nM) plus soman (1 nM) for an additional 10 min. At the end of the experiments, the preparations were washed for 10 min with drug-free ACSF. The amplitudes of events evoked at a frequency of 0.2 Hz for 3 min were averaged. The averaged amplitudes of events recorded in the presence of atropine or atropine-plus-soman and in the washing phase are expressed as percentage of the averaged amplitudes of events recorded at the same frequency for 3 min prior to exposure of the neurons to any drug. **B.** Quantitative analysis of the effect of MLA and DHβE on evoked IPSCs and on soman-induced inhibition of evoked IPSCs. Evoked IPSCs were recorded from CA1 pyramidal neurons in hippocampal slices that were exposed first to MLA (50 nM) plus DHβE (10 μM) for 5–8 min and subsequently to the admixture of the antagonists and soman (1 nM) for an additional 10 min. At the end of the experiments, the preparations were washed for 10 min with drug-free ACSF. The amplitudes of events evoked at a frequency of 0.2 Hz for 3 min were averaged. The averaged amplitudes of events recorded in the presence of drugs and in the washing phase are expressed as percentage of the averaged amplitudes of events recorded at the same frequency for 3 min under control conditions. Graph and error bars represent mean and S.E.M., respectively, of results obtained from 4 neurons at -60 mV. All experiments were carried out in the presence of CNQX and APV. According to the unpaired Student's t-test, results are significantly different from control with $p < 0.05$ (*).

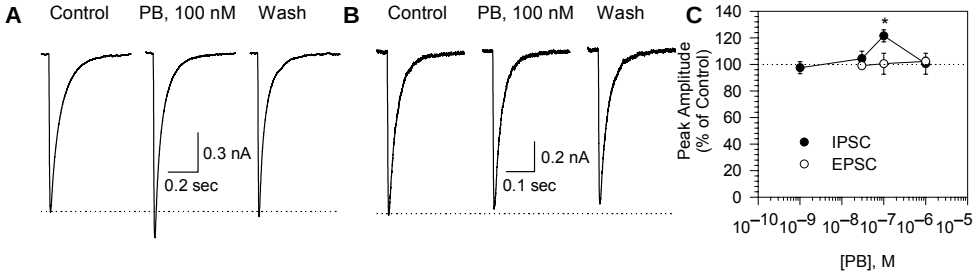

Figure 2.1.6. *PB increases the amplitude of IPSCs and does alter the amplitude of EPSCs evoked by field stimulation of the Schaffer collaterals and recorded from CA1 pyramidal neurons in rat hippocampal slices*. **A, B.** Sample recordings of evoked IPSCs (**A**) and EPSCs (**B**) obtained from two neurons under control conditions, in the presence of PB (100 nM) and after 10-min washing of the preparations with PB-free ACSF. The neurons were exposed to PB for 10 min. Evoked IPSCs were recorded in the presence of CNQX (20 μM) and APV (50 μM), and evoked EPSCs were recorded in the presence of picrotoxin (100 μM). Holding potential, -60 mV. **C.** Graph of PB concentrations vs. the amplitudes of evoked EPSCs or IPSCs normalized to control conditions. The amplitudes of EPSCs or IPSCs evoked at a frequency of 0.2 Hz for 3 min were averaged. The averaged amplitudes of events recorded in the presence of PB are expressed as percentage of the averaged amplitudes of events recorded at the same frequency for 3 min under control conditions. Graph and error bars represent mean and S.E.M., respectively, of results obtained from 4 neurons. According to the unpaired Student's t-test, results are different from control with $p < 0.05$ (*).

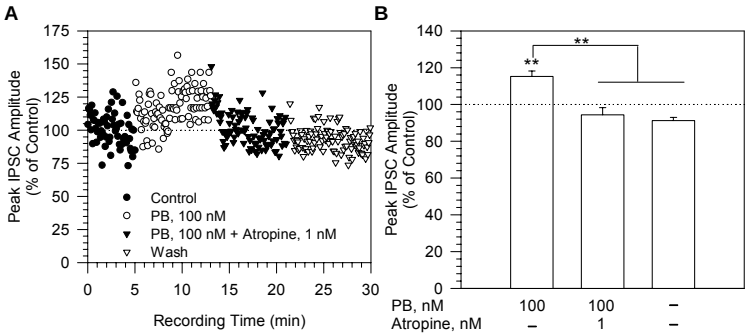

Figure 2.1.7. *Atropine blocks PB-induced potentiation of IPSCs evoked by field stimulation of the Schaffer collaterals and recorded from CA1 pyramidal neurons.* **A.** Graph of the amplitudes of IPSCs evoked at 0.2 Hz and recorded from a CA1 pyramidal neuron: (i) under control condition, (ii) in the presence of 100 nM PB, (iii) in the presence of 100 nM PB and 1 nM atropine, and (iv) during the wash-out with drug-free ACSF. **B.** Quantitative analysis of the effects of 1 nM atropine on PB-induced potentiation of evoked IPSCs. The amplitudes of IPSCs evoked at a frequency of 0.2 Hz for 3 min were averaged. The averaged amplitudes of events recorded from a given neuron in the presence of PB or atropine-plus-PB and during the washing phase are expressed as percentage of the averaged amplitudes of events recorded at the same frequency for 3 min under control conditions. Graph and error bars represent mean and S.E.M., respectively, of results obtained from 5 neurons at -60 mV. All experiments were carried out in the presence of the glutamate receptor antagonists CNQX (20 μM) and APV (50 μM). According to the ANOVA test, peak amplitudes of IPSCs recorded in the presence of PB prior to exposure of the neurons to 1 nM are significantly different from control with $p < 0.01$ (**). Finally, amplitudes of events recorded during exposure of neurons to PB-plus-atropine and after removal of both drugs were significantly different from those recorded in the presence of PB alone with $p < 0.01$ (**).

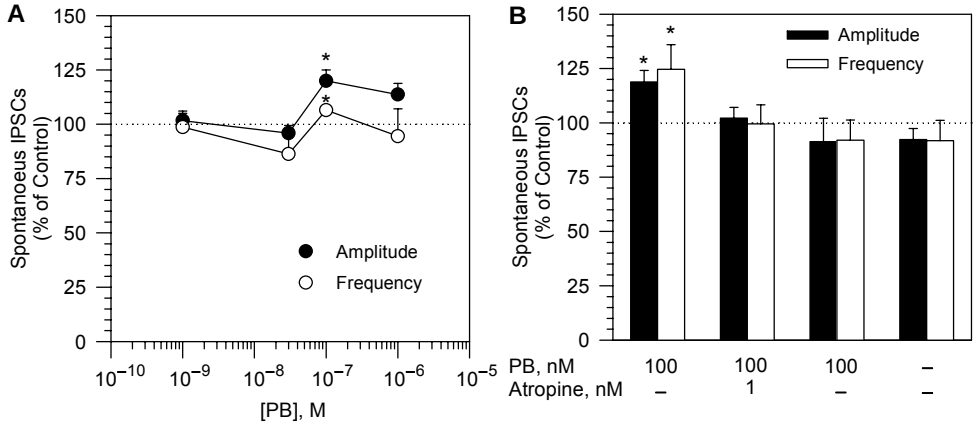

Figure 2.1.8. *Atropine blocks the effects of PB on spontaneous IPSCs recorded from CA1 pyramidal neurons in hippocampal slices where the Schaffer collaterals were stimulated at 0.2 Hz.* **A.** Analyses of the effects of PB on the amplitude and frequency of spontaneous IPSCs. The frequency and average amplitude of IPSCs recorded for 3 min in the presence of PB are expressed as percentage of the frequency and average amplitude of events recorded under control condition. Points and error bars represent mean and S.E.M., respectively, of results obtained from 4 neurons. Results are significantly different from those obtained under control conditions: *, $p < 0.05$ according to the unpaired Student's t-test. **B.** Analyses of the effects of atropine on PB-induced increase in the amplitude and frequency of spontaneous IPSCs. The neurons were first exposed to PB (100 nM) for 5–8 min and subsequently to PB (100 nM)-plus-atropine (1 nM). Following this treatment, the neurons were perfused for 10 min with ACSF containing only PB and for an additional 10 min with ACSF containing no atropine or PB. The frequency and average amplitude of IPSCs recorded for 3 min under each experimental condition are expressed as percentage of the frequency and average amplitude of events recorded under control condition. Graph and error bars represent mean and S.E.M., respectively, of results obtained from 4 neurons. Results were significantly different from those obtained under control conditions: *, $p < 0.05$ according to the unpaired Student's t-test.

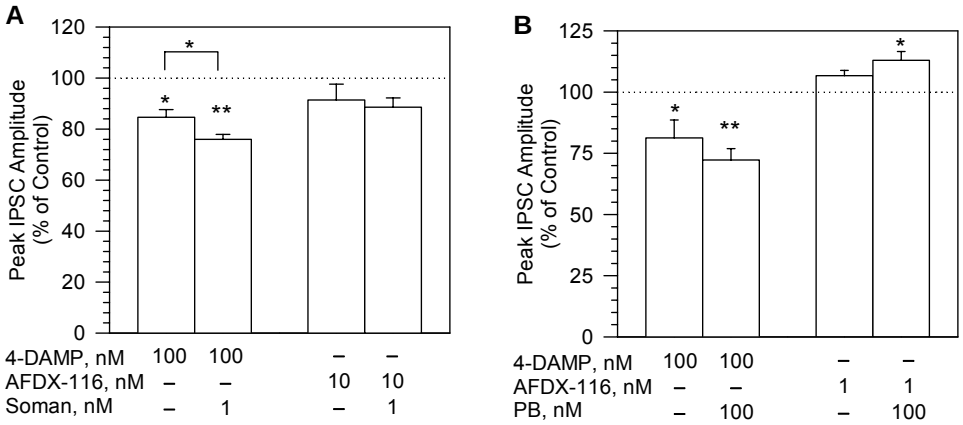

Figure 2.1.9. *Effects of AFDX-116 and 4-DAMP on soman-induced inhibition and PB-induced potentiation of evoked GABAergic transmission in hippocampal slices.* **A.** Analysis of the effects of the m3 receptor-preferring antagonist 4-DAMP and of the m2 receptor-preferring antagonist AFDX-116 on evoked IPSCs and on soman-induced inhibition of evoked IPSCs. The amplitudes of events evoked at a frequency of 0.2 Hz for 3 min were averaged. The averaged amplitudes of events recorded in the presence of a muscarinic receptor antagonist or that antagonist-plus-soman are expressed as percentage of the averaged amplitudes of events recorded at the same frequency for 3 min prior to exposure of the neurons to any drug. Each graph and error bar represents mean and S.E.M. of results obtained from 3-6 experiments. The amplitudes of currents recorded in the presence of 4-DAMP or 4-DAMP-plus-soman were significantly smaller than those recorded under control conditions: *, $p < 0.05$ and **, $p < 0.01$ according to the ANOVA test. In addition, the amplitudes of events recorded in the presence of 4-DAMP-plus-soman were significantly different from those recorded in the presence of 4-DAMP: *, $p < 0.05$ according to the ANOVA test. **B.** Quantitative analysis of the effects of the m3 receptor-preferring antagonist 4-DAMP and of the m2 receptor-preferring antagonist AFDX-116 on evoked IPSCs and on PB-induced potentiation of evoked IPSCs. The analysis is similar to that described in A. Each graph and error bar represent mean and S.E.M., respectively, of results obtained from 3–6 experiments. Amplitudes of events recorded in the presence of 4-DAMP, 4-DAMP-plus-PB, and AFDX-116-plus-PB were significantly different from those recorded under control conditions: *, $p < 0.05$; ** $p < 0.01$ according to the ANOVA test.

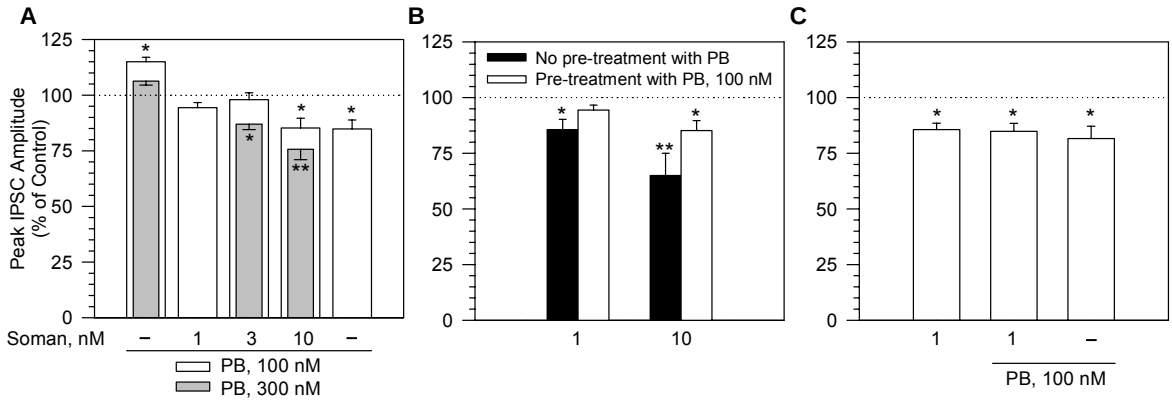

Figure 2.1.10. *Pre-exposure of the hippocampal slices to 100 nM PB masks the inhibitory effect of soman on evoked IPSCs.* **A.** Quantitative analyses of the effects of soman on evoked IPSCs recorded in the continuous presence of 100 nM or 300 nM PB. IPSCs were recorded from hippocampal slices that were exposed first to PB (100 nM), subsequently to soman (1, 3 or 10 nM) plus PB (100 nM or 300 nM) and finally to PB alone. Each perfusion lasted 5–8 min. The amplitudes of IPSCs evoked at a frequency of 0.2 Hz for 3 min were averaged. The averaged amplitudes of events recorded from a given neuron in the presence of the test compounds are expressed as percentage of the averaged amplitudes of events recorded at the same frequency for 3 min under control conditions. Graph and error bars represent mean and S.E.M., respectively, of results obtained from 3 neurons. **B.** Comparison of the effects of 1 and 10 nM soman on evoked IPSCs recorded from slices that were not pre-exposed to 100 nM PB and from slices that had been pre-exposed for 5–8 min to 100 nM PB. Data were extracted from Figs. 2B and 10A to allow mutual comparison. **C.** The inhibitory effect of soman on evoked IPSCs was unaltered when hippocampal slices were first exposed to soman (1 nM) and subsequently to soman (1 nM)-plus-PB (100 nM). The depression of the IPSCs remained after 10-min washing of the preparations with drug-free ACSF solution for at least 10 min. Analyses of the results were done according to the protocol described in **A.** Graph and error bars represent mean and S.E.M., respectively, of results obtained from 4 neurons. All experiments were carried out in the presence of CNQX (20 μM) and APV (50 μM). Holding potential, -60 mV. Wherever indicated in the graphs of panels **A**, **B** and **C**, amplitudes of events recorded in the presence of a given drug were significantly different from those of events recorded under control conditions: *, $p < 0.05$ and **, $p < 0.01$, according to the unpaired Student's t-test.

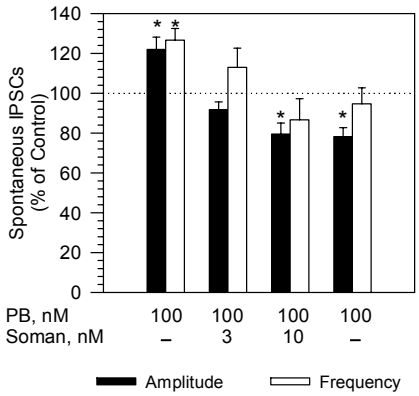

Figure 2.1.11. *Pre-exposure of the hippocampal slices to 100 nM PB masks the inhibitory effect of soman on spontaneous IPSCs recorded from CA1 neurons in hippocampal slices where the Schaffer collaterals were stimulated at 0.2 Hz.* Quantitative analyses of spontaneous IPSCs recorded from hippocampal slices exposed first to 100 nM PB and subsequently to soman (3 and 10 nM)-plus-PB (100 nM) and PB (100 nM) alone. Each perfusion lasted 5-8 min. Results obtained during a given treatment were significantly different from those obtained under control conditions: *, $p < 0.05$ according to the unpaired Student's t-test.

Section 3. Effects of paraoxon and nerve agents on neurons in the CNS

3.1. Effects of pyridostigmine, galantamine and low doses of nerve agents on neuronal survival in the CNS

Introduction

To understand the neurological effects of galantamine, pyridostigmine and nerve agents, it will be critical to determine: (i) whether the pro- and anti-apoptotic effects of these compounds are cell-type specific; (ii) the mechanisms of action underlying the pro- and anti-apoptotic effects of these compounds; and (iii) the ability of galantamine to antagonize nerve agent-induced neurotoxicity. Thus, the first part of this study was designed to determine whether galantamine (1 μM) could protect primary hippocampal cultures from degeneration induced by either the β-amyloid peptide or the protein kinase inhibitor staurosporine (STS, 100 nM) and, if so, by what mechanism. This information would lay the groundwork for further studies on the ability of galantamine to protect against brain damage caused by nerve agents.

Materials and methods

Primary hippocampal cultures were prepared according to the procedure described in Alkondon and Albuquerque, 1993. In the present study, cultures were used 10 days after plating the cells dissociated from the hippocampi of 18-day-old rat fetuses.

Results and discussion

Pre-exposure of hippocampal cultures to galantamine reduced the neuronal death induced by the β-amyloid peptide Aβ1-42 (Figure 3.1.1). Likewise, STS-induced apoptosis was lower in cultures that were pre- or co-treated with galantamine. However, STS-induced apoptosis was unaffected by post-treatment of the cultures with galantamine. Western blot analysis of the primary hippocampal cultures also revealed that the extracellular signal-regulated kinase (ERK), which controls cell viability in various systems, was activated after 24-h exposure to galantamine (1 μM). Thus, the neuroprotective action of galantamine at clinically relevant concentrations involves activation of ERK and can contribute to the therapeutic effectiveness of the drug in AD, particularly at early stages of the disease.

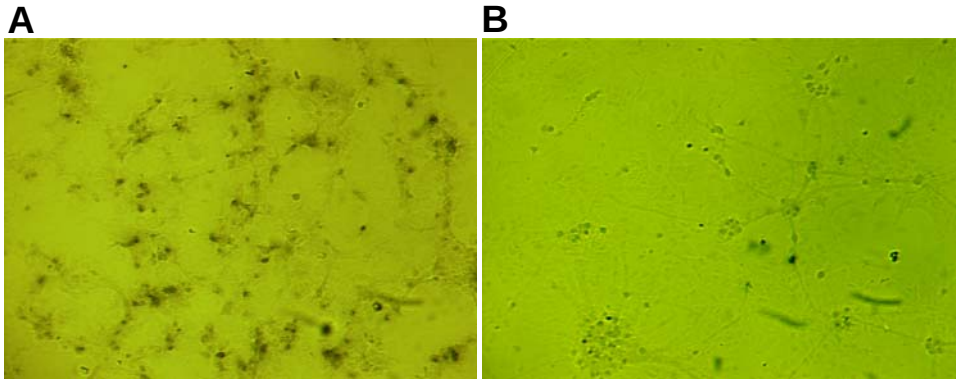

Figure 3.1.1. *Effects of galantamine on Aβ1-42-induced degeneration in primary hippocampal cultures. A.* TUNEL analysis of cultured hippocampal neurons that were exposed for 24 h to aggregated β-AP1-42 (10 μM). **B.** TUNEL analysis of cultured hippocampal neurons that were exposed for 24 h to galantamine (1 μM) and subsequently for an additional 24 h to the admixture of galantamine and β-AP1-42. Notice that the number of TUNEL-positive cells in the primary cultures that were exposed to galantamine prior to their exposure to Aβ1-42 was lower than the number of TUNEL-positive cells in cultures that were not pre-treated with galantamine. Calibration, 100 μm.

3.2. Chronic exposure to paraoxon targets spines on the basal dendrites of the ca1 hippocampal pyramidal neurons: implications to cognitive disorders

Introduction

Co-culturing of septal tissue along with hippocampal neurons results in changes in the pattern of dendritic and axonal arborization of CA1 pyramidal neurons. Thus it appears that cholinergic innervation of the hippocampus has a major impact on the development of the hippocampal neurocircuitry. As changes in the neurocircuitry of the hippocampus under underlie epileptic seizures in several experimental models, and as the OPs are known to be pro-convulsant agents, it is important to investigate the influence of low levels of OPs on septum-induced changes in the axonal and dendritic development.

Studies with another organophospate compound led us to what is probably a much more important aspect of the effects of this class of drugs on axonal and dendritic development and cytoarchitecture. Before carrying out these studies using the nerve agents, we used a readily available agent, parathion. Parathion through its oxidized active metabolite paraoxon is one of the most potent cholinesterase (ChE) inhibitor and toxic organophosphate (OP) compounds. Although banned in some developed countries including U.S., the increasing worldwide use of parathion led the World Health Organization to recognize this OP as the prime cause of accidental and occupational intoxication and fatalities. Chronic exposure to anti-ChE agents is likely to affect selectively certain brain areas leading to delayed neurological disorders. During development in animal models, cortical cholinergic disruption produces deficits in axogenesis, synaptogenesis and especially at the dendritic spines that will persist into adulthood with an impact on neuronal plasticity, long-term potentiation (LTP) and memory consolidation.

Materials and Methods

Here we studied the effects of repetitive exposure of 8 to 20 days postnatal Wistar rats, (P8-P20) to subcutaneous daily injections of low doses of paraoxon (0.1, 0.15 and 0.2 mg/kg) during the period of significant development of cholinergic system. Pyramidal neurons of the hippocampal CA1 region, as well as the overall cytoarchitecture of the hippocampal strata, were correlated with ChE levels and hippocampal staining and with choline acetyltransferase (ChAT) immunohistochemistry. At P21, 24 h after the last injection, the brain were processed for morphological and histochemical staining assays. A group of animals was allowed to recover for 7 days from the OP exposure, the assays performed at P28 and the results compared to those obtained from another group that continued to receive paraoxon up to P27.

Results and Discussion

Sub-chronic treatment of rats with paraoxon reduced the rate of body weight gain (Figure 3.2.1). Total brain ChE activity progressively decreased up to 40% of control by day 21 (Figure 3.2.2). At P28, ChE levels were further decreased to 39, 33 and 30% of control in animals exposed to 0.1, 0.15 and 0.2 mg/kg, respectively, and the ChE recovery, although significant, was not complete, reaching 75, 74 and 66% of control for the three increasing doses. ChE staining was reduced in all hippocampal and dentate gyrus regions.

Cresil violet staining showed neither cytoarchitectural changes nor signs of cell body degeneration as judged by the absence of pyknotic hyperchromatic neurons. To evaluate the effects of paraoxon on neuronal structure, CA1 pyramidal neurons were filled with Lucifer

Yellow (Figure 3.2.3). Paraoxon selectively decreased the spine density on the basal, but not on the secondary apical dendrites (Figure 3.2.4). In contrast, dendritic length and number of intersections and bifurcations of both basal and apical trees of CA1 pyramidal neurons were not affected by treatment of the animals with paraoxon (Figure 3.2.5). In addition, paraoxon decreased ChE activity in the hippocampus (Figure 3.2.6) without affecting ChAT activity (Figure 3.2.7) or the gross morphology of the pyramidal cell layer (Figure 3.2.8).

Thus, chronic exposure to low doses of paraoxon during a period of cholinergic system development, despite the overall reduction of brain ChE levels, selectively affected the basal dendrite spine density of the pyramidal neurons. This fine hippocampal alteration with serious developmental consequences to cognition and other brain functions occurred in the absence of overt cholinergic toxic signs, which serves as an alert for the insidiousness of OPs when present in a repetitive low-dose scheme. These studies are very relevant to development of antidotal and/or preventative strategies using pyridostigmine and galantamine. As protection studies continue, it will be important to determine whether this damage to the fine architecture of the brain will be prevented.

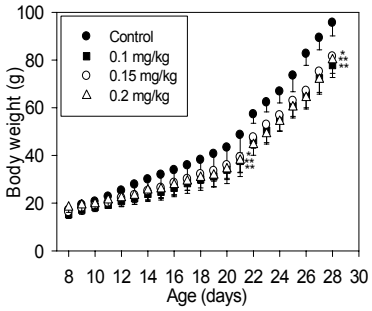

Figure 3.2.1. *Chronic paraoxon exposure decreases the rate of animal development.* Body weight was measured daily from P8 to P28, before the animals were injected with either peanut oil (control) or different concentrations of paraoxon. At P21, a 13, 14 and 27% decrease in body weight compared to control (filled circle) was found in animals exposed to 0.1 (filled square), 0.15 (open circle) and 0.2 (open triangle) mg/kg paraoxon, respectively. At P28, similar values of 14, 16 and 28% were found with increasing paraoxon concentrations. Differences were statistically significant at P21 and P28 (ANOVA and Dunnet´s test,** $p < 0.01$ and * $p < 0.05$).

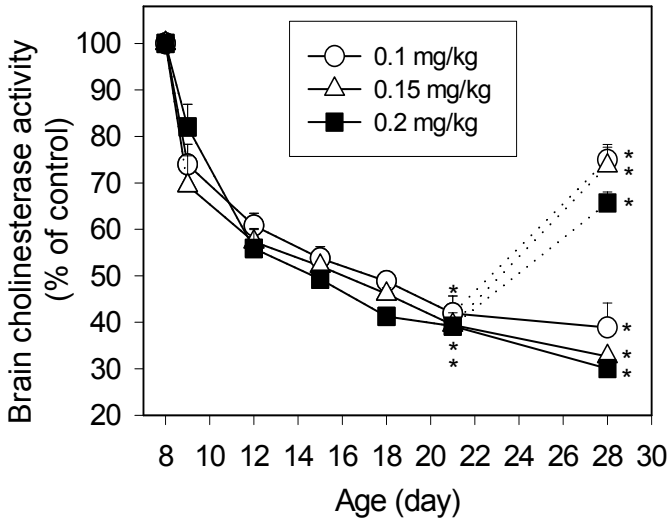

Figure 3.2.2. *Decrease of brain ChE activity during chronic paraoxon treatment.* Brain ChE activity is expressed as percentage of control *versus* days of age. ChE activity was assayed each 3 days, 24 hours after the last paraoxon injection. Animals exposed daily to 0.1 (open circle); 0.15 (open triangle) or 0.2 mg/kg (filled square) showed progressive ChE inhibition that reached 60% of control at P21 (n = 4, for each group) and 70% at P28 (n = 3). Animals receiving the last injection at P20 and examined at P28 showed significant recovery in ChE activity (dotted lines, n = 4) when compared to those continuously treated (ANOVA and SNK test, $p < 0.01$), but were still significantly below control values (ANOVA and Dunnet´s test with 8 or 12 DF,* $p < 0.01$).

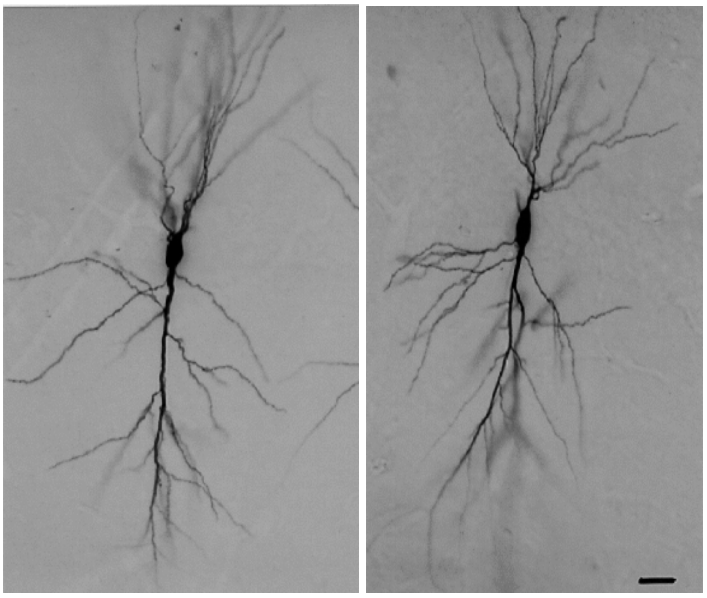

Figure 3.2.3. *Photomicrographs of Lucifer yellow-filled CA1 pyramidal neurons at P21.* Pyramidal neurons from control (A) and paraoxon (0.2 mg/kg)-injected (B) animals were filled with LY and subsequently treated with peroxidase-conjugated anti-LY antibody. Cells from the two experimental groups showed a high degree of morphological homogeneity, and paraoxon did not produce any noticeable alterations. Calibration bar: 50 μm.

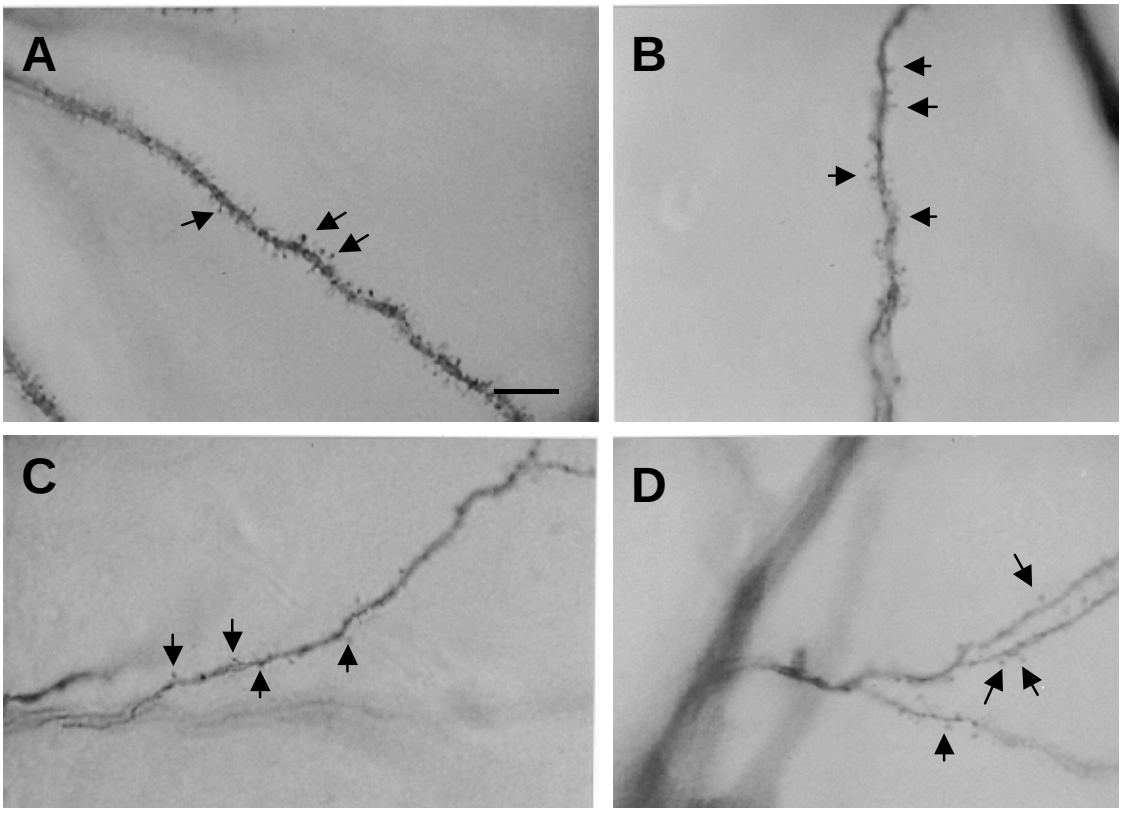

Figure 3.2.4. *Paraoxon selectively reduces the spine density on the basal dendrites of CA1 pyramidal neurons at P21*. Photomicrographs show basal and apical dendrites of pyramidal neurons filled with LY and subsequently treated with horseradish-conjugated anti-LY antibodies. A and C panels illustrate the dendritic spines of the basal tree of pyramidal neurons from control rats and from rats after treatment with 0.2 mg/kg paraoxon, respectively. The spines (indicated by the arrows), which appeared in great number on control neurons, were much fewer in number and appeared scattered along the dendrites of cells from paraoxon-treated animals. In contrast, the density of the dendritic spines on the secondary apical tree of pyramidal neurons from the control (B) and paraoxon-treated (D) animals showed no difference. Calibration bar: 5 μm.

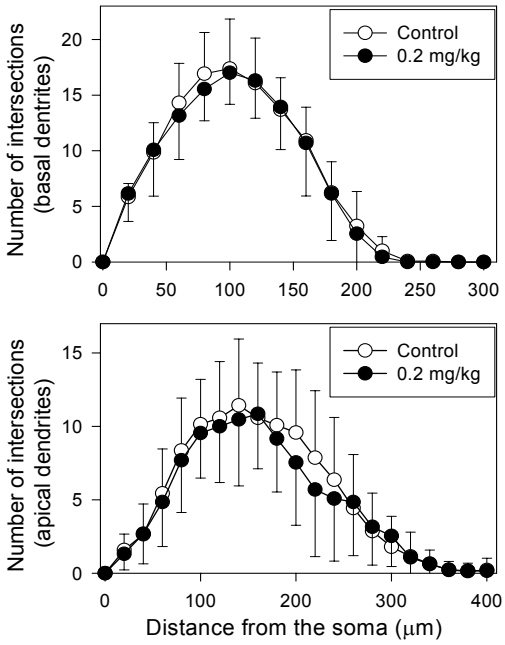

Figure 3.2.5. *Paraoxon does not alter the dendritic branching pattern of CA1 pyramidal neurons.* Sholl plots were used to describe the arborization pattern of the basal (top graph) and apical (bottom graph) dendrites at P21. The number of intersections made by the dendritic branches in cells from control (open symbols) and in 0.2 mg/kg paraoxon-treated (filled symbols) animals were plotted against the distance from the soma. The number of intersections of the basal or apical dendrites was counted within concentric circles spaced at 20-μm intervals from the center of the soma, and showed no differences between the two experimental groups. The points represent the mean ± S.D. of the mean of values for 14 neurons from control and 13 neurons from paraoxon-treated animals (4 animals for each group).

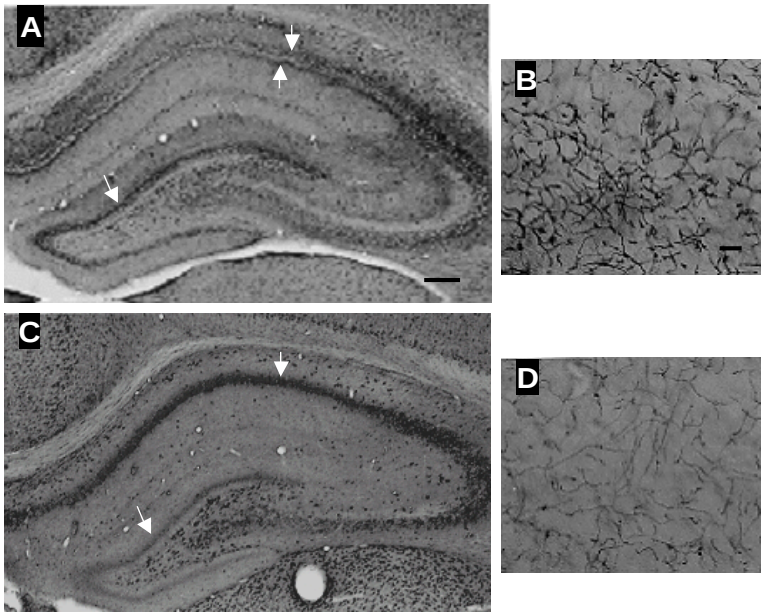

Figure 3.2.6. *Paraoxon decreases cholinesterase staining in the hippocampus and dentate gyrus.* In control slices (A), the AChE-positive fibers appeared concentrated in two bands, above and below the CA1 pyramidal layer (indicated by the arrows), and in the molecular layer of the dentate gyrus. In slices from animals treated with 0.2 mg/kg paraoxon (C), these bands in the Ammon's Horn were absent and the staining was much attenuated in the molecular layer of the dentate gyrus. Note the intense staining of the AChE-positive fibers in the detailed view of the control (B) as compared to paraoxon-treated slices (D). Calibration bars: 200 μm (A,C) and 12 μm (B,D).

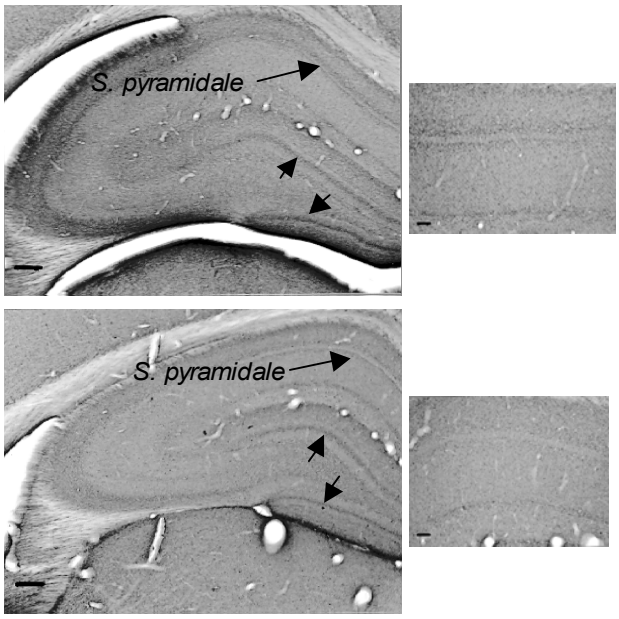

Figure 3.2.7. *Paraoxon does not alter choline acetyltransferase staining in the hippocampus and dentate gyrus.* ChAT immunohistochemistry of slices from control (top) and 0.2 mg/kg paraoxon-treated (bottom) animals shows positive staining throughout the hippocampus and dentate gyrus. A more intense staining was present at the border of the stratum pyramidale (see the detailed view, right panels) and at the internal molecular layer of the dentate gyrus (arrows). Calibration: 200 □M (left panels) and 12 □M (right panels).

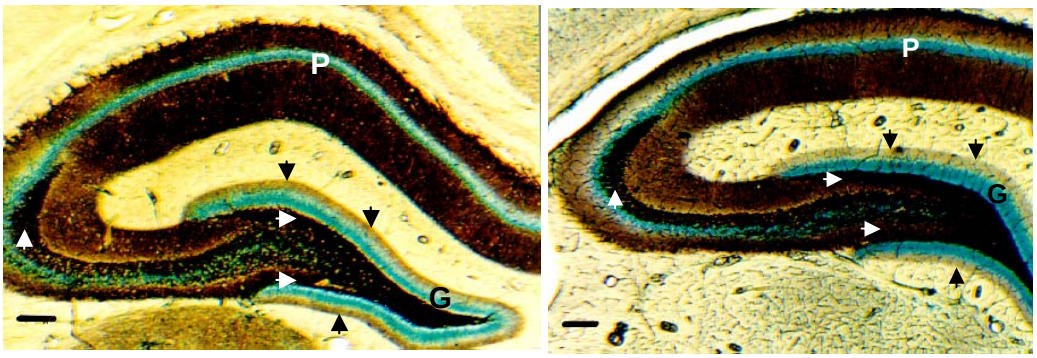

Figure 3.2.8. *Timm staining of hippocampus and dentate gyrus.* Pyramidal (P) and granular (G) cell layers (blue stain), the dentate gyrus mossy fibers (white arrows) and the associational/commissural fibers of the dentate gyrus (black arrows) and of the Ammon Horn (brown stain) are shown in Timm-stained slices. At P21, slices from control (top) and 0.2 mg/kg paraoxon-treated (bottom) animals showed no difference. Calibration bar: 200 μm.

Section 4. Countermeasures to nerve agent toxicity: initial *in vivo* studies in guinea pigs

4.1. A combination therapy consisting of galantamine and atropine effectively prevents the acute toxicity of lethal doses of soman, sarin and paraoxon: comparison with pyridostigmine and huperzine.

Materials and Methods

Animal care and treatments

Male albino guinea pigs (Crl(HA)Br; Charles River Wilmington, MA) weighing 350-420 g (5-6 week old) were used. Galantamine.HBr or galantamine methiodide at specific doses was injected intramuscularly in a hind limb, at different times and in volumes not exceeding 0.5 ml/kg, before or after subcutaneous (s.c.) injection of 1.5x or 2.0xLD50s of soman or sarin. The s.c. injection of soman or sarin was made between the shoulder blades, and the injection volume did not exceed 0.5 ml/kg. Treatment of the animals with the nerve agents was performed inside an approved fume hood and with appropriate protection as per the routine for diluting organophosphorous compounds (OPs) set forth by the U.S. Army. A gauze pad soaked with Clorox (5% sodium hypochlorite) was used to detoxify the site of injection and animals were decontaminated before disposal.

On the day of the experiments, a vial containing an aliquot (0.3 to 0.5 ml) of the U.S. Army-issued stock solution of soman (1.88-1.90 mg/ml) or sarin (1.93 mg/ml) was diluted with sterile saline to appropriate concentrations and kept on ice for the duration of the experiment. At the end of the experiments, any remainder of the diluted OP was decontaminated with 5% sodium hypochlorite prior to disposal.

Unless otherwise stated, all animals received an intramuscular (i.m.) injection of a solution of atropine sulfate (volume not exceeding 0.5 ml/kg), one min after the OP challenge, in the hind limb contralateral to the one in which the test drug, i.e. galantamine.HBr or galantamine methiodide, or control saline was injected. Solutions of each test drug were prepared at appropriate concentrations on the day of the experiment. All injections were made using disposable tuberculin syringes with 25-26 gauge needles. After all treatments, the animals were kept warm with a heat lamp and provided food and water ad lib. The animals were continuously observed for up to 8 h after the OP challenge, and every 24 h thereafter. Surviving animals were weighed every day for up to one month, and their weight in any particular day was expressed as a percentage of the weight measured on the day of the experiments. The regression coefficient of the plot of weight gain vs. days after the treatment was used as an estimate of the rate of weight gain under a given experimental condition. Onset of convulsions was the time between the OP challenge and appearance of discontinuous, involuntary skeletal muscular contractions interrupted by intervals of relaxation. Animals that showed life-threatening signs, including intense seizure activity or respiratory distress, were euthanized with CO_2. Throughout the manuscript, % of survival refers to the % of animals that were kept alive as they presented no life-threatening symptoms under a given experimental condition.

In experiments designed to investigate the involvement of the extracellular signal-regulated kinase (Erk) pathway on the effectiveness of galantamine as an antidotal therapy for OP poisoning, we used α-[amino[(4-aminophenyl) thio]methylene]-2-(trifluoromethyl)benzeneacetonitrile (SL 327) as an inhibitor of Erk kinase, with DMSO as the

vehicle. In the first set of experiments, animals received an intraperitoneal (i.p.) injection of DMSO (1-1.5 ml/kg) at 1 h prior to their treatment with 8 mg/kg galantamine.HBr or saline. At 1 h after the galantamine or saline treatment the guinea pigs received a s.c. injection of 1.5xLD50 soman. Then, at 1 min following the OP challenge, the guinea pigs were treated with 10 mg/kg atropine. Another group of animals received an i.p. injection of SL 327 (50-100 mg/kg, 1-1.5 ml/kg) instead of DMSO at 1 h prior to their treatment with 8 mg/kg galantamine or saline.

All conditions for animal maintenance conformed to appropriate federal standards and the Association for Assessment and Accreditation of Laboratory Animal Care (AAALAC) regulations and complied with the regulations and standards of the Animal Welfare Act and adhered to the principles of the Guide for the Care and Use of Laboratory Animals (NRC 1996).

Histopathological analyses of the brain of guinea pigs subjected to different treatments

Guinea pigs were anesthetized with pentobarbital at appropriate times after their treatments, subjected to transcardiacal perfusion with 0.9% saline (70 ml/min) until blood was cleared followed by perfusion with 10% formalin at room temperature. Brains were immediately removed and placed in fixative (10% formalin) for no longer than 48 h. Brains were then dehydrated and embedded in paraffin. Sections 5-μm thick were cut and dried in an incubator at 37°C for 12 h before they were stained with Fluoro-Jade B (Schmued and Hopkins, 2000). After mounting, the tissue was examined using an epifluorescent microscope with blue (450–490 nm) excitation light and a filter for fluorescein isothiocyanate. Photomicrographs were taken with a digital microscope camera (AxioCam, Zeiss, Jena, Germany).

Analysis of galantamine concentrations in the brain and plasma of guinea pigs

Brain and plasma levels of galantamine were determined by reverse phase high performance liquid chromatography (HPLC) (Claessens *et al.*, 1983; Tencheva *et al.*, 1987; Mannens, 2002) at various times after the guinea pigs received an i.m. injection of 8 mg/kg galantamine. At specific times (5, 30, 60, 120, 180 or 360 min after the galantamine injections), animals were anesthetized with CO_2. Then, blood (5-10 ml) was collected by cardiopuncture using a plastic vaccutainer heparinized system and kept in dry ice. Immediately after, the animals were exanguinated by carotid artery transection. Their brains were removed, superfused with 0.9% saline, and snap frozen in liquid nitrogen. Frozen blood samples and brains were kept at ~80°C until further processing.

Preparation of brain homogenate and extraction of galantamine

Brains were pulverized under liquid nitrogen with mortar and pestle. Typically, 1 g of pulverized brain tissue was mixed with 4 ml of high salt extraction buffer (HSEB), which consisted of 10 mM HEPES, 1.0 M NaCl, 5 mM EDTA, 5 mM EGTA, and 1% Triton X-100 (pH, 7.4), and sonicated two times on ice for 20 s. Sonicated material was freeze-thawed three times and proteins precipitated by the addition of 1/10 volume of 100% trichloroacetic acid (TCA). Samples were subjected to centrifugations for 15 min at 4 °C in a Sorvall RT6000B centrifuge with an H1000B rotor at 3000 RPM (1800 relative centrifugal force). The resulting supernatants were transferred to new tubes. The pellets were washed twice with 2.0 ml of HSEB. The supernatants and washes were pooled and made alkaline by the addition of 0.5 ml of 10 N NaOH. The aqueous phases were extracted three times with 1.5 volumes of dichloromethane. The organic phases were pooled in a glass tube and evaporated under nitrogen flow at 50 °C. The sides of the tubes were washed down with 2.0 ml of dichloromethane and evaporated again. Galantamine was recovered in 1 ml of HPLC loading buffer containing either 5 or 10 μg/ml of codeine base as internal standard. The loading buffer was composed of 85% methanol, 14% 10 mM sodium acetate, and 1% diethylamine.

Extraction of galantamine from plasma

Heparinized blood samples were centrifuged for 15 min at 4 °C at 3000 RPM, as above. Plasma was then transferred to new tubes and made alkaline by the addition of 0.25 ml of 10 N NaOH before being extracted three times with two volumes of dichloromethane. The organic phases were then dried as before and galantamine was recovered in 1 ml of HPLC loading buffer containing codeine as internal standard.

Analysis of galantamine by isocratic reverse phase HPLC

An LKB HPLC system (Bromma, Sweden) was used and consisted of a Model 2150 system controller, one Model 2150 pump, an injector valve with 0.1 ml loop, a Model 2158 UVicord SD detector equipped with a 226-nm filter, a Model 2210 single channel recorder, and a HyperClone 3 µm BDS C18 analytical column (150 x 4.6 mm) with guard column. The mobile phase (per 100 ml) consisted of 15 ml of 100 mM ammonium acetate (pH, 7.0), 15 ml acetonitrile, and 70 ml of filtered deionized water. A reasonable baseline recording at 0.8 ml/min flow rate was obtained when the column was pre-equilibrated with the mobile phase. Brain or plasma extracts were re-suspended in 1 ml of loading buffer, and 100 µl aliquots were loaded on the column. Under these conditions, galantamine eluted at 7-8 min and codeine eluted at 10-12 min. Galantamine levels were determined using the galantamine/codeine peak height ratios and a standard linear curve generated with concentrations of galantamine ranging from 0.02 to 10 µg/ml and either 5 or 10 µg/ml of codeine base.

To convert plasma galantamine concentrations from µg/ml to µM, we considered the molecular weight of galantamine as 287.4. To convert brain galantamine concentrations from µg/g to µM, we also took into account that 80% of the brain weight corresponds to water and considered that 1 g of tissue corresponds to 1 ml of water.

Radiometric enzymatic assay

Typically, 1.0 g of pulverized brain tissue was mixed with 1.0 ml of HSEB containing antiproteases (0.5 U/ml aprotinin, 30 µg/ml leupeptin, 1 mg/ml bacitracin, 2 mM benzamidine, and 5 mM N-ethylmaleimide) and subsequently sonicated for 20 s on ice. Aliquots of the resulting suspensions were used for determination of protein concentration (Pierce Micro BCA Protein Assay). The butyrylcholinesterase inhibitor tetraisopropyl pyrophosphoramide (final concentration, 1 mM) was added to the remaining suspensions and to 1 ml of heparinized blood, which were finally stored at −80°C until radiometric assay of AChE activity.

Acetylcholinesterase activity was measured with a modified two-phase radiotopic assay (Johnson and Russell, 1975) using 20 pM [^{3}H]ACh iodide (specific activity = 76 Ci/mmol), sufficient to produce approximately 200,000 cpm when totally hydrolyzed by eel AChE (2U). For the radiometric assay, 80 µl of either blood or brain suspension was mixed with 20 µl of ACh chloride and [^{3}H]ACh iodide to give a reaction volume of 100 µl (final concentration of ACh, 10 mM). Reactions were terminated by the addition of 100 µl of 1 M monochloroacetic acid, 0.5 M NaOH, and 2 M NaCl. The entire plasma sample was used for counting. However, the blood samples were centrifuged for 5 min and 100 □l of the clarified supernatant was used for counting. Four ml of the scintillation cocktail, consisting of 10% isoamyl alcohol, 0.5% 2,5 diphenyloxazole, and 0.02% 1,4 bis(4-methyl-5-phenyl-oxazol-2-yl)benzene in toluene, were added to the samples. Then, the hydrolyzed, acidified [^{3}H]acetate partitioned into the organic phase was counted on a Packard tri-carb liquid scintillation analyzer.

The *in vitro* analysis of the concentration-response relationship of galantamine-induced

AChE inhibition was made possible by comparing the enzymatic activity in untreated blood samples or brain extracts with that in blood samples or brain extracts that had been incubated for 15-30 min with known concentrations of galantamine.HBr.

Western blot analysis of Erk activation

Erk activation in the brain of guinea pigs treated with 8 mg/kg galantamine or an equivalent volume of saline was analyzed by means of western blotting (Perkins *et al.*, 2002). Animals were euthanized with CO_2 at various times after the treatments (5, 30, 60, 120, 180 and 360 min). Their brains were immediately removed, frozen in liquid nitrogen and kept at -80^{o}C until further processing.

Brains were pulverized under liquid nitrogen with a pestle and mortar. Pulverized brain tissue was then homogenized in buffer containing 20 mM Tris.HCl pH 7.5, 150 mM NaCl, 1 mM EDTA, 1 mM EGTA, 1% Triton X-100, 1% sodium dodecyl sulfate (SDS), anti-proteases (Roche Complete), and anti-phosphatases (2.5 mM sodium pyrophosphate, 1 mM β-glycerol phosphate, 1 mM sodium vanadate and 1 mM NaF). Samples were then boiled for 5 min, triturated, boiled for an additional 5 min and then placed on ice. The suspensions were subsequently sonicated and centrifuged for 5 min at 16,000 RCF. Total protein concentrations were determined using the Pierce Micro BCA kit with bovine serum albumin as standard. Samples containing equivalent amounts of protein were loaded onto 4-12% Bis-Tris gels (Invitrogen, Carlsbad, California, USA) and resolved by standard electrophoresis. Separated proteins were transferred from the gels to polyvinylidene fluoride membranes (Invitrogen, Carlsbad, California, USA). Once transferred, the membranes were incubated overnight in blocking solution containing 20 mM Tris.HCl pH 7.5, 150 mm NaCl, 0.5% Tween-20, and 5% BSA at 4^{o}C. On the next day, the membranes were incubated at room temperature for 2 h with primary antibody (rabbit anti-dually phosphorylated Erk; Promega, Madison, WI, USA), which was diluted 1:20,000 in blocking solution containing 1% BSA. The blots were washed four times for 15 min in Tris-buffered saline (20 mM Tris.HCl pH 7.5, 150 mm NaCl, 0.5% Tween-20). Subsequently, the blots were incubated at room temperature for 2 h with the secondary antibody (horseradish peroxidase-conjugated goat anti-rabbit), which was diluted 1:5,000 in the blocking solution containing 1%BSA. Afterwards, the blots were washed four times for 15 min with the Tris-buffered saline, and exposed to Kodak film using ECL chemiluminescence (Roche lumi-light, Roche, NY, USA). Finally, the blots were stripped for 30 min at 37^{o}C using the Pierce-Restore western blot stripping buffer and probed for total Erk (1:20,000; rabbit anti-total Erk, Promega) following a protocol similar to that described above.

Nerve growth factor-treated and -untreated PC12 cell extracts were used as positive controls for p-Erk and total Erk, respectively. The untreated extract was also used as a negative control for the detection of activated Erk. Appropriate controls for antibody specificity were also analyzed by probing the membranes with the secondary antibody without previous incubation with the primary antibody. Finally, appropriate dilutions for the primary and secondary antibodies were determined empirically to give a linear response over a range of extract concentrations.

The bands from the western blots were quantified on film with densitometry using a digital camera and the Image Quant software to determine the levels of immunoreactivity. Phosphorylated Erk (p-Erk) immunoreactivity was normalized to total Erk immunoreactivity and expressed as percentage of control.

Behavioral assays

Locomotor activity and stereotypy of guinea pigs were analyzed in an open field arena equipped with infrared sensors (AccuScan Instruments, Inc., Columbus, OH) as described by June *et al.* (June *et al.*, 1995). Counts obtained from the total number of interruptions of the infrared beams were automatically compiled every 5 min and processed for measures of total distance traveled and stereotypy.

Drugs

Atropine sulfate, pyridostigmine bromide, ±-huperzine A, and paraoxon were purchased from Sigma-Aldrich (St. Louis, MO). SL-327 was purchased from Sigma-Aldrich and from Tocris Bioscience (Ellisville, MO). [^{3}H]ACh iodide was purchased from Perkin Elmer Life Sciences (Boston, MA). Galantamine.HBr was a generous gift from Dr. Alfred Maelicke (Galantos Inc., Mainz, Germany). Galantamine methiodide, soman and sarin were obtained from the U.S. Army Medical Research and Development Command.

Results

Clear signs of cholinergic hyperexcitation, including miosis, increased chewing, hypersalivation, muscle fasciculations, difficulty in breathing, and loss of motor coordination, were evident at 5-15 min after the s.c. injection of 1.5xLD50 of soman (42 μg/kg) or sarin (63 μg/kg) in prepubertal male guinea pigs. Although an i.m. injection of atropine (6-16 mg/kg) immediately after the OP challenge attenuated the muscarinic signs, all animals showed tremors and intense convulsions within 15-30 min after the challenge. Atropine-treated, OP-challenged guinea pigs were euthanized as they developed life-threatening symptoms, and at 24 h after the exposure to nerve agents only 11% of the animals (7 of 65) remained alive.

All guinea pigs that were pre-treated with 5-12 mg/kg galantamine and post-treated with 10 mg/kg atropine survived the s.c. injection of 1.5xLD50 soman or sarin, with no toxic signs either before or after the OP exposure. The ED50 values of galantamine for 24-h survival of animals exposed to soman or sarin were 1.82 ± 0.37 or 2.2 ± 0.50 mg/kg, respectively (Figs. 4.1.1A,1B). The optimal dosage of galantamine changed as the OP levels increased. For example, in animals post-treated with 10 mg/kg atropine, the ED50 for galantamine to prevent the lethality of 2.0xLD50 soman was 5.1 ± 0.66 mg/kg (mean ± SEM, n = 8-10 animals/group) with 100% 24-h survival being achieved with ≥ 8 mg/kg (Fig. 4.1.1A). Effective doses of galantamine were well tolerated; only animals that received 16-20 mg/kg galantamine showed adverse symptoms, which lasted 10-15 min and included increased chewing, hypersalivation, fasciculations and tremors.

Muscarinic blockade by atropine contributed to the antidotal effectiveness. Regardless of whether animals were pre-treated with 5 or 8 mg/kg galantamine, 50% reduction of the lethality of those nerve agents was achieved with similar doses of atropine (mean ± SEM = 5.7 ± 0.47 mg/kg and 5.2 ± 0.13 mg/kg, respectively). However, a synergistic interaction occurred between galantamine and ≥ 6 mg/kg atropine; increasing the dose of galantamine from 5 to 8 mg/kg decreased the dose of atropine needed to protect the animals from the toxicity of soman (Fig. 4.1.1C). Doses of galantamine and atropine required to treat OP intoxication may be optimized using response surface methods (Carter *et al.*, 1985).

The acute toxicity of paraoxon, the active metabolite of the OP insecticide parathion, was also effectively counteracted by therapy consisting of galantamine and atropine. All guinea pigs treated with atropine (10 mg/kg, i.m.) immediately after their exposure to ≥ 1.8 mg/kg paraoxon developed life-threatening symptoms and were euthanized. In contrast, all atropine-treated animals survived with no signs of toxicity when they received galantamine (8 mg/kg, i.m.) 30 min before their exposure to 2 mg/kg paraoxon (Fig. 4.1.1D). Further, galantamine/atropine-treated animals that survived the challenge with 3 mg/kg paraoxon (Fig.

4.1.1D) displayed only brief, mild signs of intoxication that included increased chewing and slight tremors.

The effectiveness of the antidotal therapy consisting of galantamine/atropine surpassed that of a combination of pyridostigmine and atropine in preventing acute OP toxicity. Only a fraction of animals pre-treated with pyridostigmine (26-65 μg/kg) and post-treated with 10 mg/kg atropine survived the challenge with 1.5xLD50 soman (Fig. 4.1.1E). The effectiveness of this therapy increased as the dose of pyridostigmine was raised to 52 μg/kg (Fig. 4.1.1E). Increasing the dose of pyridostigmine to 65 μg/kg, however, decreased the effectiveness of the treatment, most likely because the potential benefit of increasing the protection of AChE from the actions of OPs is counteracted and eventually outweighed by the simultaneous pyridostgimine-induced inhibition of BuChE, an enzyme that serves as an endogenous scavenger of OPs (Doctor *et al.*, 1991).

The safety of the antidotal therapy consisting of galantamine/atropine was far greater than that of a combination of huperzine and atropine. Approximately 80% of the animals challenged s.c. with 1.5xLD50 soman survived if they were pretreated with 100-200 μg/kg huperzine and post-treated with 10 mg/kg atropine; the minimum dose of huperzine needed to provide 100% survival of soman-challenged, atropine-treated guinea pigs was 300 μg/kg (Fig. 4.1.1E). However, at doses $\geq$ 300 μg/kg, huperzine triggered transient, albeit incapacitating side effects that included profuse secretions, muscle fasciculations, abnormal gait, tremors, and respiratory distress. The stereotypic behavior of animals treated with huperzine was quantitatively analyzed in an open field arena, as described below.

Galantamine maintains long-term survival of OP-challenged, atropine-treated guinea pigs and has no significant effect on gross behavior of the animals: Comparison with huperzine. Even though all animals survived the first 24 h after the soman challenge when they were pre-treated with 6 mg/kg galantamine and post-treated with 6 mg/kg atropine, only 80% of them remained alive after the third day post-OP exposure (Fig. 4.1.2A). In contrast, during the entire observation period, survival remained at 100% in animals pre-treated with 5-8 mg/kg galantamine and post-treated with 10 mg/kg atropine. Increasing the dose of atropine to 16 mg/kg reduced the acute and long-term efficacy of doses of galantamine < 8 mg/kg (Fig. 4.1.2A). Thus, 10 mg/kg atropine ensures the highest long-term effectiveness of galantamine against of 1.5xLD50 soman.

Within one week after a single i.m. injection of saline, galantamine (8 mg/kg), or atropine (10 mg/kg), guinea pigs gained weight at similar rates, i.e., 2.51 $\pm$ 0.11 %/day, 2.30 $\pm$ 0.05 %/day, and 2.37 $\pm$ 0.03 %/day (Fig. 4.1.2B). In contrast, guinea pigs that received a single i.m. injection of huperzine (300 μg/kg) gained weight at a rate of 1.72 $\pm$ 0.17 %/day (Fig. 4.1.2B), which is significantly slower than that estimated for saline-injected animals ($p < 0.01$ compared to saline-injected animals according to ANOVA followed by Dunnett). Although galantamine/atropine-treated, soman-challenged animals lost on average 10% of their body weight at 24 h after the OP exposure (Fig. 4.1.2B), their rate of weight gain during the remaining recovery period (2.72 ± 0.26%/day) was not significantly different from that of saline-treated animals that were not challenged with soman. Galantamine/atropine was equally effective in maintaining the rates of weight gain of guinea pigs challenged with 1.5xLD50 sarin or 3 mg/kg paraoxon at 2.53 $\pm$ 0.20 %/day or 2.66 $\pm$ 0.21 %/day (mean $\pm$ SEM), respectively. The acute toxicity of huperzine in preventing OP poisoning was not reflected in the rates of weight gain of animals that survived the OP challenge when treated with huperzine/atropine (Fig. 4.1.2B).

In an attempt to quantify potential untoward behavioral effects of doses of galantamine and huperzine needed to prevent acute OP poisoning, the overall ambulatory activity of guinea pigs was examined in an open field arena. Previous studies reported that other centrally acting AChE inhibitors, including physostigmine, decrease locomotor activity and stereotypic behavior of rodents in the open field (Silvestre *et al.*, 1999). Further, inhibition of the N-methyl-D-aspartate (NMDA) type of glutamate receptors, a mechanism that appears to contribute to the effectiveness of huperzine in preventing OP toxicity (Gordon *et al.*, 2001), is known to increase stereotypy in rodents (Koek *et al.*, 1988).

Each guinea pig, immediately after receiving an i.m. injection of saline, galantamine (8 mg/kg) or huperzine (300 μg/kg), was placed in an open field arena equipped with infrared sensors. At the dose tested, galantamine had no significant effect on the overall locomotor activity of guinea pigs (Fig. 4.1.2C). However, huperzine increased the locomotor activity of the animals, and this effect became significant at 30 min after the treatment (Fig. 4.1.2C). At this time, a distinct pattern of locomotor stereotypy, including repetitive routes of locomotion in the open field arena, was also significantly higher in huperzine- than in saline-treated animals (Fig. 4.1.2C). These effects of huperzine resemble those of the NMDA receptor antagonists ketamine, phencyclidine and dizolcipine (Koek *et al.*, 1988).

Galantamine can be safely used as a pre- or post-treatment to counteract acute OP toxicity: Therapeutic windows of time

An effective antidotal therapy should afford long-lasting protection for first responders who will attend a population acutely exposed to toxic levels of OPs. Thus, experiments were designed to determine how long before an exposure to OPs an acute pre-treatment with galantamine would remain effective in preventing their toxicity. All atropine-treated guinea pigs that received 8 mg/kg galantamine up to 1 h before soman survived with no signs of toxicity (Fig. 4.1.3A). As the interval between the injections of galantamine and soman increased beyond 1 h, the survival decreased (Fig. 4.1.3A). Increasing the dose of galantamine to 10 mg/kg prolonged the time within which the antidotal therapy remained effective (Fig. 4.1.3A).

Considering the difficulty of predicting when a person will be exposed to toxic levels of OPs under battlefield conditions, in the case of a terrorist attack, or during handling of insecticides, experiments were also designed to determine whether post-treatment with galantamine could effectively counteract the acute toxicity of OPs. All animals treated with 8 or 10 mg/kg galantamine at 1 or 5 min after the soman challenge survived (Fig. 4.1.3B) with no signs of intoxication; rate of weight gain and gross behavior of these animals were indistinguishable from those of saline-treated animals that were not exposed to soman. Galantamine was no longer effective when administered 10 min after soman. Post-treatment with galantamine/atropine also prevented the acute toxicity of supra-lethal doses of paraoxon (Fig. 4.1.3C). The therapeutic window of time within which post-treatment with galantamine remained effective in sustaining 100% survival of the animals decreased as the dose of the OP increased (Fig. 4.1.3C).

No signs of neurotoxicity were observed in the brains of atropine-treated guinea pigs that received galantamine before or after the challenge with soman. Neurodegeneration in three areas of the brain, the pyriform cortex, the amygdala and the hippocampus, is characteristic of OP intoxication. The components of the antidotal therapy regimen, by themselves, were not neurotoxic. No signs of brain damage were detected at 24 h after an i.m. injection of saline (Fig. 4.1.4A), 8 mg/kg galantamine (Fig. 4.1.4B), or 10 mg/kg atropine (data not shown). Galantamine is a critical component of the antidotal therapy regimen, because

atropine alone was unable to prevent the well described neuronal death triggered by 1.5xLD50 soman (Fig. 4.1.4C). Large numbers of shrunken neurons that were labeled with Fluoro Jade-B (FJ-B), an anionic fluorescein derivative that binds with high affinity to degenerating cells, were consistently seen in the hippocampus, amygdala and pyriform cortex of atropine-treated guinea pigs that survived for 24 h after the challenge with 1.5xLD50 soman (Fig. 4.1.4C). In contrast, staining with FJ-B was rarely seen in brain sections of soman-challenged, atropine-treated animals that were given 8 mg/kg galantamine at 30 min before or 5 min after the OP (Figs. 4.1.4D,4E). Further, the edema observed in the hippocampus and the marked parenchymal spongy state of the amygdala and pyriform cortex of soman-exposed, atropine-treated animals were absent in animals that received galantamine 30 min before or 5 min after the nerve agent (Figs. 4.1.4C-E).

Examine potential mechanisms underlying the effectiveness of the best treatment

To help establish the clinical relevance of the doses of galantamine needed to counteract OP poisoning, plasma and brain concentrations of the drug were determined by HPLC at various times after treatment of guinea pigs with 8 mg/kg galantamine. This dose was selected because: (i) in association with atropine, it afforded full protection against OP-induced toxicity and lethality, and (ii) it was half of the minimum dose at which galantamine triggered mild side effects.

In guinea pigs, as in humans (Bickel *et al.*, 1991), plasma levels of galantamine declined with first-order kinetics. After an i.m. injection of 8 mg/kg galantamine, plasma and brain levels of the drug peaked at 30 min and decayed with half-times of 71.7 $\pm$ 14.4 min and 57.8 ± 4.31 min, respectively (Fig. 4.1.5A,5B). As shown in Fig. 4.1.3A, full protection against acute toxicity was achieved when 8 mg/kg galantamine was administered to guinea pigs up to 1 h before soman, a time when plasma and brain levels of the drug were 0.90 ± 0.01 μg/ml and 0.80 ± 0.04 μg/g, respectively (Fig. 4.1.5A, B). Since the molecular weight of galantamine is 287.4, these findings suggest that the minimal plasma concentration of galantamine needed to prevent OP toxicity and lethality is approximately 2.8 μM. Doses of galantamine recommended for treatment of AD patients are between 8 to 24 mg/day (Corey-Bloom, 2003), and peak plasma concentrations ranging from 0.2 to 3 μM have been detected in healthy human subjects treated, orally or s.c., with a single dose of 10 mg galantamine (Bickel *et al.*, 1991; Miheilova *et al.*, 1989). Thus, doses of galantamine needed to prevent OP toxicity generate peak plasma concentrations similar to those achieved with doses clinically used to treat AD.

In agreement with the concept that galantamine-induced AChE inhibition is reversible, the degree of AChE inhibition in brain and blood from galantamine-treated guinea pigs decreased as the galantamine levels declined in both compartments and became negligible at 6 h after the treatment (Fig. 4.1.5C), when plasma and brain levels of the drug were < 0.1 μg/ml and 0.1 μg/g, respectively (Fig. 4.1.5A,5B). Maximal inhibition of blood AChE activity was approximately 70% (Fig. 4.1.5C), observed at 30 min after the treatment when plasma levels of galantamine had peaked. The effectiveness of galantamine in AD patients has been correlated with AChE inhibition in blood of 40-70% (Jann *et al.*, 2002).

Maximal AChE inhibition in the brain of galantamine-treated animals was significantly different from that observed in their blood (Fig. 4.1.5C). Measured peak concentrations of galantamine were 1.6 ± 0.13 μg/ml in the plasma and 1.38 ± 0.11 μg/g in the brain. These concentrations resulted in approximately 70% and 25% inhibition of AChE in the blood and brain, respectively. Measured peak levels of galantamine in the plasma correspond to 5.6 $\pm$ 0.5 μM. Considering 80% of the brain weight as water, measured peak levels of galantamine in brain tissue would correspond to 3.8 $\pm$ 0.3 μM. Based on the concentration-response

relationships obtained for galantamine-induced inhibition of guinea pig blood and brain AChE *in vitro* (Fig. 4.1.5D), it is estimated that 5.6 μM galantamine would inhibit blood AChE activity by 68%, and 3.8 μM galantamine would inhibit brain AChE activity by 25%. In *vitro*, galantamine inhibited guinea pig blood and brain AChE with EC50s of 1.8 ± 0.38 μM and 16.9 ± 9.8 μM, respectively (mean ± SEM; Fig. 4.1.5D). In humans, blood AChE activity is also ten-fold more sensitive to inhibition by galantamine than brain AChE activity (Thomsen *et al.*, 1991).

To verify whether a large degree of blood AChE inhibition alone could explain the effectiveness of galantamine, a quaternary derivative of galantamine – galantamine methiodide – was tested for its ability to prevent OP-induced toxicity and lethality. Guinea pigs were treated i.m. with 9.3 mg/kg galantamine methiodide and 10 mg/kg atropine at 30 min before and 1 min after, respectively, their challenge with 1.5xLD50 soman. Although the same degree of inhibition of blood AChE was achieved with 8 mg/kg galantamine and 9.3 mg/kg galantamine methiodide (data not shown), the latter only protected 25% of the animals from toxicity and lethality induced by soman (Figure 4.1.6A). These findings suggest that actions of galantamine in the brain are important determinants of its ability to halt OP toxicity.

The nicotinic APL action distinguishes galantamine from other AChE inhibitors and contributes to its ability to decrease neurodegeneration and to improve synaptic transmission in the brain (Pereira *et al.*, 2002; Arias *et al.*, 2004; Kihara *et al.*, 2004). Long-lasting effects of nicotinic ligands, including galantamine, appear to result from nAChR-mediated, Ca^{2+}-dependent activation of signaling pathways, including Erk (Dajas-Bailador and Wonnacott, 2004), a critical modulator of neuronal excitability and viability. Evidence that Erk activation also has a protective role during seizures in humans and in animal models of epilepsy (Berkeley *et al.*, 2002; Jiang *et al.*, 2005) led us to ask whether treatment of guinea pigs with galantamine results in activation of Erk in the brain, and, if so, whether Erk activation contributes to the effectiveness of galantamine in preventing OP toxicity and/or lethality.

Phosphorylated, activated Erk1/2 (P-Erk1/2) in brain extracts obtained from guinea pigs at various times after their i.m. treatment with 8 mg/kg galantamine was detected by western blotting. Two bands consistent with the two Erk isoforms were seen in blots of brain extracts from guinea pigs (Figure 4.1.6C). Densitometric analyses of the blots revealed that levels of total Erk1/2 in brain extracts obtained from saline- or galantamine-treated guinea pigs were not statistically different, and, therefore, antibody to total (phosphorylated and unphosphorylated) Erk1/2 served as the control for gel loading or other technical artifacts. Ratios of P-Erk1/Erk1 in the brain of saline- and galantamine-treated animals were not significantly different, whereas ratios of P-Erk2/Erk2 increased with time up to 3 h after the galantamine treatment (Figure 4.1.6C). The nicotinic APL action, which subserves the ability of galantamine to activate the phosphatidylinositol-3 kinase pathway in a neuroblastoma cell line (Kihara *et al.*, 2004), may also underlie the Erk activation by galantamine in the guinea pig brain.

The compound α-[amino[(4-aminophenyl) thio]methylene]-2-(trifluoromethyl) benzene-acetonitrile (SL-327) was used to evaluate whether inhibition of Erk kinase, the protein kinase that phosphorylates and activates Erk, alters the effectiveness of galantamine in preventing OP toxicity and/or lethality. SL-327 was the inhibitor of choice, because it effectively crosses the blood brain barrier when administered systemically (Atkins *et al.*, 1998). Control experiments established that: (i) dimethylsulfoxide (DMSO), the vehicle used to dissolve SL-327, affected neither the toxicity of soman nor the effectiveness of galantamine in preventing it (Shih *et al.*, 2003), and (ii) a single intraperitoneal injection of 50 or 100 mg/kg SL-327 (2 ml/kg), doses previously shown to cause substantial inhibition of Erk activation in the brain of rodents (Berkeley *et al.*, 2002; Atkins *et al.*, 1998), had no significant effect on the gross behavior or rate of weight gain of guinea pigs. Thus, at 60 min after the treatment with the inhibitor, guinea

pigs received an i.m. injection of 8 mg/kg galantamine or saline. At 30 min after the galantamine or saline treatment, the animals were challenged with 1.5xLD50 soman, and at 1 min afterward they were treated with 10 mg/kg atropine. Soman-challenged guinea pigs that did not receive galantamine developed life-threatening tonic-clonic convulsions and were euthanized. Notwithstanding the treatment with SL-327, galantamine was still capable of preventing death of soman-challenged animals. However, 30 to 40 min after OP challenge, guinea pigs that received 50 and 100 mg/kg SL-327 prior to galantamine showed tremors and convulsions, respectively. Further, SL-327 decreased the effectiveness of galantamine to prevent weight loss induced by soman. The rate of weight gain of galantamine-treated, OP-challenged animals decreased from 3.1 $\pm$ 0.4 %/day to 2.3 $\pm$ 0.5%/day in the group of animals treated with DMSO and 100 mg/kg SL-327, respectively, before galantamine ($p < 0.05$; ANOVA followed by Tukey post-hoc test). These results suggest that the effectiveness of galantamine in preventing OP toxicity is mediated in part by its ability to activate Erk in the brain.

Discussion

The present study demonstrates the remarkable potential of galantamine to improve antidotal therapy for even the most deadly OPs. In combination with atropine, well-tolerated, clinically relevant doses of galantamine administered acutely either before or soon after an exposure to the nerve agents soman and sarin or of paraoxon, the active metabolite of the OP insecticide paraoxon, fully counteract the toxicity and lethality of these compounds. While atropine alone attenuates the muscarinic syndrome resulting from the exposure of the guinea pigs to the OPs, it does not afford significant protection against their lethality.

The exact mechanisms that account for the superiority of galantamine as a countermeasure against OP poisoning are yet to be fully elucidated. However, it can be postulated that the effectiveness of galantamine is related both to the higher potency with which it inhibits AChE compared to BuChE (Thomsen and Kewitz, 1990), an action that should help preserving the scavenger capacity of plasma BuChE for OPs, and to the protection of brain AChE from OP-induced irreversible inhibition. The finding that galantamine was essential to counteract soman-induced neurodegeneration in the brain supports the notion that AChE-related and/or- unrelated actions of this drug in the CNS contribute to its effectiveness. Neuronal loss in the brains of OP-intoxicated animals correlates to some extent with the intensity and duration of OP-triggered seizures (McDonough and Shih, 1997; Filliat *et al.*, 1999; Myhrer *et al.*, 2005). Yet, neurodegeneration and consequent cognitive impairment induced by OPs can be significantly reduced by therapeutic interventions that, although unable to suppress OP-triggered seizures, effectively decrease glutamate excitotoxicity (Jiang *et al.*, 2005). The ability of the galantamine-based therapy to prevent OP-induced convulsions and the well-reported neuroprotective effect of galantamine against different insults (Pereira *et al.*, 2002; Arias *et al.*, 2004; Kihara *et al.*, 2004; Nakamizo *et al.*, 2005, Capsoni *et al.*, 2002), which involves activation of intracellular pathways such as Erk, may be important determinants of the antidotal effectiveness. Since no cognitive impairment has been detected in soman-challenged animals when neuronal loss in their brains remains below a certain threshold (Filliat *et al.*, 1999), galantamine is likely to maintain normal cognitive performance of OP-exposed subjects.

Inhibition of brain AChE by > 60-70% has been shown to trigger severe incapacitating effects, including seizures (Todulli *et al.*, 1999). Maximal degrees of inhibition of AChE activities observed in guinea pigs treated with doses of galantamine that effectively counteracted OP intoxication were about 75% in blood and 30% in brain. All other centrally acting AChE inhibitors studied to date, including huperzine, acutely prevent OP toxicity when used at doses that decrease blood AChE activity by >70% (Desphande *et al.*, 1986; Grunwald *et al.*, 1994; Fricke *et al.*, 1994; Lallement *et al.*, 2002). However, brain AChE activity is inhibited to a similar large extent by these drugs (Lallement *et al.*, 2002). Therefore, while a

high degree of reversible and selective AChE inhibition in the blood appears to be necessary to acutely counteract the peripheral toxic effects of OPs, a low degree of reversible inhibition of brain AChE may be essential to protect a significant pool of the enzyme from OP-induced irreversible inhibition and critical to limit the occurrence of untoward side effects of centrally acting reversible AChE inhibitors.

Development of effective and safe antidotes against OP toxicity will help improve treatment of victims of a terrorist attack with nerve agents and help reduce the mortality associated with OP insecticide poisoning worldwide. The demonstration that an acute treatment with a galantamine-based therapy effectively and safely counteracts OP poisoning is, therefore, of utmost relevance for farmworkers and others who handle OP insecticides, for the general population under threat of OP exposure in terrorist attacks, and for soldiers, who, despite the Geneva Protocol, may be exposed to deadly nerve agents in the course of battle.

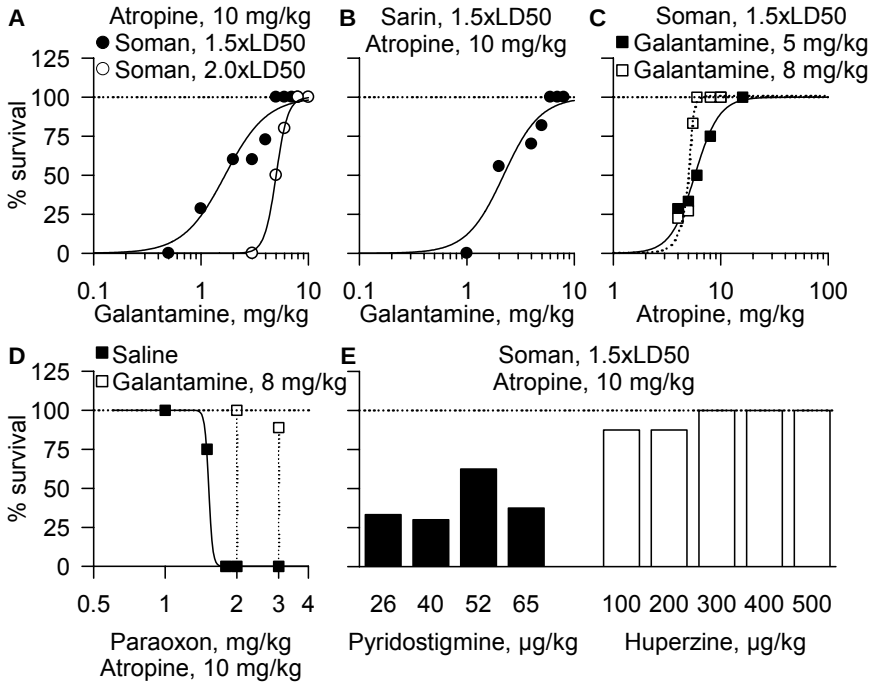

Figure 4.1.1. *Pre-treatment with galantamine prevents the acute toxicity of lethal doses of OPs: Comparison with pyridostigmine and huperzine.* In all experiments, guinea pigs received an i.m. injection of selected doses of galantamine, pyridostigmine, or huperzine followed 30 min later by a single s.c. injection of 1.5xLD50 (42 μg/kg) or 2.0xLD50 (56 μg/kg) soman, 1.5xLD50 sarin (56 μg/kg, s.c.), or indicated doses of paraoxon. At 1 min after the OP challenge, all animals received atropine (1-10 mg/kg, i.m.). A-C, dose-response relationships for galantamine or atropine to maintain 24-h survival of animals challenged with nerve agents. D, dose-response relationship for paraoxon-induced decrease in 24-h survival of atropine-treated guinea pigs that were pre-treated with saline or galantamine. E, effects of increasing doses of pyridostigmine or huperzine in maintaining 24-h survival of soman-challenged, atropine-treated animals. Each group had 8-12 animals. Percent survival represents the % of animals that were kept alive as they presented no life-threatening symptoms.

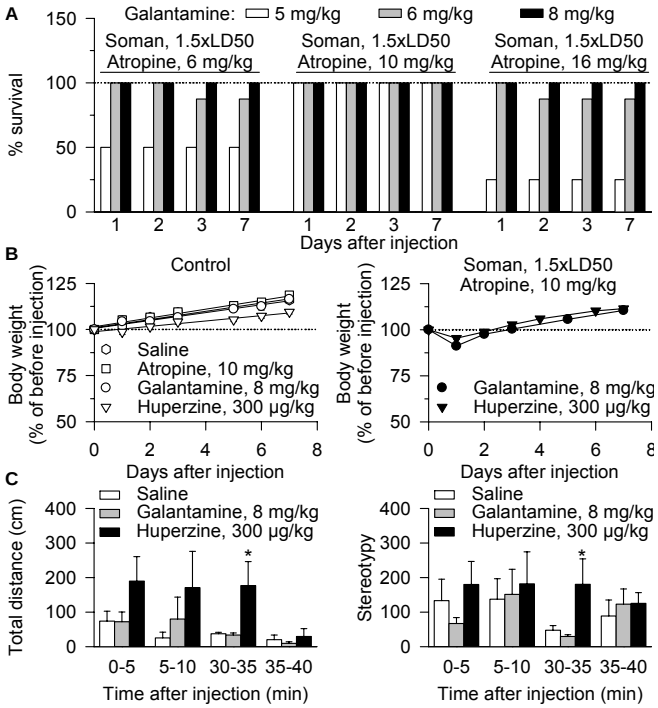

Figure 4.1.2. *Long-term effectiveness and acute toxicity of different antidotal therapies against OP poisoning.* **A.** Seven-day survival of guinea pigs treated with galantamine at 30 min before and atropine at 1 min after their challenge with 1.5xLD50 soman. Each group had 8 to 12 animals. **B.** Seven-day follow-up of the weight of animals subjected to different treatments. Weights are expressed as % of the weights measured 1 h before the first treatment. Control groups consist of animals that received a single i.m. injection of atropine, galantamine, huperzine or saline. The soman/atropine groups consist of animals treated with galantamine or huperzine at 30 min before and atropine at 1 min after soman (n = 5-8 animals/treatment). **C.** Graphs of average total distance traveled and stereotypy of guinea pigs at the indicated times after their received an i.m. injection of saline, galantamine, or huperzine (n = 6 animals/treatment). In **B** and **C**, results are presented as mean $\pm$ SEM. Asterisk indicates that results from huperzine- and saline-treated animals are significantly different at $p < 0.05$ (ANOVA followed by Dunnett post-hoc test).

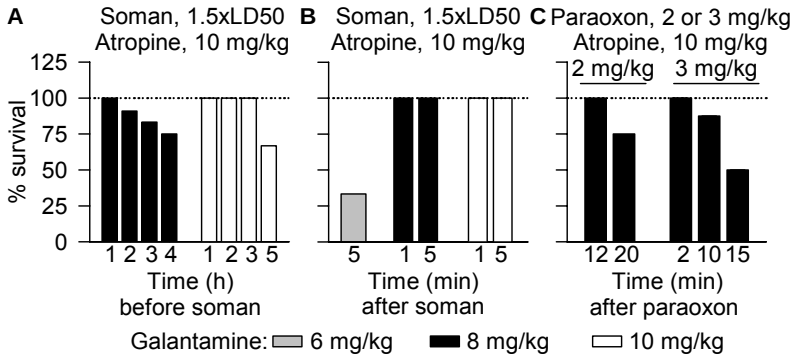

Figure 4.1.3. *Efficacy of galantamine as a pre- or post-treatment for OP poisoning is dose and time dependent.* A. 24-h survival of animals that received a single i.m. injection of 8 or 10 mg/kg galantamine at 1, 2, 3, 4, or 5 h before the s.c. injection of 1.5xLD50 soman that was followed 1 min later by an i.m. injection of 10 mg/kg atropine. B and C. Panels display the 24-h survival of animals that received a single i.m. injection of specific doses of galantamine at different times after their challenge with 1.5xLD50 soman or 2-3 mg/kg paraoxon, respectively. Each group had 8-10 animals.

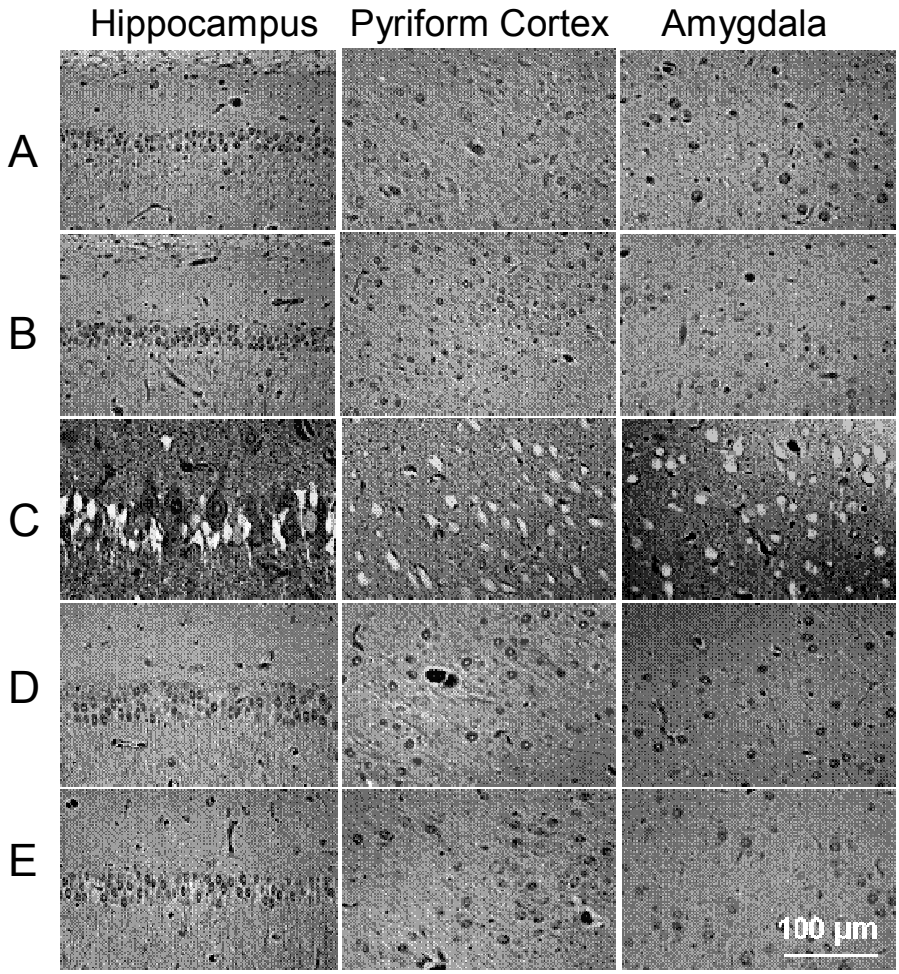

Figure 4.1.4. *Soman-induced neurodegeneration is not present in the hippocampus, pyriform cortex and amygdala of guinea pigs pre- or post-treated with galantamine.* A and B. Representative photomicrographs of the hippocampal CA1 field, the pyriform cortex and the amygadala of guinea pigs that were euthanized 24 h after an i.m. injection of saline (A) or 8 mg/kg galantamine (B). No FJ-B-positive neurons were seen in the brains of these animals. C. Large numbers of FJ-B-positive neurons were seen in all three index areas of the brain of a guinea pig that survived for 24 h after the challenge with 1.5xLD50 soman. D and E. FJ-B-positive neurons were rarely seen in brain sections of animals that received galantamine (8 mg/kg, i.m.) at 30 min before (D) or 5 min after (E) soman. In C-E, all animals received atropine (10 mg/kg, i.m.) at 1 min after the OP and were euthanized at 24 h after the OP challenge. Photomicrographs are representative of results obtained from each group, which had 5 animals.

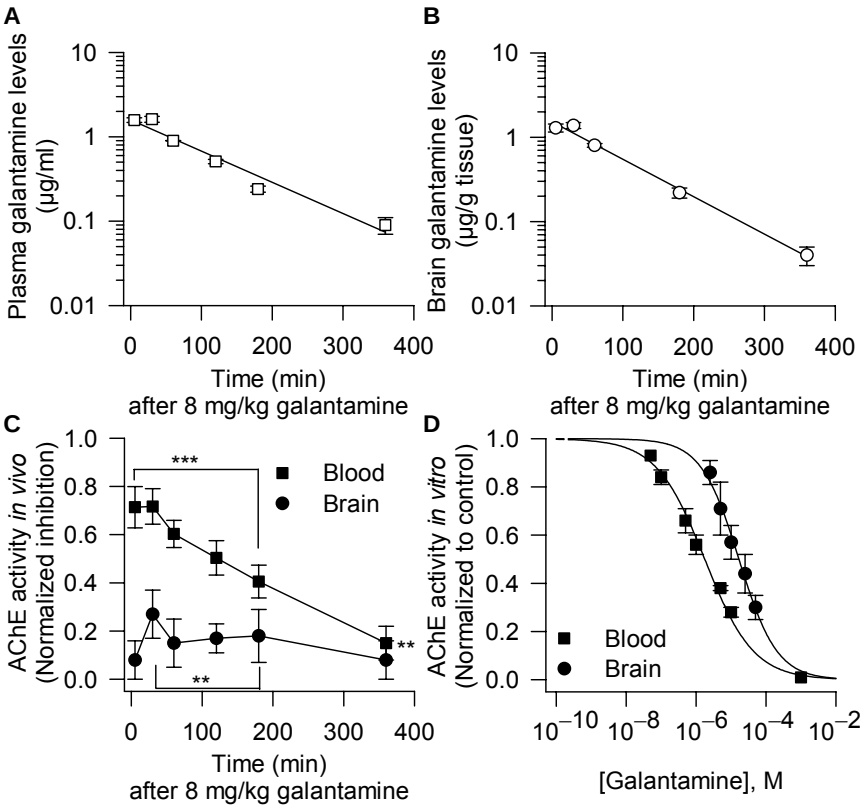

Figure 4.1.5. *Differential sensitivity of brain and blood AChE activities to inhibition by galantamine in vivo and in vitro.* **A** and **B**. Logarithm of the concentrations of galantamine measured in blood and brain samples obtained at various times after treatment of guinea pigs (n = 4-6 animals/time point) with galantamine (8 mg/kg, i.m) is plotted against time. **C.** AChE activity measured in samples from saline-treated animals was taken as 1 and used to normalize the enzyme activity measured in samples obtained at various times after treatment of animals with galantamine (8 mg/kg, i.m.). Normalized inhibition (1 – normalized activity) is plotted against the time at which samples were obtained. Asterisks indicate that results from galantamine- and saline-treated animals are significantly different at $p < 0.001$ (***) or < 0.01 (**) (ANOVA followed by Dunnett post-hoc test). In **A-C**, the first point corresponds to results obtained at 5 min after the treatment. **D.** Increasing concentrations of galantamine were added *in vitro* to brain homogenates and blood samples obtained from naive animals. AChE activity in untreated samples was taken as 1 and used to normalize activity measured in galantamine-treated samples. The graph of normalized AChE activity vs. galantamine concentrations was fitted with the Hill equation. Results are presented as mean and SEM (n = 4-6 animals/galantamine concentration).

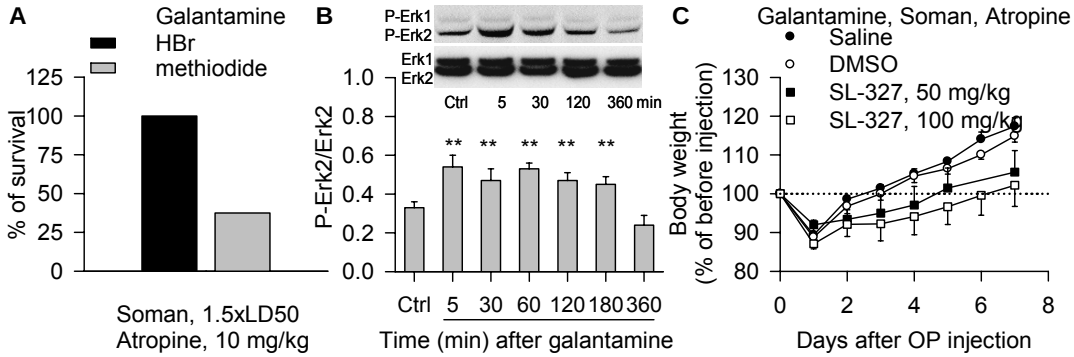

Figure 4.1.6. *Mechanisms that contribute to the effectiveness of galantamine as an antidotal therapy for OP poisoning.* A. Plot of the 24-h survival of guinea pigs treated with 8 mg/kg galantamine hydrobromide or an equivalent dose of the quaternary derivative of galantamine, galantamine methiodide (9.3 mg/kg) at 30 min prior to their challenge with 1.5xLD50 soman. The lower survival of the animals treated with galantamine methiodide suggested that actions of galantamine in the CNS are important for its effectiveness. Each experimental group included 8-12 animals. B. Galantamine induces Erk activation in the brain of guinea pigs. Brains were removed from guinea pigs at 5, 30, 120 and 360 min after they received an i.m. injection of 8 mg/kg galantamine. Control animals received an i.m. injection of an equivalent volume of saline. Each experimental group consisted of 3 animals. Proteins in brain extracts were resolved by electrophoresis, transferred to PVDF membranes, and immunoblotted with an antibody specific for P-Erk1/2 (inset). Blots were subsequently stripped and reprobed with an antibody to Erk1/2 (inset). Protein levels were quantified by densitometric scanning, and the results are expressed as P-Erk/Erk ratios for each time point after the injection of galantamine. Data are presented as mean and S.E.M. of results obtained from 3 animals. Asterisks indicate that results obtained at any given time after treatment with galantamine are significantly different from control. **, $p < 0.01$ (ANOVA followed by Dunnet post-hoc test). C. Galantamine-induced Erk activation contributes to its effectiveness as an antidote for OP poisoning. Weight gain of animals that received an i.p. injection of 2 ml/kg of saline, DMSO or SL-327 (50 or 100 mg/kg) at 1 h prior to their treatment with 8 mg/kg galantamine. At 1 h after the galantamine treatment, the animals were challenged with 1.5xLD50 soman. All animals in A-C received an i.m. injection of 10 mg/kg atropine at 1 min after the OP challenge. Symbols represent the mean and S.E.M. of results obtained from 5 animals.

Overall Conclusions

Studies supported by DAMD-17-95C-5063 have led to a better understanding of non-cholinesterase effects of the nerve agents sarin, soman and VX and some OP insecticides on the mammalian CNS and, ultimately, to an extremely promising treatment regimen that has been patented and licensed. It is likely that, as a result of this fundamental research, there will be a countermeasure to nerve agent toxicity made available to soldiers and to the general population that is far improved over the current regimen.

Our studies were focused on the nerve agents sarin, soman and VX, but they also included OPs commonly used as pesticides, such as paraoxon. They covered a wide range of possible countermeasures, including pyridostigmine, atropine, donepezil, huperzine, rivastigmine and galantmine. Experimental approaches included electrophysiological investigations of synaptic transmission in hippocampal slices from rats and from humans, and in primary cultures of rat hippocampal neurons. Excitotoxic effects of the nerve agents VX, sarin and soman in the CNS were documented and the underlying mechanisms analyzed using a variety of pharmacological approaches. It was determined that excitotoxic effects can be attributed primarily to a selective inhibition of action potential-dependent GABAergic transmission. This effect is caused in part by a direct interaction of the OPs with muscarinic receptors present on GABAergic neurons.

Seizures and convulsions are the prevalent toxic signs following intoxication with nerve agents. These seizures, if not rapidly reverted, can progress to status epilepticus and contribute to serious brain damage (Kadar *et al.*, 1994; Suzuki *et al.*, 1997). Initially, the seizures were considered to be a consequence of the high concentrations of ACh following blockade of AChE; however, we have demonstrated that the OP VX can interfere with neuronal synaptic transmission in different ways, not only causing an imbalance between the action potential-dependent excitatory and inhibitory synaptic transmissions, but also increasing the action potential-independent transmitter release (Rocha *et al.*, 1999) via a mechanism unrelated to the cholinesterase inhibition. In contrast, sarin, at low concentrations, has a more specific effect in the mammalian hippocampus, affecting only the action potential-dependent inhibitory synaptic transmission. A selective blockade by sarin of GABAergic transmission, particularly in the hippocampus, could conceivably contribute to the convulsions caused by the OP, and, that being the case, compounds that are able to enhance the inhibitory GABAergic transmission in the CNS might be considered as possible countermeasures.

Currently, the management of OP intoxication includes the use of oximes (Brightman *et al.*, 1995), benzodiazepines and the muscarinic antagonist atropine. It is interesting to note that, atropine poorly crosses the blood-brain-barrier, and very low concentrations of this drug are likely to be achieved in the CNS following the regular doses used to prevent and/or treat OP-induced intoxication. Thus, our finding that, at very low concentrations (1-10 nM), atropine increases the GABAergic neurotransmission in the hippocampus, indicates that atropine may be beneficial to prevent and/or reverse the convulsions induced by sarin.

We then explored the mechanism by which pyridostigmine could be providing a protective effect against nerve agent toxicity. Potentiation of GABAergic transmission by 100 nM PB functionally antagonized soman-induced inhibition of GABAergic transmission, but only when hippocampal slices were pre-treated with PB. We showed further that, acting via m3 receptors present on GABAergic neurons, PB at 100 nM effectively prevents inhibition of GABAergic transmission induced by the interactions of soman with m2 receptors located on GABAergic neurons. Therefore, PB, acting via m3 receptors, can effectively counteract effects arising from the interactions of soman with m2 receptors in the brain.

In parallel *in vitro* morphological studies, we found that chronic exposure to low doses of paraoxon during a period of cholinergic system development, despite the overall reduction of brain ChE levels, selectively affects the spine density of basal dendrites of the pyramidal neurons. This fine hippocampal alteration with serious developmental consequences to cognition and other brain functions occurred in the absence of overt cholinergic toxic signs, which serves as an alert for the insidiousness of OPs when present in a repetitive low-dose scheme. These studies are very relevant to development of antidotal and/or preventative strategies using pyridostigmine and galantamine.

As studies progressed it became apparent that galantamine offers a far superior protection than current regimens. Galantamine was already under study in our laboratory for its actions as an allosteric potentiating ligand (APL) of nicotinic acetylcholine receptors in the CSN. Studies were begun in guinea pigs, and we were able to demonstrate the remarkable potential of galantamine to improve antidotal therapy for even the most deadly OPs. In combination with atropine, well-tolerated, clinically relevant doses of galantamine administered acutely either before or soon after an exposure to the nerve agents soman and sarin or of paraoxon, the active metabolite of the OP insecticide paraoxon, fully counteract the toxicity and lethality of these compounds. While atropine alone attenuates the muscarinic syndrome resulting from the exposure of the guinea pigs to the OPs, it does not afford significant protection against their lethality.

The exact mechanisms that account for the superiority of galantamine as a countermeasure against OP poisoning are yet to be fully elucidated. However, it can be postulated that the effectiveness of galantamine is related both to the higher potency with which it inhibits AChE compared to BuChE (Thomsen and Kewitz, 1990), an action that should help preserving the scavenger capacity of plasma BuChE for OPs, and to the protection of brain AChE from OP-induced irreversible inhibition. The finding that galantamine was essential to counteract soman-induced neurodegeneration in the brain supports the notion that AChE-related and/or- unrelated actions of this drug in the CNS contribute to its effectiveness. Neuronal loss in the brains of OP-intoxicated animals correlates to some extent with the intensity and duration of OP-triggered seizures (McDonough and Shih, 1997; Filliat *et al.*, 1999; Myhrer *et al.*, 2005). Yet, neurodegeneration and consequent cognitive impairment induced by OPs can be significantly reduced by therapeutic interventions that, although unable to suppress OP-triggered seizures, effectively decrease glutamate excitotoxicity (Jiang *et al.*, 2005). The ability of the galantamine-based therapy to prevent OP-induced convulsions and the well-reported neuroprotective effect of galantamine against different insults (Pereira *et al.*, 2002; Arias *et al.*, 2004; Kihara *et al.*, 2004; Nakamizo *et al.*, 2005, Capsoni *et al.*, 2002), which involves activation of intracellular pathways such as Erk, may be important determinants of the antidotal effectiveness. Since no cognitive impairment has been detected in soman-challenged animals when neuronal loss in their brains remains below a certain threshold (Filliat *et al.*, 1999), galantamine is likely to maintain normal cognitive performance of OP-exposed subjects.

Inhibition of brain AChE by > 60-70% has been shown to trigger severe incapacitating effects, including seizures (Todulli *et al.*, 1999). Maximal degrees of inhibition of AChE activities observed in guinea pigs treated with doses of galantamine that effectively counteracted OP intoxication were about 75% in blood and 30% in brain. All other centrally acting AChE inhibitors studied to date, including huperzine, acutely prevent OP toxicity when used at doses that decrease blood AChE activity by >70% (Desphande *et al.*, 1986; Grunwald *et al.*, 1994; Fricke *et al.*, 1994; Lallement *et al.*, 2002). However, brain AChE activity is inhibited to a similar large extent by these drugs (Lallement *et al.*, 2002). Therefore, while a high degree of reversible and selective AChE inhibition in the blood appears to be necessary to acutely counteract the peripheral toxic effects of OPs, a low degree of reversible inhibition of

brain AChE may be essential to protect a significant pool of the enzyme from OP-induced irreversible inhibition and critical to limit the occurrence of untoward side effects of centrally acting reversible AChE inhibitors.

Development of effective and safe antidotes against OP toxicity will help improve treatment of victims of a terrorist attack with nerve agents and help reduce the mortality associated with OP insecticide poisoning worldwide. The demonstration that an acute treatment with a galantamine-based therapy effectively and safely counteracts OP poisoning is, therefore, of utmost relevance for farm workers and others who handle OP insecticides, for the general population under threat of OP exposure in terrorist attacks, and for soldiers, who, despite the Geneva Protocol, may be exposed to deadly nerve agents in the course of battle.

It is clear from our DOD-funded studies reported herein that the toxicity of nerve agents and other OP compounds cannot be solely explained by their ability to irreversibly inhibit AChE. While this mechanism contributes to their toxicity, other targets are equally affected by the OPs. Our studies reveal an interaction of nerve agents with muscarinic receptors that severely compromises neuronal functions in the brain, an effect that is amplified by direct interference of the agents with intracellular mechanisms underlying neuronal viability and synaptic plasticity. Thus, it comes at no surprise that a potentially effective countermeasure against OP poisoning is a drug that has multiple mechanisms of action relevant to counteract the toxic effects of OP compounds. In this regard, galantamine, acting both as a weak cholinesterase inhibitor and a nicotinic allosteric potentiating ligand, effectively and safely prevents and treats OP intoxication.

References

Albuquerque EX, Alkondon M, Deshpande SS, Cintra, WM, Brossi A. The role of carbamates and oximes in reversing toxicity of organophosphorus compounds: a perspective into mechanisms. In: *Neurotox '88: Molecular basis of drug and pesticide action,* Lunt GG, ed., Cambridge, Elsevier Publish., 1988, pp 349-373.

Albuquerque EX, Aracava Y, Idriss M, Schönenberger B, Brossi A, Deshpande SS. Activation and blockade of the nicotinic and glutamatergic synapses by reversible and irreversible cholinesterase inhibitors. In: *Neurobiology of Acetylcholine,* Dunn NJ and Perlman RL, eds., New York, Plenum Publishing Corp., 1987, pp 301-328.

Albuquerque EX, Deshpande SS, Kawabuchi M, Aracava Y, Idriss M, Rickett DL, Boyne AF. Multiple actions of anticholinesterase agents on chemosensitive synapses: molecular basis for prophylaxis and treatment of organophosphate poisoning. *Fund Appl Toxicol* 1985; 5: S182-S203.

Albuquerque EX, Pereira EFR, Braga MFM, Alkondon M. Contribution of nicotinic receptors to the function of synapses in the central nervous system: The action of choline as a selective agonist of α7 receptors. *J Physiol (Paris)*, 1998; 92: 309-316.

Albuquerque EX, Swanson KL, Montes JG, Aracava Y. Molecular targets and synaptic effects of carbamates, organophosphates, oximes, and pyridiniums: Implications for prophylaxis and therapy of organophosphate toxicity. *Report to U.S. Army Research and Development Command* 1994; 243 pp.

Alkondon M and Albuquerque EX. Diversity of nicotinic acetylcholine receptors in rat hippocampal neurons. I. Pharmacological and functional evidence for distinct structural subtypes. *J Pharmacol Exp Ther*, 1993; 265: 1455-1473.

Alkondon M, Pereira EFR, Barbosa CT, Albuquerque EX. Neuronal nicotinic acetylcholine receptor activation modulates γ-aminobutyric acid release from CA1 neurons of rat hippocampal slices. *J Pharmacol Exp Ther* 1997; 283: 1396-1411.

Alkondon M, Pereira EFR, Eisenberg HM, Albuquerque EX. Choline and selective antagonists

identify receptors that modulate GABA release from CA1 interneurons in rat hippocampal slices. *J Neurosci* 1999; 19: 2693-2705.
Aramakis VB and Metherate R. Nicotine selectively enhances NMDA receptor-mediated synaptic transmission during post-natal development in sensory neocortex. *J Neurosci* 1998; 18: 8485-8495.
Arias, E., Ales, E., Gabilan, N.H., Cano-Abad, M.F., Villarroya, M., Garcia, A.G., & Lopez, M.G. *Neuropharmacology* 2004; 46, 103-114.
Atkins, C.M., Selcher, J.C., Petraitis, J.J., Trzaskos, J.M., Sweatt, J.D. The MAPK cascade is required for mammalian associative learning. *Nat. Neurosci.* 1998, 1, 602-609.
Bajgar, J. Organophosphates/nerve agent poisoning: mechanism of action, diagnosis, prophylaxis, and treatment. *Adv Clin Chem* 2004; 38, 151-216.
Bakry NMS, El-Rashidy AH, Eldefrawi AT, Eldefrawi M.E. Direct actions of organophosphate anticholinesterases on nicotinic and muscarinic acetylcholine receptors. *J Biochem Toxicol* 1988; 3: 235-259.
Behrends JC and ten Bruggencate G. Cholinergic modulation of synaptic inhibition in the guinea pig hippocampus in vitro: excitation of GABAergic interneurons and inhibition of GABA-release. *J Neurophysiol* 1993; 69, 626-629.
Berkeley, JL, Decker, MJ, Levey, AI. The role of muscarinic acetylcholine receptor-mediated activation of extracellular signal-regulated kinase 1/2 in pilocarpine-induced seizures. *J Neurochem* 2002; 82, 192-201.
Bickel, U, Thomsen, T, Weber, W, Fischer, JP, Bachus, R, Nitz, M, Kewitz, H. Pharmacokinetics of galanthamine in humans and corresponding cholinesterase inhibition. *Clin Pharmacol Ther* 1991; 50, 420-428.
Braga MFM, Pereira EFR, Albuquerque EX. Nanomolar concentration of lead inhibit glutamatergic and GABAergic transmission in hippocampal neurons. *Brain Research* 1999; 826, 22-34.
Brightman T, Ye JG, Ortiz-Jimenez E, Wen-Hsien Wu F, McArdle JJ. 2,3-Butanedione monoxime protects mice against the convulsant effect of picrotoxin by facilitating GABA-activated currents. *Brain Research* 1995; 678, 110-116.
Buckley, NA, Karalliedde, L, Dawson, A, Senanayake, N, Eddleston, M. Where is the evidence for treatments used in pesticide poisoning? Is clinical toxicology fiddling while the developing world burns? *J Toxicol Clin Toxicol* 2004; 42, 113-116.
Capsoni, S, Giannotta, S, Cattaneo, A. Nerve growth factor and galantamine ameliorate early signs of neurodegeneration in anti-nerve growth factor mice. *Proc Natl Acad Sci USA 2002;* 99, 12432-12437.
Carter, WH, Jones, DE, Carchman, RA. Application of response surface methods for evaluating the interactions of soman, atropine, and pralidioxime chloride. *Fundam Appl Toxicol* 1985; 5, S232-241.
Claessens, HA, van Thiel, M, Westra, P, Soeterboek, AM. High-performance liquid chromatographic determination of galanthamine, a long-acting anticholinesterase drug, in serum, urine and bile. *J Chromatogr* 1983; 275, 345-353.
Corey-Bloom, Galantamine: a review of its use in Alzheimer's disease and vascular dementia. *Int J Clin Pract* 2003; 57, 219-223.
Coupland, R and Leins, KR. Science and prohibited weapons. *Science* 2005; 308, 1841.
Cox, CL, Metherate, R, Ashe, JH. Modulation of cellular excitability in neocortex: Muscarinic receptor and second messenger-mediated actions of acetylcholine. *Synapse* 1994; 16, 123-136.
Cunha, RA, Constantino, MD, Ribeiro, JA. Inhibition of [^{3}H]γ-aminobutyric acid release by kainate receptor activation in rat hippocampal synaptosomes. *Eur. J. Pharmacol.* 1997; 323, 167-172.
Dajas-Bailador, F., Wonnacott, S. Nicotinic acetylcholine receptors and the regulation of neuronal signalling. *Trends Pharmacol. Sci.* 2004; 25, 317-324.

Dempster J. Computer analysis of electrophysiological signals. In: *Microcomputers in physiology: A practical approach,* Sattelle DB, ed.Oxford IRL Press 1989, pp 51-93.

Deshpande, SS, Viana, GB, Kauffman, FC, Rickett, DL Albuquerque, EX. Effectiveness of physostigmine as a pretreatment drug for protection of rats from organophosphate poisoning. *Fundam. Appl. Toxicol.* 1986; 6, 566-577.

Doctor, BP, Raveh, L, Wolfe, AD, Maxwell, DM, Ashani, Y. Enzymes as pretreatment drugs for organophosphate toxicity. *Neurosci. Biobehav. Rev.* 1991; 15, 123-128.

Dreyer, R. [Treatment of epilepsy with Nivaline?] *Munch. Med. Wochenschr.* 1968; 110, 1481.

Eldefrawi AT, Jett D, Eldefrawi ME. Direct actions of organophosphorus anticholinesterases on muscarinic receptors. In: *Organophosphates chemistry, fate, and effects,* Chambers JE and Levi PE, eds., New York Academy Press 1992, pp 259-270.

Figenschou A, Hu GY, Storm JF. Cholinergic modulation of the action potential in rat hippocampal neurons. *Eur J Neurosci* 1996; 8: 211-219.

Filliat, P, Baubichon, D, Burckhart, MF, Pernot-Marino, I, Foquin, A, Masqueliez, C, Perrichon, C, Carpentier, P, Lallement, G. Memory impairment after soman intoxication in rat: correlation with central neuropathology. Improvement with anticholinergic and antiglutamatergic therapeutics. *Neurotoxicology* 1999; 20, 535-549.

Fricke, RF, Koplovitz, I, Scharf, BA, Rockwood, GA, Olson, CT, Hobson, DW, Blank, JA. *Drug Chem. Toxicol.* 1994; 17, 15-34.

Ghanem, E and Raushel, FM. *Toxicol. Appl. Pharmacol*. 2005; 207, 459-470.

Gordon, RK, Nigam, SV, Weitz, JA, Dave, JR, Doctor, BP, Vec, HS *J. Appl. Toxicol.* 2001; 21, S47-S51.

Gray R, Rajan AS, Radcliffe KA, Yakehiro M, Dani JA. Hippocampal synaptic transmission enhanced by low concentrations of nicotine. *Nature* 1996; 383: 713-716.

Grunwald, J, Raveh, L, Doctor, BP, Ashani, Y *Life Sci.* 1994; 54, 991-997.

Gunderson, CH, Lehman, CR, Sidell, FR, Jabbari, B. Nerve agents: a review. *Neurology* 1992; 42, 946-950.

Haley RW and Kurt TL. Self-reported exposure to the neurotoxic chemical combinations in the Gulf War. *JAMA* 1997; 277, 231-237.

Hamill, OP, Marty, A, Neher, E, Sakamann, B, Sigworth, FJ. Improved patch-clamp techniques for high resolution current recording from cells and cell-free membrane patches. *Pflügers Arch.* 1981; 391, 85-100.

Idriss MK, Aguayo LG, Rickett DL, Albuquerque EX. Organophosphate and carbamate compounds have pre- and postjunctional effects at the insect glutamatergic synapses. *J Pharmacol Exp Ther* 1986; 239, 279-285.

Jann, MW, Shirley, KL,, Small, GW. Clinical pharmacokinetics and pharmacodynamics of cholinesterase inhibitors. *Clin. Pharmacokinet.* 2002; 41, 719-739.

Jarolimek, W., and Misgeld, U. $GABA_B$ receptor-mediated inhibition of tetrodotoxin-resistant GABA release in rodent hippocampal CA1 pyramidal cells. *J. Neurosci.* 1997; 17: 1025-1032.

Jett, DA, Abdallah, EAM, El-Fakahany, EE, Eldefrawi, ME, Eldefrawi, AT. High affinity activation by paraoxon of a muscarinic receptor subtype in rat brain striatum. *Pesticide Bioch Physiol* 1991; 39, 149-157.

Jiang, W, Van Cleemput, J, Sheerin, AH, Ji, SP, Zhang, Y, Saucier, DM, Corcoran, ME, Zhang, X. Involvement of extracellular regulated kinase and p38 kinase in hippocampal seizure tolerance. *J. Neurosci. Res.* 2005; 81, 581-588.

Johnson, CD and Russell, RL. A rapid, simple radiometric assay for cholinesterase, suitable for multiple determinations. *Anal. Biochem.* 1975*;* 64, 229-238.

June, HL, Duemler, SE, Greene, TL, Williams, JA, Lin, M, Devaraju, SL, Chen, SH, Lewis, MJ, Murphy, JM. *J. Pharmacol. Exp. Ther.* 1995; 274, 1105-1112.

Kadar T, Shapira S, Cohen G, Sahar R, Alkalay D, Raveh L. Sarin-induced neuropathology in rats. *Human Exp Toxicol* 1994; 14: 252-259.

Karalliedde, L, Senanayake, N. Organophosphorus insecticide poisoning. *Br. J. Anesth.* 1989; 65, 736-750.

Karczmar, AG. Acute and long lasting central actions of organophosphorus agents. *Fundam App. Toxicol* 1984; 4(2 part2): S1-S17.

Kihara, T, Sawada, H, Nakamizo, T, Kanki, R, Yamashita, H, Maelicke, A, Shimohama, S. Galantamine modulates nicotinic receptor and blocks Abeta-enhanced glutamate toxicity. *Biochem. Biophys. Res. Commun.* 2004; 325, 976-982.

Kimura F and Baughman RW. Distinct muscarinic receptor subtypes suppress excitatory and inhibitory synaptic response in cortical neurons. *J Neurophysiol* 1997; 77: 709-716.

Koek, W, Woods, JH, Winger, GD. MK-801, a proposed noncompetitive antagonist of excitatory amino acid neurotransmission, produces phencyclidine-like behavioral effects in pigeons, rats and rhesus monkeys. *J. Pharmacol. Exp. Ther.* 1988; 245, 969-974.

Lallement, G, Baille, V, Baubichon, D, Carpentier, P, Collombet, JM, Filliat, P, Foquin, A, Four, E, Masqueliez, C, Testylier, G, Tonduli, L., Dorandeu, F. Review of the value of huperzine as pretreatment of organophosphate poisoning. *Neurotoxicology* 2002; 23, 1-5.

Lallement G, Dorandeu F, Filliat P, Carpentier P, Baille, V, Blanchet G. Medical management of organophosphate-induced seizure. *J Physiol (Paris)* 1998; 92: 369-373.

Leadbeater, L, Inns, RH, Rylands, JM. Treatment of poisoning by soman. *Fundam. Appl. Toxicol.* 1985; 5, S225-231.

Losev, NA and Tkachenko, EI. [Effect of N- and M-cholinergic-potentiating and cholinergic-blocking agents on the epileptogenesis of a penicillin focus in the dorsal hippocampus] *Biull. Eksp. Biol. Med.* 1986; 101, 436-438.

Mannens, GS. The metabolism and excretion of galantamine in rats, dogs, and humans. *Drug Metab. Dispos.* 2002; 30, 553-563.

Marin P, Hamon B, Glowinski J, Premont J. Nicotine-induced inhibition of phospholipase A2. *J Pharmacol Exp Ther* 1997; 280, 1277-1283.

Maxwell, DM, Brecht, KM, Lenz, DE, O'Neill, BL. Effect of carboxylesterase inhibition on carbamate protection against soman toxicity. *J. Pharmacol.Exp. Ther.* 1988; 246, 986-991.

McDonough, JHJr. and Shih, TM. Neuropharmacological mechanisms of nerve agent-induced seizure and neuropathology. Neuropharmacological mechanisms of nerve agent-induced neuropathology. *Neurosci Biobehav Rev* 1997; 21, 559-579.

McDonough, JH, McLeaod, CG, Nipwoda, MT. Direct microinjection of soman or VX into the amygdala produces repetitive limbic convulsions and neuropathology. *Brain Res.* 1987; 435, 123-137.

McKinney, M, Miller, JH, Aagaard, PJ. Pharmacological characterization of the rat hippocampal muscarinic autoreceptor. *J. Pharmacol. Exp. Ther.* 1993; 264, 74-78.

Mihailova, D, Yamboliev, I, Zhivkova, Z, Tencheva, J, Jovovich, V. Pharmacokinetics of galanthamine hydrobromide after single subcutaneous and oral dosage in humans. *Pharmacology* 1989; 39, 50-58.

Morton RA and Davies CH. Regulation of muscarinic acetylcholine receptor-mediated synaptic responses by adenosine receptors in the rat hippocampus. *J Physiol* 1997; 501, 775-90.

Myhrer, T,, Andersen, JM, Nguyen, NH, Aas, P. Soman-induced convulsions in rats terminated with pharmacological agents after 45 min: neuropathology and cognitive performance. *Neurotoxicology* 2005; 26, 39-48.

Nakamizo, T, Kawamata, J, Yamashita, H, Kanki, R, Kihara, T, Sawada, H, Akaike, A, Shimohama S. Stimulation of nicotinic acetylcholine receptors protects motor neurons. *Biochem. Biophys. Res. Commun.* 2005; 330, 1285-1289.

Okumura T, Takasu N, Ishimatsu S. Report on 640 victims of the Tokyo subway sarin attack. *Ann Emerg Med* 1996; 28, 129-135.

Pereira, EFR, Hilmas, C, Santos, MD, Alkondon, M, Maelicke, A, Albuquerque, E.X.. Unconventional ligands and modulators of nicotinic receptors. *J. Neurobiol.*2002; 53, 479-500.

Perkins, D, Pereira, EFR, Gober, M, Yarowsky, PJ, Aurelian, L. The herpes simplex virus type 2 R1 protein kinase (ICP10 PK) blocks apoptosis in hippocampal neurons, involving activation of the MEK/MAPK survival pathway. *J. Virol.* 2002; 76, 1435-1449.

Pitler TA and Alger BE. Cholinergic excitation of GABAergic interneurons in the rat hippocampal slice. *J Physiol* 1992; 450, 127-142.

Rao KS, Aracava Y, Rickett DL, Albuquerque EX. Noncompetitive blockade of the nicotinic acetylcholine receptor-ion channels complex by an irreversible cholinesterase inhibitor. *J Pharmacol Exp Ther* 1987; 240, 337-344.

Raveh L, Grunwald J, Markus D, Papier Y, Cohen G, Ashani Y. Human butyrylcholinesterase as a general prophylactic antidote for nerve agents toxicity. In vitro and in vivo quantitative characterization. *Biochem Pharmacol* 1993; 45, 2465-2474.

Rocha, ES, Alkondon, M, Swanson, KL, Albuquerque, EX. Stimulatory effect of VX on excitatory synapses of cultured hippocampal neurons. *Soc. Neurosci. Abstr.* 1996a; 22:1740.

Rocha, ES, Aracava, Y, Albuquerque, EX. VX enhances transmitter release in cultured hippocampal neurons. *Soc. Neurosci. Abstr.* 1992; 18, 634.

Rocha, ES, Pereira, EFR, Swanson, KL, Albuquerque, EX. Novel molecular targets in the central nervous system for the actions of cholinesterase inhibitors: alterations of modulatory processes. *Proceedings of the 1996 Medical Defense Bioscience Review.* 1996b;1635-1643.

Rocha ES, Santos MD, Chebabo SR, Aracava Y, Albuquerque EX. Low concentrations of the organophosphate VX affect spontaneous and evoked transmitter release from hippocampal neurons: Toxicological relevance of cholinesterase-independent actions. *Toxicol Appl Pharmacol* 1999*;* 159, 31-40.

Rocha ES, Swanson KL, Aracava Y, Goolsby JE, Maelicke A, Albuquerque EX. Paraoxon: Cholinesterase-independent stimulation of transmitter release and selective block of ligand -gated ion channels in cultured hippocampal neurons. *J Pharmacol Exp Ther* 1996; 278, 1175-1187.

Romano Jr., JA, King, JM. Psychological casualties resulting from chemical and biological weapons. *Mil. Med.* 2001; 166, 21-22.

Rouse ST, Thomas TM, Levey A. Muscarinic acetylcholine receptor subtype, m2: Diverse functional implications of differential synaptic localization. *Life Sciences* 1997; 60, 1031-1038.

Santos, M.D., Pereira, E.F.R., Aracava, Y., Castro, N.G., Fawcett, W.P., Randall, W.R., and Albuquerque, E.X. Low concentrations of pyridostigmine prevent soman-induced inhibition of GABAergic transmission in the central nervous system: Involvement of muscarinic receptors. *J Pharmacol Exp Ther* 2003; 304, 254-265.

Sanz B, Exposito I, Mora F. M1 acetylcholine stimulation increases the extracellular concentrations of glutamate and GABA in the medial prefrontal cortex. *Neurochem Res* 1997; 22, 281-286.

Sapolsky, RM. The stress of Gulf War syndrome. *Nature* 1998; 395, 308-309.

Sawyer TW, Weiss MT, Boulet CA, Hansen AS. Toxicity of organophosphate nerve agents and related phosphonylated oximes compared to their anticholinesterase activity in neuron cultures. *Fund. Appl Toxicol* 1991; 17, 208-219.

Schmued, L. C., Hopkins, K.J. Fluoro-Jade B: a high affinity fluorescent marker for the localization of neuronal degeneration. *Brain Res.* 2000; 874, 123-130.

Shih, TM, Duniho, SM, McDonough, JH. *Toxicol. Appl. Pharmacol.* 2003; 188, 69-80.

Siebler, M, Köeller, H, Schmalenbach, C, Müller, HW. GABA activated chloride currents in cultured rat hippocampal and septal region neurons can be inhibited by curare and

atropine. *Neurosci Letters* 1988; 93, 220-224.
Silveira CLP, Eldefrawi AT, Eldefrawi ME. Putative M2 muscarinic receptors of rat heart have high affinity for organophosphorus anticholinesterases. *Toxicol Appl Pharmacol* 1990; 103, 474-481.
Silvestre, JS, Fernandez, AG, Palacios, JM. Preliminary evidence for an involvement of the cholinergic system in the sedative effects of rolipram in rats. *Pharmacol. Biochem. Behav.* 1999; 64, 1-5.
Sivam SP, Hyoscine B, Ho IK. An assessment of comparative acute toxicity of diisopropylfluorophosphate, tabun, sarin, and soman in relation to cholinergic and GABAergic enzyme activities in rat. *Fund Appl Toxicol* 1984; 4, 531-538.
Solberg, Y and Belking, M. The role of excitotoxicity in organophosphorus nerve agents central poisoning. *Trends in Pharmacol. Sci.* 1997; 18, 183-185.
Suzuki J, Kohno T, Tsukagosi M, Furuhata T, Yamazaki K. Eighteen cases exposed to sarin in Matsumoto, *Japan Int Med* 1997; 36, 466-470.
Tariot, PN, Scheineider, L, Porsteinsson, AP. Treating Alzheimer's disease. Pharmacologic options now and in the near future. *Postgrad. Med.* 1997; 101, 73-76, 81, 84 passim.
Taylor P. Anticholinesterase agents. In: *Goodman & Gilman's: Pharmacological Basis of Therapeutics,* Hardman, JG and Limbird LE., eds., New York McGraw-Hill, 1996, pp 161-176.
Tencheva, J, Yamboliev, I, Zhivkova, Z. Reversed-phase liquid chromatography for the determination of galanthamine and its metabolites in human plasma and urine. *J. Chromatogr.* 1987; 421, 396-400.
Thesleff S, Sellin LC, Tagerud S. Tetrahydro-aminoacridine (tacrine) stimulates neurosecretion at mammalian motor endplates. *Br J Pharmacol* 1990; 100, 487-490.
Thomsen, T,, Kaden, B, Fischer, JP, Bickel, U, Barz, H, Gusztony, G, Cervos-Navarro, J, Kewitz, H. Inhibition of acetylcholinesterase activity in human brain tissue and erythrocytes by galanthamine, physostigmine and tacrine. *Eur J Clin Chem Clin Biochem.* 1991; 29, 487-492.
Thomsen, T and Kewitz, H. Selective inhibition of human acetylcholinesterase by galanthamine in vitro and in vivo. *Life Sci.* 1990; 46, 1553-1558.
Tonduli, LS, Testylier, G, Pernot Marino, I, Lallement, G. Triggering of soman-induced seizures in rats: multiparametric analysis with special correlation between enzymatic, neurochemical and electrophysiological data. *J. Neurosci. Res.* 1999; 58, 464-473.
Wetherell, J, Hall, T, Passingham, S. Physostigmine and hyoscine improves protection against the lethal and incapacitating effects of nerve agent poisoning in the guinea-pig. *Neurotoxicology* 2002; 23, 341-349.

Relevant Publications from Dr. Albuquerque's laboratory (those directly supported by this contraction are indicated with an asterisk)

Albuquerque, E.X., Pereira, E.F.R., Castro, N.G., Alkondon, M., Reinhardt, S., Schroder, H., and Maelicke, A. Nicotinic receptor function in the mammalian central nervous system. Ann. N.Y. Acad. Sci. 757:48-72, 1995.

Castro, N.G. and Albuquerque, E.X. α-Bungarotoxin-sensitive hippocampal nicotinic receptor channel has a high calcium permeability. Biophys. J. 68: 516-524, 1995.

Ishihara, K., Montes, J. and Albuquerque, E.X. Ontogenically related properties of N-methyl-D-aspartate receptors in rat hippocampal neurons and the age-specific sensitivity of developing neurons to lead. J. Pharmacol. Exp. Ther. 273:1459-1470, 1995.

Ishihara, K., Alkondon, M., Montes, J.G., and Albuquerque, E.X. Nicotinic responses in acutely dissociated rat hippocampal neurons and the selective blockade of fast desensitizing nicotinic currents by lead. J. Pharmacol. Exp. Ther. 273:1471-1482, 1995.

Albuquerque, E.X., Pereira, E.F.R., Castro, N.G., and Alkondon, M. Neuronal nicotinic receptors: Function, modulation, and structure. Seminars in the Neurosciences 7:91-101, 1995.

Storch, A., Schrattenholz, A., Cooper, J.C., Ghani, E.M.A., Gutbrod, O., Weber, K.-H., Reinhardt, S., Lobron, C., Hermsen, B. Soskic, V., Pereira, E.F.R., Albuquerque, E.X., Methfessel, C., and Maelicke, A. Physostigmine, galanthamine and codeine act as non-competitive agonists on clonal rat pheocromocytoma cells. Eur. J. Pharmacol. 290:207-219, 1995.

Alkondon, M. And Albuquerque, E.X. Diversity of nicotinic receptors in rat hippocampal neurons. III. Agonist actions of the novel alkaloid epibatidine and analysis of type II current. J. Pharmacol. Exp. Ther. 274:771-782, 1995.

Swanson, K.L., Alkondon, M., Pereira, E.F.R., and Albuquerque, E.X. The search for subtype-selective nicotinic acetylcholine receptor agonists. In: Chemistry and Toxicology of Alkaloids, ed. M. Blum, pp. 191-280, 1995.

Grando, S.A., Horton, R.M., Pereira, E.F.R., Diethelm-Okita, B.M., George, P.M., Albuquerque, E.X. and Conti-Fine, B.M. A nicotinic acetylcholine receptor regulating cell adhesion and motility is expressed in human keratinocytes. J. Invest. Dermatol. 105: 774-781, 1995.

Maelicke, A., Schrattenholz, A., Storch, A., Schroder, B., Gutbrod, O., Methfessel, C., Weber, K.H., Pereira, E.F.R., Alkondon, M., and Albuquerque, E.X. Noncompetitive agonism at nicotinic acetylcholine receptors: Functional significance for CNS signal transduction. J. Receptor & Signal Transduction Res. 15: 333 353, 1995.

Schrattenholz, A., Pereira, E.F.R., Methfessel, C., Roth, U., Weber, K.-H., Albuquerque, E.X., and Maelicke, A. Agonist responses of neuronal nicotinic acetylcholine receptors are potentiated by a novel class of allosterically acting ligands. Mol. Pharmacol. 49:1-6, 1996.

Bonfante-Cabarcas, R., Swanson, K.L., Alkondon, M., and Albuquerque, E.X. Diversity of nicotinic acetylcholine receptors in rat hippocampal neurons IV. Regulation by external Ca2+ of

α-bungarotoxin-sensitive receptor function and rectification induced by internal Mg2+. J. Pharmacol. Exp. Ther. 277:432-444, 1996.

Maelicke, A., and Albuquerque, E.X. New approach to drug therapy in Alzheimer's dementia. Drug Discovery Today 1:53-59, 1996.

Barbosa, C.T.F., Alkondon, M., Aracava, Y., Maelicke, A., and Albuquerque, E.X. Ligand-gated ion channels in acutely dissociated rat hippocampal neurons with long dendrites. Neurosci. Lett. 210:177-180, 1996.

Rocha, E.S., Swanson, K.L., Aracava, Y., Goolsby, J.E., Maelicke, A., and Albuquerque, E.X. Paraoxon: Cholinesterase-independent stimulation of transmitter release and selective block of ligand-gated ion channels in cultured hippocampal neurons. J. Pharmacol. Exp. Ther. 278:1175-1187, 1996.

Alkondon, M., Rocha, E.S., Maelicke, A., and Albuquerque, E.X. Diversity of nicotinic acetylcholine receptors in brain neurons V. α-Bungarotoxin-sensitive nicotinic receptors in olfactory bulb neurons, and presynaptic modulation of glutamate release. J. Pharmacol. Exp. Ther. 278:1460-1471, 1996.

Pereira, E.F.R., Alkondon, M, McIntosh, J.M. and Albuquerque, E.X. α-Conotoxin-ImI, a competitive nicotinic antagonist at α-bungarotoxin-sensitive neuronal nicotinic receptors. J. Pharmacol. Exp. Ther. 278:1472-1483, 1996.

Marchioro, M., Swanson, K.L., Aracava, Y., and Albuquerque, E.X. Glycine- and calcium-dependent effects of lead on N-methyl-D-aspartate receptor function in rat hippocampal neurons. J. Pharmacol. Exp. Ther. 279:143-153, 1996.

Alkondon, M., Pereira, E.F.R., and Albuquerque, E.X. Mapping the location of functional nicotinic and γ-aminobutyric acid receptors on hippocampal neurons. J. Pharmacol. Exp. Ther. 279:1491-1506, 1996.

Rocha, E.S., Pereira, E.F.R., Swanson, K.L., and Albuquerque, E.X. Novel molecular targets in the central nervous system for the actions of cholinesterase inhibitors: Alterations of modulatory processes. 1996 Medical Defense Bioscience Review, Proceedings Volume III, 1635-1643, 1996.

Albuquerque, E.X., Pereira, E.F.R., Bonfante-Cabarcas, R., Marchioro, M., Matsubayashi, H., Alkondon, M., and Maelicke, A. Nicotinic acetylcholine receptors on hippocampal neurons: Cell compartment-specific expression and modulatory control of channel activity. Prog. Brain Res. 109:111-124, 1996.

Albuquerque, E.X., Pereira, E.F.R., Alkondon, M., Schrattenholz, A., and Maelicke, A. Nicotinic acetylcholine receptors on hippocampal neurons: Distribution on the neuronal surface and modulation of receptor activity. J. Receptor & Signal Transduction Res. 17: 243-266, 1997.

Maelicke, A., Coban, T., Storch, A., Schrattenholz, A., Pereira, E.F.R., and Albuquerque, E.X. Allosteric modulation of torpedo nicotinic acetylcholine receptor ion channel activity by noncompetitive agonists. J. Receptor & Signal Transduction Research 17: 11-28, 1997.

Matsubayashi, H., Swanson, K.L., and Albuquerque, E.X. Amantadine inhibits nicotinic

acetylcholine receptor function in hippocampal neurons. J. Pharmacol. Exp. Ther. 281: 834-844, 1997.

Albuquerque, E.X., Alkondon, M., Pereira, E.F.R., Castro, N.G., Schrattenholz, A., Barbosa, C.T.F., Bonfante-Cabarcas, R., Aracava, Y., Eisenberg, H., and Maelicke, A. Properties of neuronal nicotinic acetylcholine receptors: Pharmacological characterization and modulation of synaptic function. J. Pharmacol. Exp. Ther. 280: 1117-1136, 1997. (Otto Krayer Award Lecture in Pharmacology and Experimental Therapeutics).
Albuquerque, E.X. Acetylcholine receptors, nicotinic. In: Elsevier=s Encyclopedia of Neuroscience, George Adelman and Barry H. Smith, Eds. Amsterdam: Elsevier B.V., 1997.

Swanson, K.L., Marchioro, M., Ishihara, K., Alkondon, M., Pereira, E.F.R. and Albuquerque, E.X. ANeuronal targets of lead in the hippocampus: Relationship to low-level lead intoxication.@ In Comprehensive Toxicology I.G. Sipes, C.A. McQueen, A.J. Gandolfi (Eds.) Volume 11 Nervous System and Behavioral Toxicology H.E. Lowndes, K.R. Reuhl (Eds.) Elsevier, Oxford pp. 471-493, 1997.

*Camara, A.L., Braga, M.F.M., Rocha, E.S., Santos, M.D., Cortes, W.S., Cintra, W.M., Aracava, Y., Maelicke, A., and Albuquerque, E.X. Methamidophos: An anticholinesterase without significant effects on postsynaptic receptors or transmitter release. NeuroToxicology 18:589-602, 1997.

Alkondon, M., Pereira, E.F.R., Cortes, W.S., Maelicke, A., and Albuquerque, E.X. Choline is a selective agonist of α7 nicotinic acetylcholine receptors in the rat brain neurons. Eur. J. Neurosci. 9: 2734-2742, 1997.
Alkondon, M., Pereira, E.F.R., Barbosa, C.T.F., and Albuquerque, E.X. Neuronal nicotinic acetylcholine receptor activation modulates γ-aminobutyric acid release from CA1 neurons of rat hippocampal slices. J. Pharmacol. Exp. Ther. 283:1396-1411, 1997.

Matsubayashi, H., Alkondon, M., Pereira, E.F.R., Swanson, K.L., and Albuquerque, E.X. Strychnine: A potent competitive antagonist of α-bungarotoxin-sensitive nicotinic acetylcholine receptors in rat hippocampal neurons. J. Pharmacol. Exp. Ther. 284: 904-913, 1998.

Macklin, Kevin D., Maus, A.D.J., Pereira, E.F.R., Albuquerque, E.X., and Conti-Fine, B.M. Human vascular endothelial cells express functional nicotinic acetylcholine receptors. J. Pharmacol. Exp. Ther. 287:435-439, 1998.

Alkondon, M., Pereira, E.F.R., and Albuquerque, E.X. α-Bungarotoxin- and methyllycaconitine-sensitive nicotinic receptors mediate fast synaptic transmission in interneurons of rat hippocampal slices. Brain Research 810:257-263, 1998.

Pereira, E.F.R., Alkondon, M., Albuquerque, E.X., and Maelicke, A. AFunctional diversity of nicotinic acetylcholine receptors in the mammalian central nervous system: Physiological relevance.@ in: Neuronal Nicotinic Receptors: Pharmacology and Therapeutic Opportunities, Eds. Stephen P. Arneric and Jorge D. Brioni, John Wiley and Sons, Inc., 161-186, 1998.
Maus, A.D.J., Pereira, E.F.R., Karachunski, P.I., Horton, R.M., Navaneetham, D., Macklin, K., Cortes, W.S., Albuquerque, E.X., and Conti-Fine, B.M. Human and rodent bronchial epithelial cells express functional nicotinic receptors. Mol. Pharmacol. 54:779-788, 1998.

Albuquerque, E.X., Pereira, E.F.R., Braga, M.R.M., and Alkondon, M. Contribution of nicotinic receptors to the function of synapses in the central nervous system: The action of cholineas a selective agonist of α7 receptors. J. Physiol. (Paris) 92:309-316, 1998.

Albuquerque, E.X., Pereira, E.F.R., Braga, M.F.M., Matsubayashi, H., and Alkondon, M. Neuronal nicotinic receptors modulate synaptic function in the hippocampus and are sensitive to blockade by the convulsant strychnine and by the anti-Parkinson drug amantadine. Toxicol. Lett. 102-103: 211-218, 1998.

*Rocha, E.S., Chebabo, S.R., Santos, M.D., Aracava, Y., and Albuquerque, E.X. An analysis of low level doses of cholinesterase inhibitors in cultured neurons and hippocampal slices of rats. Drug and Chemical Toxicology. 21: 191-200, 1998.

Braga, M.R.M., Pereira, E.F.R., and Albuquerque, E.X. Nanomolar concentrations of lead inhibit glutamatergic and gabaergic transmission in hippocampal neurons. Brain Res. 826: 22-34, 1999.

Braga, M.F.M., Pereira, E.F.R., Marchioro, M., and Albuquerque, E.X. Lead increases tetrodotoxin-insensitive spontaneous release of glutamate and GABA from hippocampal neurons. Brain Res. 826: 10-21, 1999.

Alkondon, M., Pereira, E.F.R., Eisenberg, H.M., and Albuquerque, E.X. Choline and selective antagonists identify two subtypes of nicotinic acetylcholine receptors that modulate GABA release from CA1 interneurons in rat hippocampal slices. J. Neurosci. 19: 2693-2705, 1999.

Albuquerque, E.X. Acetylcholine receptors, nicotinic. In: Elsevier=s Encyclopedia of Neuroscience, 2nd enlarged and revised edition, George Adelman and Barry H. Smith, Eds. Amsterdam: Elsevier B.V., 1999. pp. 7-12.

Rocha, E.S., Santos, M.D., Chebabo, S.R., Aracava, Y., and Albuquerque, E.X. Low concentrations of VX affect spontaneous and evoked transmitter release from hippocampal neurons: Toxicological relevance of cholinesterase-independent actions. Tox. Appl. Pharmacol. 159: 31-40, 1999.

Fischer, U., Reinhardt, S., Albuquerque, E.X., and Maelicke, A. Expression of functional α7 nicotinic acetylcholine receptor during muscle development and denervation. Eur. J. Neurosci. 11: 2856 2864, 1999.

Wevers, A., Monteggia, L., Nowacki, S., Bloch, W., Schütz, U., Lindstrom, J., Pereira, E.F.R., Arneric, S., Sullivan, J., Eisenberg, H. Giacobini, E., Gass, P., deVos, R.A.I, Jansen, S.E.N.H., Maelicke, A., Albuquerque, E.X. and Schröder, H. Expression of nicotinic acetylcholine receptor subunits in the cerebral cortex in Alzheimer's disease: Histotopographical correlation with amyloid plaques and hyperphosphorylated tau-protein. Eur. J. Neurosci. 11: 2551-2555, 1999.

*Chebabo, S.R., Santos, M.D., and Albuquerque, E.X. The organophosphate sarin, at low concentrations, inhibits the evoked release of GABA in hippocampal slices of rat. Neurotoxicology 20:871-882, 1999.

Alkondon, M., Pereira, E.F.R., Eisenberg, H.M., and Albuquerque, E.X. Nicotinic receptor activity in human cerebral cortical interneurons: A mechanism for inhibition and disinhibition of neuronal networks. J. Neurosci. 20:66-75, 2000.

Albuquerque, E.X., Pereira, E.F.R., Alkondon, M., Eisenberg, H.M., and Maelicke, A. ANeuronal nicotinic receptors and synaptic transmission in the central nervous system.@ In

Handbook of Experimental Pharmacology, F. Clementi, C. Gotti and D. Fornasari, eds., New York: Springer Verlag. Chapter 13 "Functional, Pharmacological and Modulatory Properties of the nAChRs@, pp.337-358.

Alkondon, M., Braga, M.F., Pereira, E.F., Maelicke, A., and Albuquerque, E.X. α7 nicotinic acetylcholine receptors and modulation of gabaergic synaptic transmission in the hippocampus. Eur. J. Pharmacol. 393:59 67, 2000.

Albuquerque, E.X., Pereira, E.F.R., Mike, A., Eisenberg, H.M., Maelicke, A., and Alkondon, M. Neuronal nicotinic receptors in synaptic functions in humans and rats: Physiological and clinical relevance. Behav. Brain Res. 113:131-141, 2000.

Maelicke, A., Schrattenholz, A., Samochocki, M., Radina, M., and Albuquerque, E.X. Allosterically potentiating ligands of nicotinic receptors as a treatment strategy for Alzheimer=s disease. Behav. Brain Res. 113:199-206, 2000.

Maelicke, A., and Albuquerque, E.X. Allosteric modulation of nicotinic acetylcholine receptors as a treatment strategy for Alzheimer's disease. Eur. J. Pharmacol. 393: 165-170, 2000.
Mike, A., Pereira, E.F.R., and Albuquerque, E.X. Ca2+-sensitive inhibition by Pb2+ of α7-containing nicotinic acetylcholine receptors in hippocampal neurons. Brain Res. 873:112-123, 2000.

Mike, A., Castro, N.G., and Albuquerque, E.X. Choline and acetylcholine have similar kinetic properties of activation and desensitization on the α7 nicotinic receptors in rat hippocampal neurons. Brain Research 882:155-168, 2000.

Alkondon, M., Pereira, E.F.R., Almeida, L.E.F., Randall, W.R., and Albuquerque, E.X. Nicotine at concentrations found in cigarette smokers activates and desensitizes nicotinic acetylcholine receptors in CA1 interneurons of rat hippocampus. Neuropharmacology 39:2726-2739, 2000.

Almeida, L.E.F., Pereira, E.F.R., Alkondon, M., Fawcett, W.P., Randall, W.R., and Albuquerque, E.X. The opioid antagonist naltrexone inhibits activity and alters expression of α7 and α4β2 nicotinic receptors: Implications for smoking cessation programs. Neuropharmacology 39:2740-2755, 2000.

Samochocki, M., Zerlin, M., Josttock, R., Groot, Kormelink, P.J., Luyten, W.H., Albuquerque, E.X. and Maelicke, A. Galantamine is an allosterically potentiating ligand of the human alpha4/beta2 nAChR. Acta Neurol. Scand. Suppl. 176:68-73, 2000.

Peçanha, E.P., Fraga, C.A.M., Barreir, E.J., Braga, M.R.M., Pereira, E.F.R., and Albuquerque, E.X. Synthesis and pharmacological evaluation of a new 2-azabicyclo[3.3.0]octane derivative. J. Braz. Chem. Soc. 12: 408-412, 2001.

Maelicke, A., Samochocki, M., Jostock, R., Fehrenbacher, A., Ludwig, J., Albuquerque, E.X. and Zerlin, M. Allosteric sensitization of nicotinic receptors by galantamine, a new treatment strategy for Alzheimer=s disease. Biol. Psychiatry 49:279-288, 2001.

Albuquerque, E.X., Santos, M.D., Alkondon, M., and Pereira, E.F.R., and Maelicke, A. Modulation of nicotinic receptor activity in the central nervous system: a novel approach to the treatment of Alzheimer disease. Alzheimer Dis. Assoc. Disord. 15 Suppl. 1: S19-25, 2001.

Hilmas, C., Pereira, E.F.R., Alkondon, M., Rassoulpour, A, Schwarcz R., and Albuquerque,

E.X. The brain metabolite hynurenic acid inhibits α7 nicotinic receptor activity and increases non-α7 nicotinic receptor expression: Physiopathological implications. J. Neurosci. 21:7463-7473, 2001.

da Silva, A.J.M., Melo, P.A., Silva, N.M.V., Brito, F.V., Buarque, C.D., de Souza, D.V., Rodrigues, V.P., Poças, E.S.C., Nöel, F., Albuquerque, E.X., and Costa, P.R.R. Synthesis and preliminary pharmacological evaluation of coumestans with different patterns of oxygenation. Bioorganic & Med. Chem. Lett. 11:283-286, 2001.

Gonzalez-Serratos, H., Chang, R., Pereira, E.F.R., Castro, N.G., Aracava, Y., Melo, P.A., Lima, P.C., Fraga, C.A.M., Barreiro, E.J., and Albuquerque, E.X. A novel thienylhydrazone, (2-thienylidene)3,4-methylenedioxybenzoylhydrazine, increases inotropism and decreases fatigue of skeletal muscle. J. Pharmacol. Exp. Ther. 299:558-566, 2001.

Alkondon, M., and Albuquerque, E.X. Nicotinic acetylcholine receptor α7 and α4β2 subtypes differentially control GABAergic input to CA1 neurons in rat hippocampus. J. Neurophysiol. 86:3043-3055, 2001.

Pereira, E.F.R., Santos, M.D., Engelhardt, E., Cavalcanti, J.L.SA., Temponi, F.M. and Albuquerque, E.X. A galantamine no tratamento da coença de Alzheimer: de pesquisa ao paciente. (Galantamine in the treatment of Alzheimer=s disease: from research to patient). Revista Brasileira de Neurologia 37:6-17, 2001.

Wang, Y., Pereira, E.F., Maus, A.D., Ostlie, N.S., Navaneetham, D., Lei, S., Albuquerque, E.X., and Conti-Fine, B.M. Human bronchial epithelial and endothelial cells express alpha7 nicotinic acetylcholine receptors. Mol. Pharmacol. 60:1201-1209, 2001.

Alkondon, M., and Albuquerque, E.X. A non-α7 nicotinic acetylcholine receptor modulates excitatory input to hippocampal CA1 interneurons.. J. Neurophysiol. 87:1651-1654, 2002.

*Santos, M.D., Alkondon, M., Pereira, E.F.R., Aracava, Y., Eisenberg, H.M., Maelicke, A., and Albuquerque, E.X. The nicotinic allosteric potentiating ligand galantamine facilitates synaptic transmission in the mammalian central nervous system. Mol. Pharmacol. 61:1222-1234, 2002.

Priel, M.R., and Albuquerque, E.X. Short-term effects of pilocarpine on rat hippocampal neurons in culture. Epilepsia 43:Suppl. 5:40-46, 2002.

*Pereira, E.F., Hilmas, C., Santos, M.D., Alkondon, M., Maelicke, A., and Albuquerque, E.X. Unconventional ligands and modulators of nicotinic receptors. J. Neurobiol. 53:479-500, 2002.

*Santos, M.D., Pereira, E.F.R., Aracava, Y., Castro, N.G., Fawcett, W.P., Randall, W.R., and Albuquerque, E.X. Low concentrations of pyridostigmine prevent soman-induced inhibition of GABAergic transmission in the central nervous system: Involvement of muscarinic receptors. J. Pharmacol. Exp. Ther. 304:254-265, 2003.

Menegatti R, Cunha AC, Ferreira VF, Perreira EF, El Nabawi A, Eldefrawi AT, Albuquerque EX, Neves G, Rates SM, Fraga CA, Barreiro EJ. Design, synthesis and pharmacological profile of novel dopamine D2 receptor ligands. Bioorg Med Chem. 11:4807 4813, 2003

Alkondon, M., and Albuquerque, E.X. The nicotinic acetylcholine receptor subtypes and their function in the hippocampus and cerebral cortex. Prog. Brain Res. 145:109-120, 2003.

*Samochocki, M., Höffle, A., Fehrenbacher, A., Jostock, R., Ludwig, J., Christner, C., Radina, M., Zerlin, M., Ullmer, C., Pereira, E.F.R., Fels, G., Lübbert, H., Albuquerque, E.X., and Maelicke, A. Galantamine is an allosterically potentiating ligand of neuronal nicotinic but not of muscarinic acetylcholine receptors. J. Pharmacol. Exp. Ther. 305:1024-1036, 2003.

Alkondon, M., Pereira, E.F.R., and Albuquerque. NMDA and AMPA receptors contribute to the nicotinic cholinergic excitation of CA1 interneurons in the rat hippocampus. J. Neurophysiol. 90:1613-1625, 2003.

*Santos, H.R., Cintra, W.M., Aracava, Y., Maciel, C.M., Castro, N.G., and Albuquerque, E.X. Spine density and dendritic branching pattern of hippocampal CA1 pyramidal neurons in neonatal rats chronically exposed to the organophosphate paraoxon. J. Neurotoxicol. 25:481-494, 2004.

Almeida, L.E.F., Pereira, E.F.R., Camara, A.L., Maelicke, A., and Albuquerque, E.X. Sensitivity of neuronal nicotinic acetylcholine receptors to the opiate antagonists naltrexone and naloxone: receptor blockade and up-regulation. Bioorganic & Medical Chemistry Letters 14:1879-1887, 2004.

Alkondon, M., Pereira, E.F.R., Yu, P., Arruda, E.Z., Almeida, E.F., Guidetti, P., Fawcett, W.P., Sapko, M.T., Randall, W.R., Schwarcz, R., Tagle, D.A., and Albuquerque, E.X. Targeted deletion of the kynurenine aminotransferase II gene reveals a critical role of engodenous kynurenic acid in the regulation of synaptic transmission via α7 nicotinic receptors in the hippocampus. J. Neurosci. 24:4635-4648, 2004.

Braga, M.F.M., Pereira, E.F.R., Mike, A., and Albuquerque, E.X. Pb2+ via protein kinase C inhibits nicotinic cholinergic modulation of synaptic transmission the hippocampus. J. Pharmacol. Exp. Ther. 311:700-710, 2004.

Alkondon, M., and Albuquerque, E.X. The nicotinic acetylcholine receptor subtypes and their function in the hippocampus and cerebral cortex. Prog. Brain Res. 145:109-120, 2004.

Aracava, Y., Pereira, E.F.R., Maelicke, A., and Albuquerque, E.X. Memantine blocks α7* nicotinic receptors more potently than n-mthyl-D-aspartate receptors in rat hippocampal neurons. J. Pharmacol. Exp. Ther. 312:1195-1205, 2004.

Alkondon, M., and Albuquerque, E.X. Nicotinic receptor subtypes in rat hippocampal slices are differentially sensitive to desensitization and early in vivo functional up-regulation by nicotine and to block by buproprion. J. Pharmacol. Exp. Ther. 313:740-750, 2005.

Rassoulpour, A., Wu, H.-Q., Albuquerque, E.X., Schwarcz, R. Prolonged nicotine administration results in biphasic, brain-specific changes in kynurenate levels in the rat. Neuropsychopharmacology 30:687-704, 2005.

Santos, H.R., Ribeiro, H.S., Setti-Perdigao, P., Albuquerque, E.X., and Castro, N.G. The magnitude of α7 nicotinic receptor currents in rat hippocampal neurons is dependent upon GABAergic activity and depolarization. J. Pharmacol. Exp. Ther. 2006 Jul 12; [Epub ahead of print] PMID: 16837558

Alkondon, M., and Albuquerque, E.X. Subtype-specific inhibition of nicotinic acetylcholine receptors by choline: a regulatory pathway. J. Pharmacol. Exp. Ther. 2006 Jul;318(1):268-75. Epub 2006 Mar 24.

*Albuquerque, E.X., Pereira, E.F.R. Aracava, Y., Fawcett, W.P. Oliveira, M., Randall, W.R., Hamilton, T.A., Kan, R.K., Fomano, Jr., J.A., and Adler, M. Effective countermeasure against poisoning by organophosphorus insecticides and nerve agents. Proc. Nat. Acad. Sci. U.S.A. 103:13220-13225, 2006.

Popa, R., Pereira, E.F.R., Lopes, C., Maelicke, A., and Albuquerque, E.X. The n-butylcarbamate derivative of galantamine acts as an allosteric potentiating ligand on α7 nicotinic receptors in hippocampal neurons: Clinical implications for treatment of Alzheimer's disease. J. Mol. Neurosci. in press

PRESENTATIONS/ABSTRACTS:

Pereira, E.F.R., Crista, C., Randall, W.R., and Albuquerque, E.X. Interactions between kynurenic acid and galantamine on α7 nicotinic receptors in hippocampal neurons. Abstr. Soc. Neurosci., #11419, 2003.

Popa, R., Pereira, E.F.R., Cintra, W.M., Maelicke, A., and Albuquerque, E.X. At clinically relevant concentrations galantaminone, a metabolite of galantamine, does not affect □7 nicotinic receptor activity in hippocampal neurons. Abstr. Soc. Neurosci., #9433, 2003.

Oliveira, M., Gary, T.M., Fawcett, W.P., Randall, W.R., Albuquerque, E.X., and Pereira, E.F.R. Neuroprotective effects of galantamine, a drug used to treat alzheimer's disease, in primary hippocampal cultures. Abstr. Soc. Neurosci., # (in press) 2004.

Albuquerque, E.X., Santos, H.R., Cintra, W.M., Maciel, C.M., Castro, N.G., and Aracava, Y. Chronic exposure to organophosphate targets spines on the basal dendrites of the CA1 hippocampal pyramidal neurons: Implications to cognitive disorders. U.S. Aarmy Medical Defense Bioscience Review 2004.

Oliveira; M., Gary, T.M., Fawcett, W.P., Randall, W.R., Albuquerque, E.X., and Pereira, E.F.R. Neuroprotective effects of galantamine, a drug used to treat Alzheimer's disease, in primary hippocampal cultures. Abstr. Soc. Neurosci. #216.15, 2004.

Fawcett; W.P., Pereira. E.F.R., Aracava, Y., Oliveira. M., Randall. W.R., Adler. M., Romano. J., and Albuquerque, E.X.. An in vivo analysis of the effects of galantamine in guinea pigs. Abstr. Soc. Neurosci. #954.11, 2005.

Aracava, Y., Periera, E.F.R., Fawcett, W.P., Oliveira, M., Randall, W.R., Hamilton, T., Kan, R.K., Adler, M., Romano, Jr., J.A., and Albuquerque, E.X. An effective countermeasure against poisoning by organophosphorus insecticides and nerve agents. Abstr. Soc. Neurosci. #684.17, 2006.

Alkondon, M., Pereira, E. F. R., and Albuquerque, E. X. Strain-specific nicotinic cholinergic modulation of glutamate transmission in the CA1 field of the rat hippocampus. Abstr. Soc. Neurosci. #326.4, 2006.

Caminha, I., Albuquerque, E. X., and Pereira. E. F. Interactions between galantamine and kynurenic acid on α7 nicotinic receptors in hippocampal and striatal neurons. Abstr. Soc. Neurosci. #524.1, 2006.

Lopes, C., Pereira, E. F. R., Schwarcz, R., Burt, D.R., and Albuquerque, E. X. Interactions

between galantamine and kynurenic acid on α7 nicotinic receptors in hippocampal and striatal neurons. Abstr. Soc. Neurosci. #524.4, 2006.

Albuquerque, E. X., and Alkondon; M. Choline differentially activates and inhibits three nicotinic acetylcholine receptor subtypes in rat hippocampal slices. Abstr. Soc. Neurosci. #524.10, 2006.

Aracava, Y., Pereira, E.F.R., Fawcett, W.P., Oliveira, M., Randall, W. R., Hamilton, T. Kan, R. K., Adler, M., Romano, Jr., J. A., and Albuquerque, E. X. An effective countermeasure against poisoning by organophosphorus insecticides and nerve agents. Abstr. Soc. Neurosci. #684.17, 2006.